Identification of Block Oriented Nonlinear Models using Relay

Trusna Meher

Identification of Block Oriented Nonlinear Models using Relay

Submitted in partial fulfilment of the requirements for the degree of

Doctor of Philosophy

by

Trusna Meher

under the supervision of

Prof. Somanath Majhi

Department of Electronics and Electrical Engineering

Indian Institute of Technology Guwahati

Guwahati-781039, Assam, India

January 2021

To my parents (Anita Meher and Dhaneswar Meher)

and my sister (Trupti Meher).

Certificate

This is to certify that the thesis entitled "**Identification of block oriented nonlinear models using relay**", submitted by **Trusna Meher** (Roll No.:136102020), a research scholar in the department of Electronics and Electrical Engineering, Indian Institute of Technology Guwahati, for the award of the degree of **Doctor of Philosophy**, is a record of an original research work carried out by her under my supervision and guidance. The dissertation has fulfilled all requirements as per the regulations of the institute and in my opinion has reached the standard needed for submission. The results embodied in this dissertation have not been submitted to any other University or Institute for the award of any degree or diploma.

Prof. Somanath Majhi
Dept. of Electronics and Electrical Engg.,
Indian Institute of Technology Guwahati,
Guwahati - 781039, Assam, India.

Date:

Place: Guwahati

Declaration

I declare that this written submission represents my ideas in my own words, and where others' ideas or words have been included, I have adequately cited and referenced the original sources. I also declare that I have adhered to all principles of academic honesty and integrity and have not misrepresented or fabricated or falsified any idea/data/fact/source in my submission. I understand that any violation of the above will be cause for disciplinary action by the Institute and can also evoke penal action from the sources which have thus not been properly cited or from whom proper permission has not been taken when needed.

Trusna Meher

Roll No.: 136102020

Date:

Place: Guwahati

Acknowledgements

As this highly nonlinear journey of my life comes to an end, I would like to thank a lot of people, without their inputs this thesis would never have approached its equilibrium state. First and foremost, I am grateful to my supervisor Prof. Somanath Majhi for his constant guidance and valuable research inputs. Without his constant evaluation of my work, this thesis would never have materialized. His ethics of preparing his students not only for research but also as reviewers, teachers, and future academicians will help us in our journeys beyond our post-graduation.

I would like to express my deepest gratitude to my DC (doctoral committee) members, Prof. C. Mahanta, Dr. S. K. Nayak, and Dr. S. Nath for their constant monitoring of my work and suggestions for improvement. I would like to thank all my TA (teaching assistant) supervisors, Dr. G. Trivedi, Dr. R. K. Sonkar, Dr. S. Ganguly, Dr. R. Adda, and Prof. H. B. Nemade. I am also grateful to all other faculty members of the Department of Electronics and Electrical Engineering, IIT Guwahati for all the seminars/talks/conferences, etc. which enriches our academic values. I thank all the staff members of the department, especially Mr. Mukut, Late Mr. Uday, Mr. Dasharath, Mr. Sandeep, Mr. Mazid, Ms. Khurshida, Ms. Chayanika, and Mr. Sanjib.

A student's journey inside the campus is highly dependent on certain work-groups who take care of our day to day needs. I would like to thank all the securities, mess workers, canteen owners, cleaners, store owners, gardeners, etc. for their honest works. I would like to mention a few of them; Mr. Ratul Ali for the special juice and shakes and for allowing me to tie Rakhi defying boundaries of religions, the security Mr. Bitul and cleaner Ms. Nimoli for caring for my plants, the Core 2 canteen owners Ratan and Rajib dada. To keep the mind healthy, extracurricular activities play an important role. I am thankful to my Odissi guru Mr. D. Barua and my fellow

dance mates (Mrs. Tumpa Manna, Irshya, Kheya, and all others). My sincere gratitude to Mrs. Patel, Mrs. Dwivedi, Dr. P. Alagarsamy for helping me arrange spaces for the practice.

This research journey would have been incomplete without the support of teachers, lab mates, and fellow researchers from the department. I would like to thank all past and present faculties of the control system lab, Dr. D. Pal, Dr. S. Krishnaswamy, Dr. I. Kar, Dr. H. Sekhawat, and Dr. C. Bhawal. I thank my friends from the department, Anirudhha, Abhijit, Gautam, Tarique, Aditya, Sumi, Uddipana, Dr. Gargi, Kamakshi, Dr. Vivek, Dr. Jitu, Dr. Niladri, Gayatri, Nama, Dr. Amit, Vineeta, Prabhakar, and Sami. My gratitude to all the seniors who guided me during difficult times especially Dr. Kashi, Dr. Mridul, Mr. Suman, Ms. Karnika, Mr. Sushanta, Dr. Tousif, Dr. Nabanita, Dr. Bajrangbali, Dr. Sourabh and Dr. Arghya. Thanks to all the lovely juniors Kasturi, Anindya, Raju, Shiv, Tamen, and Manmohan.

Most of my life I have lived at campuses, away from home so friends plays the most important role in my every journey. A big thank you to Afreen, Kaushik, Ila, Dikhshant, Shivangi, Apari, Dr. Sanju, Dr. Camelia, Mitali, Dr. Madhvi, and Dr. Upasana. To my lovely siblings from other mothers Avinash, Srini, Surendra, Lokesh, Harsha, Harish, Mounica, Manikanta, and Ravi, a very big thank you. A special thank you to Sunita, Shreetam, Deepak, Namrata mam, Aseem, and Arvin. How can I forget our Sambalpuri group ?? Thank you, Tushar, Swarup, Saroj, Dr. Kunal, Dr. Ranjan, Biswajit, Dr. Dileep, Dinabandhu, Dr. A. Sahu, Smita mam, and Ansi for giving me the feeling of home away from home. Last of the friends but the most special, the ones I count as my constants, the ones who plan their life with me, the 3am buddies, I can go on writing about them but it will all be less: Sweta, Soumyashree, Dr. Pratibha, and Guru, I am forever indebted to you.

I would thank my family for their immense support throughout my life. My special brothers from other mothers who have been guarding me since childhood, Chandramani, Dharam, Govinda, Manoj, Hemanta, and Dr. Gopabandhu, thank you all. Dada and Nani, thank you for always boosting my self-confidence. I am forever grateful to my Maa and Bapa without whom I wouldn't have survived so far, who have nurtured a family of love, not blood, every word of appreciation would not suffice to express my gratitude towards them. Lastly, to my beloved sister

Trupti, thank you for all the sweetness you have brought to my life.

Thank you all !

Trusna Meher

Abstract

Relay feedback identification technique is widely used in process control industries, but its application is limited mainly to linear systems. This thesis focuses on extending the applicability of relay feedback to nonlinear system identification. For the said purpose, two nonlinear models have been studied, the Wiener and the Hammerstein model. Requirements of many tests and sometimes a complete change of set-up have been reported in the literature. This thesis work tries to resolve these issues by using the same set-up and no tedious resetting of the relay. It is also found in the literature that the nature of the linear subsystem is restricted to first-order or second-order with distinct real roots. The present work has successfully included a second-order linear subsystem with other kinds of roots. It also includes negative roots (i.e., right side poles) thereby applicable to unstable systems as well, given the condition that a stable limit cycle can be induced by the relay feedback set-up. Thus, the two nonlinear models considered in this work are somewhat more general compared to the reported literature. The identification procedure has been applied to various linear systems as well because the linear system is a special case of both the nonlinear models. Simulation studies are carried out to validate the proposed identification methodologies against some existing relay auto-tuning methods utilizing various examples from the literature. In the end, an attempt has been made to model a non-ideal buck converter as a Hammerstein model in the simulation thereby giving an insight into practical implementation.

Contents

List of Figures

List of Tables

List of Tables

Acronyms

AI artificial intelligence. 10

BONL block oriented nonlinear. vii, 1, 3–7, 46, 106

ESR equivalent series resistance. 99

FOPDT first-order plus dead-time. vii, 8, 11, 23, 24, 26, 30, 31, 38, 40–42, 47, 57, 61, 68, 69, 71, 79

ISE integrated square error. ix, 28, 32, 33, 37, 69, 76, 80, 101, 103

LSE least square error. 6, 46, 105

PID proportional-integral-derivative. 40

SOPDT second-order plus dead-time. viii, 7, 8, 11, 17, 22, 23, 25, 26, 31, 34, 35, 37, 40, 42, 47, 51, 56, 57, 60, 73, 78, 86, 94

Chapter 1

Introduction

1.1 Nonlinear Systems

This thesis deals with a class of nonlinear systems called the block oriented nonlinear (BONL) model. This naturally brings two fundamental questions:

1) **What are systems ??** In general, a system is any isolated whole under any environment that is of interest to someone. Mathematically, it is an equation/map which relates the inputs and outputs and hence defines a process [3]. Symbolically, for a single input single output case, a system can be given as

$$y = T[u] \tag{1.1}$$

where T is called an operator that represents the equation/map between the input u and the output y. The system's input and output are usually functions of some independent variable like position or time. If time t is the only independent variable, (1.1) can be re-written as

$$y(t) = T[u(t)] \tag{1.2}$$

The operator T is usually an integral operator due to its ability to capture the memory. Physically realizable systems are causal and hence the output depends only on the past memory. Linear integral operators are used to represent linear systems, and nonlinear systems are represented us-

ing nonlinear operators. However, there are other forms of representing systems as well, and partial differential equation is one of them. A system can be represented in various ways and all representations are inter-related. The integral operator representation is the solution of partial differential equations. The partial differential equation representation is widely used and can be generalized into what is called state space representation. Throughout this thesis work, the state space representation is used. However, some insights into the integral operator representation are given wherever required.

2) **What are nonlinear systems ??** Systems whose input to output behaviors are not proportional; mathematically, a nonlinear system is a process whose dynamics can not be modeled using linear equations/maps. Dynamics is the subject that deals with the behaviors of systems evolving with time.

The history of dynamics started with Newton's work on calculus in the mid-1660s. The work on nonlinear dynamics began with the geometric approach of Poincaré in the late 1800s who also hinted at the possibility of chaos. Pioneering works on nonlinear dynamics are done by van der Pol, Birkhoff, Kolmogorov, Lorenz, Feigenbaum, Mandelbrot, etc. For an insightful and further deep analysis of nonlinear dynamics, a reading of the book by Strogatz [4] is highly recommended. A nonlinear system in its simplest form can be represented using a set of nonlinear differential equations given as

$$\dot{\mathbf{x}} = \mathbf{f}(\mathbf{x}, t) \tag{1.3}$$

where $\mathbf{x}$ is an $n \times 1$ state vector in which each elements is a state variable including the output, $\mathbf{f}$ is a $n \times 1$ vector of nonlinear functions and n is the order of the system [5]. A geometric space with the states of the system as the variables along the axes is called state space. The solution of the equation (1.3) describes the behavior of the nonlinear system. The importance of nonlinear modeling is its ability to capture unique behaviors like bifurcations, chaos, fractals, etc. which is ignored by linear modeling. Almost all naturally occurring systems are nonlinear. Linear system itself is a special class of nonlinear systems where the function $\mathbf{f}$ is linear therefore, its dynamics

are written in the state space form

$$\dot{\mathbf{x}} = \mathbf{A}(t)\mathbf{x} \tag{1.4}$$

where $\mathbf{A}(t)$ is a matrix of dimension $n \times n$ [5]. Naturally, this hints that the bulk of nonlinear systems comprises of various classes. BONL models are an example of one such class, some other examples are nonlinear oscillators, iterated maps, neural networks, etc. What makes nonlinear systems complex to study is that there is no single unifying approach to study them. Having said that it is not impossible that in the future such a unifying approach will not exist.

1.2 Block Oriented Nonlinear Models

During the 1990s, two nonlinear models were developed independently pertaining to various applications, those were the Wiener and the Hammerstein models. The original models proposed were quite complex which are later on simplified to form the present day popular versions which consist of only a dynamic linear (DL) and static nonlinear (SNL) subsystem blocks. A Hammerstein model consists of a static nonlinear subsystem block proceeded by a dynamic linear subsystem whereas in the Wiener model the position of the linear and nonlinear subsystem blocks are reversed as shown in Figure 1.1. A series combination of these two models gives another two BONL models as shown in Figure 1.2 and 1.3. Similarly, many other nonlinear structures were developed by combining the two subsystem blocks in various fashions: series, parallel, series-parallel, etc. Later on, these groups of structures became known as the BONL models. Block-structured models can also be used for feedback systems as in Figure 1.4. Parallel BONL models are suitable for modeling multichannel topology systems, e.g., electric power distribution, communication nets, multicell parallel power converters, etc.[6]. The nonlinearity in BONL models can also be considered dynamic which will lead to high complexity which is an active area of research. However, this research work deals only with static nonlinearity. Also, out of all probable structures, this work is based only on the two basic BONL models, the Wiener and the Hammerstein.

(a) The Hammerstein Model (b) The Wiener Model

Figure 1.1: The two basic BONL models

Figure 1.2: The Hammerstein-Wiener Model

Figure 1.3: The Wiener-Hammerstein Model

The subsystems in any BONL models may or may not be physically separable. Therefore, the intermediate signal between them may not be always available for measurement. One advantage of the block-oriented model is that it can accommodate any parametric or non-parametric model within itself. For example, the linear subsystems may be parametric (transfer functions, state-space representations, etc.) or non-parametric (impulse response, frequency response, FIR, IIR etc.). The nonlinear elements may, in turn, be parametric or non-parametric, memory or memory-less. Finally, the system components may be interconnected in different ways (series/ parallel/feedback)[6]. This flexibility of block-oriented models makes them a preferable choice for practical applications. Another important advantage of these models is that they permit the use of standard linear controller design methods which is possible because the static nonlinearity in the process can be canceled by inserting an inverse at the appropriate position in the loop. Many processes can be described using block-oriented models such as pH neutralization system(Huang et al. [7]), continuous stirred tank reactor (CSTR) system (Huang et al. [7]), van der Pol's oscillator (Slotine et al. [5]), communication channels (Min et al. [8]), gas turbines (Holcomb et al. [9]), solid oxide fuel cells (Jurado [10]), muscle modeling (Chou [11]), thermal systems (Wang et al. [12]). The biggest disadvantage of the BONL model is its inability to capture behaviors of non-linear systems globally such as chaos and bifurcation. However, due to its ease towards

practical implementation and flexibility to accommodate any computational approach has made it popular among researchers.

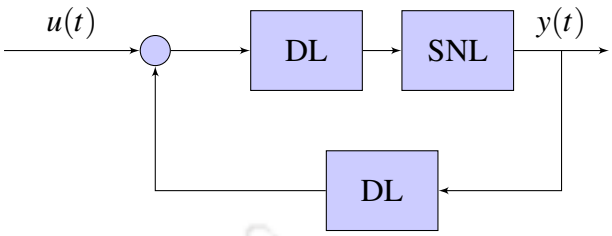

Figure 1.4: A feedback BONL model.

1.3 System Identification

There are two basic aspects to analyze a system for control: modeling and identification. Modeling deals with finding a suitable model structure that can be used to relate all the inputs and outputs of the given system. Identification deals with finding the parameters of the chosen model. This thesis work deals with only identification. It has been assumed that the model is known prior i.e., BONL models.

Modeling can be of three types, namely- white box or observational modeling, black-box modeling, and grey-box modeling [6]. Defining a system directly by the known laws of sciences is called white box or observational modeling which is the most accurate way of modeling a system. However, it is not always possible to know all the underlying of a system and hence the natural principles involved in it.

When limited or no data are available, observational modeling gets tough so, one has to rely on black-box or grey-box modeling. Black-box modeling is usually opted when absolutely nothing is known about the system, only input, and output data can be analyzed. Black-box modeling techniques include neural networks, fuzzy or neuro-fuzzy models, wavelets, etc.[13]. Black-box modeling has the drawback that it gives no physical meaning to the real process. Grey-box modeling is employed when limited observational data is available. BONL models are grey-box models. There are various methods developed in the literature to find out whether a BONL

model structure is suitable for the given system or not. The work on this thesis will not deal with structure detection rather, it will focus only on identification.

A vast literature has been already established for the identification of BONL models which includes functional series approaches, correlation analysis, neural network models, fuzzy models, differential equations models, regression models, etc. The least square error (LSE) based estimation, correlation analysis, etc. are analytic methods that require Gaussian white noise or random binary sequence kind of stochastic inputs which are easier to implement in algorithms but difficult to implement practically. Therefore, many application oriented practical methods are also developed to identify BONL models which utilize deterministic signals like the impulse, step, square, sine, etc. Relay feedback is such a method that produces a deterministic output signal, i.e., persistent oscillatory output with no input. The following section will present a brief introduction to identification using a relay.

1.4 Identification using Relay

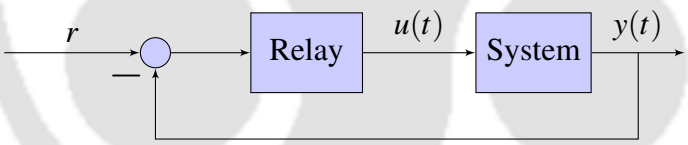

Figure 1.5: A typical relay feedback identification setup

A relay is simply a switch. Åström and Hägglund [14] were the first to propose an identification scheme using a relay in feedback which they termed as relay auto-tuning. The general structure employed for relay identification is shown in Figure 1.5, where r denotes the setpoint, y is the system output and u is the relay output or the system input. Generally, two types of relays are used, unbiased (symmetrical) and biased (asymmetrical). Sometimes, hysteresis is also added to the relay to prevent chattering. A relay feedback test without hysteresis is called an *ideal* relay test. Oscillation induced by relay on a linear system can be explained by describing function analysis. Åström and Hägglund [14] gives the details of limit cycles in relay feedback for linear systems using describing function analysis. However, the oscillation induced by relay on a non-

linear system like the BONL model can not be explained simply using the describing function analysis. In this thesis work, the relay is adjusted heuristically to get oscillation. The condition of oscillation in BONL systems in relay feedback requires in-depth analysis and has been suggested as future work.

1.5 Motivation

Despite being a successful technique, relay feedback identification is majorly limited to linear systems. This thesis work is an attempt at exploiting the ease and practicability of relay feedback from linear domains to block oriented nonlinear models. Building on simple state space calculations, this research shows the simplicity with which relay feedback can be effectively used for the identification of the Hammerstein and the Wiener models. The use of relay feedback in BONL models first began in the identification of chemical processes [15] and is still limited mostly to the chemical domain; this further motivated to build a more generalized scheme for probable application in various other industries. There are a vast number of approaches available to identify BONL models, the focus of this work is not to develop another competent method rather improve on the drawbacks of already existing relay feedback techniques. The specific drawbacks with respect to each BONL models (Wiener/ Hammerstein) has been given at the introduction of each chapters regarding them. This is because each models has a vast literature of their own hence needs to be addressed separately.

1.6 Thesis Organization

This thesis consists of five chapters including this chapter of introduction. A brief overview of each chapter is given below

- Chapter 2 : This chapter begins with a thorough literature review on the Wiener model identification. Then the identification setup, as well as the model, is described in the problem formulation. A Wiener model with a second-order plus dead time (SOPDT) linear

subsystem is considered. The procedure for identifying the model has been developed using state space equations on the limit cycle output. Not all but wider probable cases of the linear subsystem in the Wiener model which include real roots, complex conjugate roots, first-order plus dead-time FOPDT systems, integrating SOPDT, repeated roots, integrator as well as unstable cases are considered. The proposed method is simple and requires less prior knowledge about the system. The technique being somehow general, can be applied effectively to linear and unstable systems as well. Simulation examples for each case are considered to demonstrate the efficacy of the proposed identification scheme. A brief discussion on convergence, complexity, and online identification are also presented.

- Chapter 3 : An in-depth literature review on the identification of the Hammerstein model is presented first. The identification problem is then stated and discussed. Based on the similar technique of relay auto-tuning, the identification scheme is developed. First, a SOPDT Hammerstein model is considered with all probable cases of subsystems: real roots, complex conjugate roots, FOPDT systems, integrating SOPDT, repeated roots, integrator as well as unstable cases. Thereafter the identification scheme is extended to the study of an *n*th order critically damped Hammerstein model. Similar to the previous case of the Wiener model, the identification method applies to unstable cases as well. Examples from the literature are taken for each case and simulated to demonstrate the proposed identification scheme. In the end, some brief discussions of online identification, complexity, and convergence are also presented.

- Chapter 4 : This chapter proposes an efficient grey-box identification method for modeling a buck converter beyond the conventional linearized model. The buck converter is modeled as a Hammerstein nonlinear system that captures its quasi-linear behavior. The identification technique developed in the previous chapter is utilized here. A simulation is carried out and discussed to validate the procedure.

- Chapter 5 : This chapter summarizes the key contributions of the thesis and then gives a list of probable future research related to this work.

Chapter 2

Wiener Model Identification

In the 1880s Vito Volterra developed a functional series that can be used to describe dynamic, nonlinear, time-invariant systems. The series later on named after him as the Volterra series. Volterra series is a direct generalization of the Taylor series: a brief derivation of the same has been given below, for a detailed derivation, the paper by Schetzen [3] is recommended. When a system is causal, dynamic, linear and time-invariant (LTI), the output can be represented as the convolution of input $u(t)$ with the system's unit impulse response $h(t)$ i.e., the operator T in equation (1.2) is a convolution integral for LTI systems and is given as:

$$y(t) = \int_0^\infty h(\tau)u(t-\tau)d\tau \tag{2.1}$$

It is known that convolution represents the memory, therefore, the unit impulse response represents a linear system whose output depends on past inputs. When the LTI system has no memory it can be represented as a simple straight line, i.e., $y(t) = cu(t)$ where c is the slope. Therefore, the graph of a static (no-memory) nonlinear system is a curve and can be represented using a Taylor series as

$$y(t) = \sum_{i=0}^{\infty} c_i u^i(t) \tag{2.2}$$

where c_i are the Taylor series coefficients. When (2.2) is extended to dynamic nonlinear

time-invariant systems, it can be written using (2.1) as

$$y(t) = h_0 + \int_0^\infty h_1(\tau_1)u(t-\tau_1)d\tau_1 + \int_0^\infty \int_0^\infty h_2(\tau_1,\tau_2)u(t-\tau_1)u(t-\tau_2)d\tau_1 d\tau_2 + \cdots \quad (2.3)$$

This series is known as the Volterra series in recognition of Vito Volterra's contributions to it and the functions $h(\tau_1,\tau_2,\cdots\cdots,\tau_i)$ are known as the Volterra kernels of the system. Although Volterra's functional representation is theoretically sound, difficulty in kernel measurement and convergence were two major limitations for its practical implementation [3]. Wiener simplified Volterra series representation for finite memory time-invariant non-linear systems which later on became known as the Wiener model. The actual model proposed by Wiener represented a dynamic non-linear system as a combination of dynamic linear time-invariant (LTI) subsystem followed by a static nonlinearity; the LTI subsystem is represented using Laguerre network and the static non-linearity is represented using the Hermite polynomials [16]. The present-day popular Wiener model (shown in Figure 1.1b) is a highly simplified version of the original model proposed by Wiener and was first studied by Billings and Fakhouri [17].

A vast number of approaches has been developed to identify Wiener model pertaining to the required application/goals. Identification based on correlation analysis are proposed by Billings and Fakhouri [17], Schetzen [3]. Methods such as kernels, functional series or regression based techniques are developed by Greblicki [18]-[19], Tötterman and Toivonen [20], Fang and Chow [21]. Bai [22], Giri et al. [23] studied frequency domain identification methods. Major identification techniques are developed using optimization algorithms such as by Hagenblad and Ljung [24], Hagenblad et al. [25], Tang et al. [26], Wang and Ding [27], Liu et al. [28], Zhou et al. [29]. Recently, identification using least square recursive algorithms are studied by Ding et al. [30]. Guo et al. [31] developed AI friendly approach using quantized inputs and binary-valued outputs. Mohamed and Kar [32] have used differential mean value theorem and stochastic contraction theory for estimating Wiener models. Wiener models are successfully applied to many processes as well; biological systems [33, 34], pH neutralization processes [35, 7, 36], distillation column modeling [15].

Luyben and Eskinat [15] were the first to use relay feedback for identifying Wiener and Ham-

merstein models. They adjusted the relay height to get a symmetric output, thereby canceling the effect of the nonlinearity. This allowed them to use describing function techniques of linear auto-tune modeling. However, their equations gave singular solutions because the output frequency is independent of relay height, and in their work, they used frequency response analysis. To get non-trivial solutions, they used different known dynamic elements in the loop to change the frequency. This is an easy solution, however not efficient because as pointed out by them the choice of a dynamic element relies on the complexity of the system which means prior knowledge is required. Also, adding a known dynamic element may pose a difficulty if the method is considered for online identification. Luyben and Eskinat [15]'s method relied mostly on the experimental solution instead of theoretical analysis. Huang et al. [2] used a two-stage identification procedure to identify the Wiener model using relay feedback. In the first stage, the static nonlinearity and its inverse are estimated using an optimization procedure. In the second stage, the input relay settings are adjusted to cancel the static linearity thereby converting the Wiener model into a simple linear FOPDT or SOPDT system, the linear subsystem is then identified using the relay output. Lee et al. [1] made use of an adjustable PI controller in the relay feedback loop to identify the Wiener model. Lee et al. [1]'s method is a convenient tool for online identification which decoupled the linear and non-linear subsystem identification part. Jeng et al. [37] used a predesigned relay heights setting experiment to identify the Wiener model; the nonlinearity is identified using a least-square algorithm whereas the linear subsystem is identified using frequency domain analysis of the output. Mehta and Majhi [38] used a relay with hysteresis to identify the Wiener model with only a critically damped linear subsystem, they used a simple state space-based technique. Hanjalić and Jurić [39] used a frequency domain approach to identify the Wiener model where the relay is used in the feedback path instead of the conventional feed-forward path.

Most of the work mentioned above were restricted only to critically damped or over damped linear subsystems. Although, Jeng et al. [37] and Hanjalić and Jurić [39] considers a more general SOPDT linear subsystem, they used frequency domain techniques. Also, none of the earlier methods have considered unstable linear subsystem. The proposed method in this thesis considers a more general SOPDT linear subsystem including unstable poles and uses time domain analysis.

One advantage of the identification technique is that there is no need of knowing a prior the stability of poles of the linear subsystem, it can be inferred directly from the calculated value of the time constants.

The work in this chapter has been published in [40].

2.1 Problem Formulation

The setup for identification of the Wiener model is the same as any typical identification setup used in relay feedback as shown in Figure 1.5. The detailed setup indicating all associated signals is shown in Figure 2.2.

An ideal symmetric relay with hysteresis is used for identification. Practically relay is never ideal therefore, hysteresis is considered which also prevents relay chattering in the presence of measurement noise. The relay characteristics are shown in Figure 2.1.

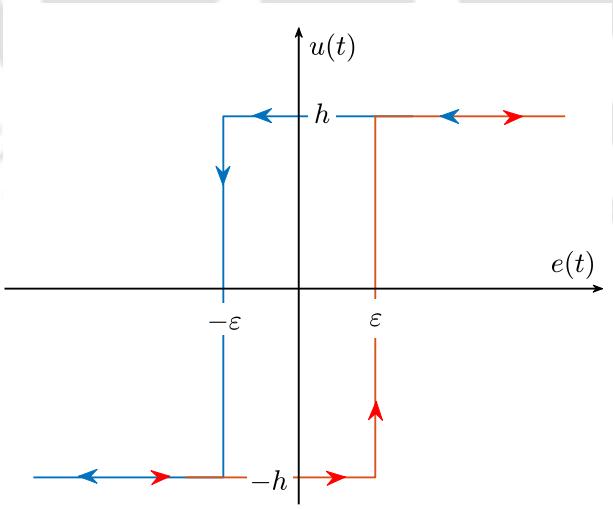

Figure 2.1: Graphical characteristic of a relay with hysteresis.

The hysteretic relay output or the system input in the identification setup of Fig 2.2 is given

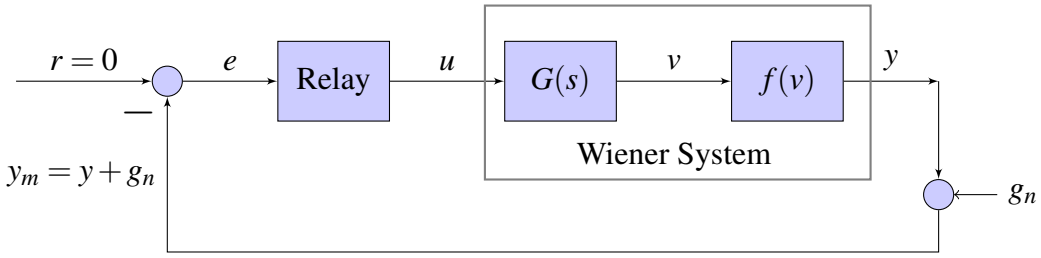

Figure 2.2: Setup used for the identification of Wiener model

as

$$u(t) = \begin{cases} h & \text{if} \quad e(t) \geqslant \varepsilon \\ -h & \text{if} \quad e(t) \leqslant -\varepsilon \\ h & \text{if} \quad e(t) \in (-\varepsilon, \varepsilon) \quad \text{and} \quad e(\delta(t)) = \varepsilon \\ -h & \text{if} \quad e(t) \in (-\varepsilon, \varepsilon) \quad \text{and} \quad e(\delta(t)) = -\varepsilon \end{cases} \tag{2.4}$$

where, $\delta(t)$ is the value of time at the last threshold attained. The article by Macki et al. [41] is recommended for more details on relay with hysteresis. The signal, g_n is the additive white Gaussian noise added at the output and r is the set point reference. For simplicity of calculation, r is taken as 0 as the operating point of the system is considered to be the origin. However, for systems with operating point other than origin, the operating point can be brought back to origin with a simple change of coordinates in which case the value of r has to be changed accordingly. The measurement noise ($g_n(t)$) is assumed to be prevented from entering the system by changing the width of hysteresis, heuristically. Therefore, only the measured output $y_m(t)$ is noisy whereas system input, $u(t)$ and intermediate signal, $v(t)$ are noise free. This is a simplified situation whereas in real application, there are other noises beside measurement noise, a treatment of which could make for future studies.

It is to be noted that in the presence of white noise $g_n(t)$, $y(t)$ in all the equations represent the denoised signal extracted from $y_m(t)$. All calculations involved in system identification is done using this denoised output, $y(t)$ instead of measured output $y_m(t)$ because: the proposed method is not an adaptive or iterative method where the whole output signal for a certain duration is required for the identification. This method requires measurements on a few cycles of the

oscillatory output, it doesn't require the whole output signal. Therefore, the noisy output, $y_m(t)$ can be denoised separately outside the setup, and only the required measurements are taken for identification.

The relay output is the input to the system whose structure is a Wiener model. The linear subsystem used has transfer function $G(s)$ as

$$G(s) = \frac{e^{-\theta s}}{(T_1 s+1)(T_2 s+1)} \tag{2.5}$$

where θ is the time delay and the poles of $G(s)$ i.e., $\frac{-1}{T_1}$ and $\frac{-1}{T_2}$ can be real/complex, all possible cases are treated separately. The system is considered to be stable/unstable depending on the sign of T_1 and T_2. The DC gain in the transfer function $G(s)$ is assumed one because its effect can be considered along with the static nonlinearity. The static nonlinearity is assumed to be passive and monotonic which is estimated as a polynomial of the form

$$f(v(t)) = \sum_{j=1}^{p} \alpha_j v^j(t) \tag{2.6}$$

where, α_j's are constants and p is the order of the polynomial. Passivity makes the nonlinearity bounded only to the first and third quadrants. Passivity is required to ensure limit cycle oscillation. If the nonliearity is present also in second and fourth quadrant it will induce a 180 degree phase shift i.e., a negative gain which is when added to the negative feedback gives 360 degree phase shift hence, no oscillation. A detail on passive nonlinearities can be found in chapter 6 of Khalil [42]. The requirement of monotonicity will be discussed in subsection 2.5.3 because the explanation depends on the identification procedure. However, the static nonlinearity has to be continuous as discontinuous nonlinearities will not produce limit cycle oscillation and absence of limit cycle oscillation doesn't mean a discontinuity in the nonlinearity. All these restrictions on the nonlinearity makes the polynomial form suitable for representation. However, other functional forms can also be considered such as Hermite polynomial originally used by Arnold [16] or exponential functions as suggested by Luyben and Eskinat [15]. Similarly, rational functions, transcendental functions, orthogonal polynomials, Fourier series, wavelets, regression analysis,

neural networks etc. can also be explored to consider nonlinear function representation.

As stated earlier in Sec. 1.2, the intermediate signal $v(t)$ may not always be available for measurement. When $v(t)$ is available for measurement, the identification is straight forward and easy. Therefore, considering the worst case, $v(t)$ is assumed to be immeasurable. The overall system dynamics of the Wiener system in Figure 2.2 can be written as

$$y(t) = f(v(t)) = \sum_{i=1}^{p} \alpha_i v^i(t) \tag{2.7}$$

$$\dot{\mathbf{X}}(t) = \mathbf{A}\mathbf{X}(t) + \mathbf{B}u(t-\theta) \tag{2.8}$$

$$v(t) = \mathbf{C}\mathbf{X}(t) \tag{2.9}$$

where,

$$\mathbf{A} = \begin{bmatrix} -\frac{1}{T_1} & 0 \\ 0 & -\frac{1}{T_2} \end{bmatrix}; \qquad \mathbf{B} = \begin{bmatrix} 1 \\ 1 \end{bmatrix}$$

$$\mathbf{C} = \frac{1}{(T_1 - T_2)} \begin{bmatrix} 1 & -1 \end{bmatrix}; \qquad \mathbf{X}(t) = \begin{bmatrix} x_1(t) \\ x_2(t) \end{bmatrix}$$

and subject to the condition that $T_1 \neq T_2$. The critically damped case when $T_1 = T_2$ has been discussed separately. Considering the set-up in Figure 2.2 and all the assumptions stated above, the final problem is to identify $G(s)$ and $f(v)$ with the knowledge of only $u(t)$ and $y(t)$.

2.2 Wiener Model of Second-Order Systems

The proposed identification method is divided into two stages: in the first stage, the linear sub-system of the Wiener model, $G(s)$ is identified. Then using the obtained data, the nonlinearity, $f(v)$ for the required time interval is estimated in the second stage. The relay heights are set as h and $-h$ along with hysteresis width of ε and $-\varepsilon$. All the calculations are carried out considering $g_n = 0$, in other words considering $y(t)$ as the denoised output; the reason for this is explained

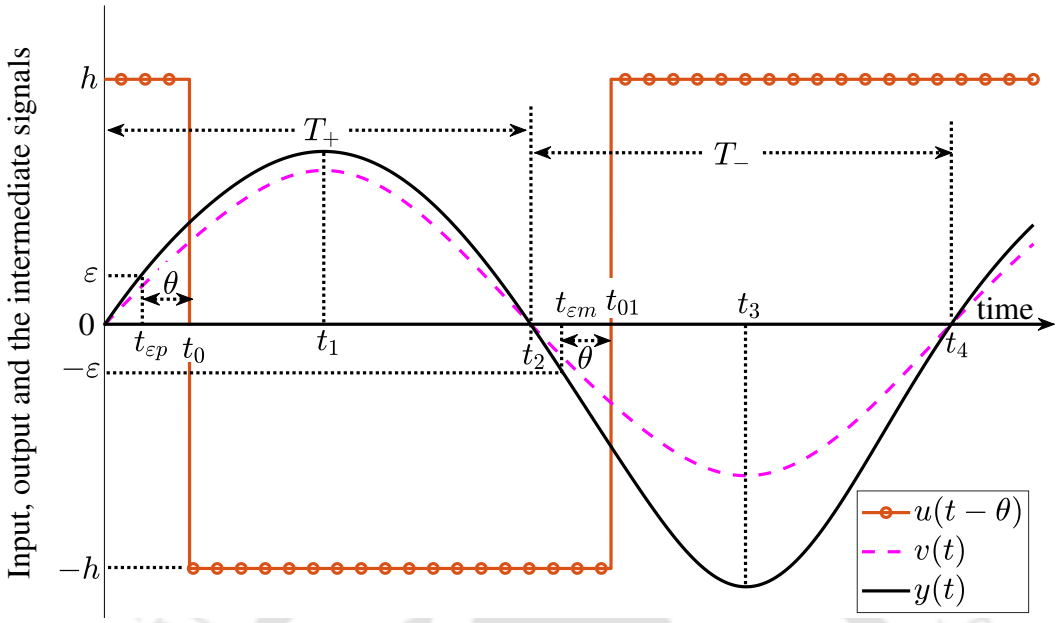

Figure 2.3: Typical output of a Wiener model with order higher than one of the linear subsystem.

in the previous section. The typical output of a second-order Wiener system is given in Figure 2.3. The relay output $u(t)$ is a step signal which switches when $e(t) = -y(t)$ attains $\pm\varepsilon$. The delayed relay output $u(t-\theta)$ is shown instead of $u(t)$ to show the effect of considering delay in $G(s)$. However, it is to be noted that $u(t)$ is measurable whereas $u(t-\theta)$ is not. As the LTI subsystem in the Wiener model is of second-order, therefore, it gives a sinusoidal type output $v(t)$ in response to $u(t)$ as shown in Figure 2.3. The nonlinearity being static changes only the magnitude of $v(t)$ and doesn't shift it. Moreover, the nonlinearity is assumed to be monotonic, therefore, the peak of $v(t)$ and $y(t)$ occurs at the same time. The various time measurements in the graph of Figure 2.3 are defined as

- $t = 0$ is the time where $y(t) = 0$ i.e. the beginning of the positive half cycle of the chosen full cycle of $y(t)$.
- $t_{\varepsilon p}$ is the time at which $y(t) = \varepsilon$ or the relay output $u(t)$ switches. In the presence of white noise $g_n(t)$, the denoised output $y(t)$ may not switch exactly at $+\varepsilon$. Therefore, $t_{\varepsilon p}$ is measured as the time at which $u(t)$ crosses the time axis.
- t_0 is the time at which the delayed relay output $u(t-\theta)$ crosses the time axis which is not measurable directly. For the measurement of t_0 and hence θ, the procedure mentioned by

Majhi [43] is used. If the model is of a lower order, then the model is usually estimated with its exact order which is assumed to be known. In that case, the time delay θ is measured as the duration from relay switching to the duration at which an abrupt change in nth order derivative of the output occurs. But higher order systems are usually represented as second-order plus dead time (SOPDT) with an effective time delay of θ_E. In such a case, the effective delay is measured as the duration between relay switching to the duration at which the nearby optimum of the second derivative of system output occurs. Note that the plots in Figure 2.3 is only for systems with small time delays. When the delay is high, the output may have ripples instead of having a smooth peak because the delay will allow transient to persist longer.

- t_1 is the time instance where $y(t)$ attains peak. In the presence of noise, it is taken as the instance where the first derivative of the denoised output crosses the time axis.
- t_2 is the time where the positive half cycle of $y(t)$ ends or $y(t)$ crosses the time axis hence, $y(t_2) = 0$.
- $t_{\varepsilon m}, t_{01}$ and t_3 in the negative half cycle are the same as what $t_{\varepsilon p}, t_0$ and t_1 are in the positive half cycle.
- t_4 is the end of the chosen complete cycle and the beginning of a new one of $y(t)$ and hence, $y(t_4) = 0$.
- T_+ is the time period during which the output is positive and T_- is the time period during which the output is negative.

This typical output plot of Figure 2.3 and the above-mentioned instances of time serves as the reference for all the proceeding derivations.

2.2.1 Linear Subsystem Identification

Linear subsystem identification includes finding the time constants T_1 and T_2 of the LTI transfer function, $G(s)$. The calculation of delay has been already mentioned in the previous section.

From equation (2.9),

$$x_1(t) - x_2(t) = v(t)(T_1 - T_2) \tag{2.10}$$

$$\Rightarrow \dot{x}_1(t) - \dot{x}_2(t) = \dot{v}(t)(T_1 - T_2) \tag{2.11}$$

Expanding equation (2.8) and using (2.11) ,

$$\dot{x}_1(t) - \dot{x}_2(t) = \frac{x_2(t)}{T_2} - \frac{x_1(t)}{T_1} = \dot{v}(t)(T_1 - T_2) \tag{2.12}$$

From the graph of Figure 2.3 and (2.12),

$$v(0) = 0$$

$$\Rightarrow x_1(0) = x_2(0) = x(0) \quad \text{(say)} \tag{2.13}$$

Solving equation (2.8) for time range $0 \leqslant t \leqslant t_0$ during which the input to the plant remains piece-wise constant, $u(t-\theta) = h$ (refer Figure 2.3),

$$\mathbf{X}(t) = \mathbf{e}^{\mathbf{A}t}\mathbf{X}(0) - (\mathbf{I} - \mathbf{e}^{\mathbf{A}t})\mathbf{A}^{-1}\mathbf{B}h \tag{2.14}$$

$$\Rightarrow \begin{bmatrix} x_1(t) \\ x_2(t) \end{bmatrix} = \begin{bmatrix} x(0)e^{\frac{-t}{T_1}} + hT_1(1 - e^{\frac{-t}{T_1}}) \\ x(0)e^{\frac{-t}{T_2}} + hT_2(1 - e^{\frac{-t}{T_2}}) \end{bmatrix} \tag{2.15}$$

Again, solving equation (2.8) for time range $t_0 \leqslant t \leqslant t_{01}$ during which the input to the plant remains piece-wise constant, $u(t-\theta) = -h$ (refer Figure 2.3),

$$\mathbf{X}(t) = \mathbf{e}^{\mathbf{A}t}\mathbf{X}(0) + (\mathbf{I} + \mathbf{e}^{\mathbf{A}t} - 2\mathbf{e}^{\mathbf{A}(t-t_0)})\mathbf{A}^{-1}\mathbf{B}h \tag{2.16}$$

$$\Rightarrow \begin{bmatrix} x_1(t) \\ x_2(t) \end{bmatrix} = \begin{bmatrix} x(0)e^{\frac{-t}{T_1}} - hT_1(1 + e^{\frac{-t}{T_1}} - 2e^{\frac{(t_0-t)}{T_1}}) \\ x(0)e^{\frac{-t}{T_2}} - hT_2(1 + e^{\frac{-t}{T_2}} - 2e^{\frac{(t_0-t)}{T_2}}) \end{bmatrix} \tag{2.17}$$

Now, using (2.17) in $v(t_2) = 0$ and solving gives,

$$x(0)\left(e^{\frac{-t_2}{T_1}} - e^{\frac{-t_2}{T_2}}\right) = h\left[T_1(1+e^{\frac{-t_2}{T_1}} - 2e^{\frac{t_0-t_2}{T_1}}) - T_2(1+e^{\frac{-t_2}{T_2}} - 2e^{\frac{t_0-t_2}{T_2}})\right] \tag{2.18}$$

Case-I: When $t_1 \leq t_0$, solving $\dot{v}(t_1) = 0$ using (2.15) and (2.11) gives

$$x(0)\left[\frac{e^{\frac{-t_1}{T_1}}}{T_1} - \frac{e^{\frac{-t_1}{T_2}}}{T_2}\right] = h\left(e^{\frac{-t_1}{T_1}} - e^{\frac{-t_1}{T_2}}\right) \tag{2.19}$$

Dividing (2.18) by (2.19) and solving gives

$$1 + \frac{\left(T_2 e^{\frac{-t_2}{T_2}} e^{\frac{-t_1}{T_1}} - T_1 e^{\frac{-t_2}{T_1}} e^{\frac{-t_1}{T_2}}\right)}{\left(T_2 e^{\frac{-t_1}{T_1}} - T_1 e^{\frac{-t_1}{T_2}}\right)} = \frac{2\left(T_1 e^{\frac{t_0-t_2}{T_1}} - T_2 e^{\frac{t_0-t_2}{T_2}}\right)}{T_1 - T_2} \tag{2.20}$$

Case-II: When $t_1 \geq t_0$, solving $\dot{v}(t_1) = 0$ using (2.17) and (2.11) gives

$$x(0)\left[\frac{e^{\frac{-t_1}{T_1}}}{T_1} - \frac{e^{\frac{-t_1}{T_2}}}{T_2}\right] = h\left(e^{\frac{-t_1}{T_1}} - e^{\frac{-t_1}{T_2}} - 2\left(e^{\frac{t_0-t_1}{T_1}} - e^{\frac{t_0-t_1}{T_2}}\right)\right) \tag{2.21}$$

Dividing (2.18) by (2.21) and solving gives

$$1 + \frac{\left(T_1 e^{\frac{-t_1}{T_2}} - T_2 e^{\frac{-t_1}{T_1}}\right)}{\left(T_1 e^{\frac{-t_2}{T_1}} e^{\frac{-t_1}{T_2}} - T_2 e^{\frac{-t_2}{T_2}} e^{\frac{-t_1}{T_1}}\right)} = \frac{2\left(T_1 e^{\frac{t_0}{T_1}} - T_2 e^{\frac{t_0}{T_2}}\right)}{T_1 - T_2} \tag{2.22}$$

Solving equation (2.8) for time range $t_{01} \leqslant t \leqslant t_4$ during which the input to the plant remains piece-wise constant, $u(t-\theta) = h$ (refer Figure 2.3),

$$\mathbf{X}(t) = \mathbf{e}^{\mathbf{A}t}\mathbf{X}(0) - (\mathbf{I} - \mathbf{e}^{\mathbf{A}t} + 2\mathbf{e}^{\mathbf{A}(t-t_0)} - 2\mathbf{e}^{\mathbf{A}(t-t_{01})})\mathbf{A}^{-1}\mathbf{B}h \tag{2.23}$$

$$\Rightarrow \begin{bmatrix} x_1(t) \\ x_2(t) \end{bmatrix} = \begin{bmatrix} x(0)e^{\frac{-t}{T_1}} + hT_1(1 - e^{\frac{-t}{T_1}} + 2e^{\frac{t_0-t}{T_1}} - 2e^{\frac{t_{01}-t}{T_1}}) \\ x(0)e^{\frac{-t}{T_2}} + hT_2(1 - e^{\frac{-t}{T_2}} + 2e^{\frac{t_0-t}{T_2}} - 2e^{\frac{t_{01}-t}{T_2}}) \end{bmatrix} \tag{2.24}$$

By periodicity of the intermediate signal $v(t)$, $\mathbf{X}(0) = \mathbf{X}(t_4)$, when substituted in (2.24) gives

$$\begin{aligned} x(0) &= x(0)e^{\frac{-t_4}{T_1}} + hT_1(1 - e^{\frac{-t_4}{T_1}} + 2e^{\frac{t_0-t_4}{T_1}} - 2e^{\frac{t_{01}-t_4}{T_1}}) \\ \Rightarrow x(0)(1 - e^{\frac{-t_4}{T_1}}) &= hT_1(1 - e^{\frac{-t_4}{T_1}} + 2e^{\frac{t_0-t_4}{T_1}} - 2e^{\frac{t_{01}-t_4}{T_1}}) \end{aligned} \tag{2.25}$$

and,

$$\begin{aligned} x(0) &= x(0)e^{\frac{-t_4}{T_2}} + hT_2(1 - e^{\frac{-t_4}{T_2}} + 2e^{\frac{t_0-t}{T_2}} - 2e^{\frac{t_{01}-t_4}{T_2}}) \\ \Rightarrow x(0)(1 - e^{\frac{-t_4}{T_2}}) &= hT_2(1 - e^{\frac{-t_4}{T_2}} + 2e^{\frac{t_0-t}{T_2}} - 2e^{\frac{t_{01}-t_4}{T_2}}) \end{aligned} \tag{2.26}$$

Dividing (2.25) by (2.26) and solving gives,

$$\frac{T_2}{T_1} = \frac{1 + \frac{2(e^{\frac{t_0}{T_1}} - e^{\frac{t_{01}}{T_1}})}{e^{\frac{t_4}{T_1}} - 1}}{1 + \frac{2(e^{\frac{t_0}{T_2}} - e^{\frac{t_{01}}{T_2}})}{e^{\frac{t_4}{T_2}} - 1}} \tag{2.27}$$

Now, equations (2.20)/(2.22) and (2.27) will be treated separately for various kinds of roots in the denominator of the linear subsystem.

(i) real roots

When the roots of $G(s)$ are real then the two non-linear equations (2.20)/ (2.22) and (2.27) are explicitly used to evaluate T_1 and T_2.

(ii) complex conjugate roots

When the roots of $G(s)$ are complex conjugates,

$$\frac{1}{T_1} = a + ib \quad \text{and} \quad \frac{1}{T_2} = a - ib \tag{2.28}$$

Putting these values in $G(s)$ will not affect the denominator therefore, it can be directly used in equations (2.20)/(2.22) and (2.27). Hence, putting the values of T_1 and T_2 from equation (2.28),

the equations (2.20)/(2.22) and (2.27) can be re-written in terms of a and b as,

$$e^{at_2} + \frac{a\sin\Big(b(t_1-t_2)\Big) - b\cos\Big(b(t_1-t_2)\Big)}{a\sin(bt_1) - b\cos(bt_1)} + \frac{2}{b}e^{at_0}\left(a\sin\Big(b(t_0-t_2)\Big) - b\cos\Big(b(t_0-t_2)\Big)\right) = 0 \tag{2.29}$$

$$e^{-at_2} + \frac{a\sin(bt_1) - b\cos(bt_1)}{a\sin\Big(b(t_1-t_2)\Big) - b\cos\Big(b(t_1-t_2)\Big)} + \frac{2}{b}e^{a(t_0-t_2)}\Big(a\sin(bt_0) - b\cos(bt_0)\Big) = 0 \tag{2.30}$$

$$\begin{aligned} e^{-at_4} + e^{at_4} - 2\cos(bt_4) = \\ 2e^{at_0}\left[\frac{a}{b}\left(\sin\Big(b(t_0-t_4)\Big) - e^{-at_4}\sin(bt_0)\right) - \cos\Big(b(t_0-t_4)\Big) + e^{-at_4}\cos(bt_0)\right] \\ -2e^{at_{01}}\left[\frac{a}{b}\left(\sin\Big(b(t_{01}-t_4)\Big) - e^{-at_4}\sin(bt_{01})\right) - \cos\Big(b(t_{01}-t_4)\Big) + e^{-at_4}\cos(bt_{01})\right] \end{aligned} \tag{2.31}$$

(iii) repeated roots

The matrices for repeated roots case in the equations (2.8) and (2.9) are modified as follows,

$$\mathbf{A} = \begin{bmatrix} -a & 1 \\ 0 & -a \end{bmatrix}; \qquad \mathbf{B} = \begin{bmatrix} 0 \\ 1 \end{bmatrix}; \qquad \mathbf{C} = a^2\begin{bmatrix} 1 & 0 \end{bmatrix}$$

where, $a = \frac{1}{T_1}$. Substituting these matrices in (2.8) and (2.9), the following equations are obtained,

$$\dot{x}_1(t) = -ax_1(t) + x_2(t) \tag{2.32}$$

$$\dot{x}_1(t) = -ax_2(t) + u(t-\theta) \tag{2.33}$$

$$v(t) = a^2x_1(t) \tag{2.34}$$

From Figure 2.3, $v(0) = 0 \Rightarrow x_1(0) = 0$, therefore, solving (2.8) for time range $t_0 \leqslant t \leqslant t_{01}$

now gives,

$$\mathbf{X}(t) = x_2(0)e^{-at}\begin{bmatrix} t \\ 1 \end{bmatrix} - \frac{h}{a^2}\begin{bmatrix} 1+e^{-at}-2e^{a(t_0-t)}+ae^{-at}\Big(t-2(t-t_0)e^{at_0}\Big) \\ a\Big(1+e^{-at}-2e^{a(t_0-t)}\Big) \end{bmatrix} \tag{2.35}$$

Now, using (2.35) in $v(t_2) = 0$ and solving gives,

$$x_2(0) = \frac{h\Big(1+e^{at_2}-2e^{at_0}+a\Big(t_2-2(t_2-t_0)e^{at_0}\Big)\Big)}{t_2a^2} \tag{2.36}$$

Given the non-linearity to be monotonic, for the critically damped case, $t_1 \geqslant t_0$, always. Therefore, solving $\dot{v}(t_1) = 0$ using (2.35) gives,

$$x_2(0) = \frac{h\Big(2(t_1-t_0)e^{at_0}-t_1\Big)}{1-at_1} \tag{2.37}$$

Equating (2.36) and (2.37) gives the equation to find a and hence T_1 as

$$1-a(t_1-t_2)+e^{at_2}(1-at_1) = 2e^{at_0}[1+a(t_2-t_1+t_0)+a^2t_0(t_1-t_2)] \tag{2.38}$$

(iv) integrating second-order

The transfer function for integrating SOPDT is given as,

$$G(s) = \frac{e^{-\theta s}}{s(T_1s+1)} \tag{2.39}$$

which can be considered as a special case of SOPDT where one pole tends to zero, i.e., $\frac{1}{T_2} \to 0$. In other term, the time constant T_2 is very high compared to T_1, however can be canceled with the linear static gain at the numerator of $G(s)$ i.e.,

$$G(s) = \frac{T_2e^{-\theta s}}{(T_2s+1)(T_1s+1)} \tag{2.40}$$

but, $T_2 >> 1$

$$\therefore \quad G(s) = \frac{T_2 e^{-\theta s}}{T_2 s(T_1 s+1)} = \frac{e^{-\theta s}}{s(T_1 s+1)}$$

Therefore, the value of T_1 can be obtained by solving the non-linear equations (2.20)/(2.22) and (2.27) considering a very high initial value of T_2 compared to T_1. It will be shown in the simulation too that considering a relatively high initial value of T_2 compared to T_1 for solving the non-linear equations (2.20)/(2.22) and (2.27), gives very accurate estimate of T_1 while T_2 comes nearly equal to the considered initial estimate of it.

(v) first-order

A FOPDT system can be easily detected by studying the shape of the output $y(t)$ which will be nearly triangular in shape. For FOPDT case, in Figure 2.3, $t_0 = t_1$ and in the equation of $G(s)$, $T_2 = 0$. Substituting these values in (2.20) or (2.22) gives the equation to find T_1 as

$$1 + e^{\frac{t_2}{T_1}} = 2e^{\frac{t_0}{T_1}} \tag{2.41}$$

(vi) integrator

For an integrator with dead time, the transfer function $G(s)$ is written as

$$G(s) = \frac{e^{-\theta s}}{s} \tag{2.42}$$

which can be seen as a special case of integrating SOPDT or the first-order type subsystem. Considering it as a special case of FOPDT type system with $\frac{1}{T_1} \to 0$, $G(s)$ can be re-written as

$$G(s) = \frac{T_1 e^{-\theta s}}{T_1 s+1} \simeq \frac{T_1 e^{-\theta s}}{T_1 s} = \frac{e^{-\theta s}}{s}$$

In another term, the very high time constant T_1 gets canceled with the high linear static gain at the numerator. Note that this assumption will not affect the actual linear static gain as from the beginning of this section it has been considered with the nonlinear subsystem block. Therefore,

no calculations are required to find any time constant in this. It will be verified in the simulation example that by treating an integrator as a FOPDT system and hence evaluating T_1 using equation (2.41) gives a very high value. The unknowns required to be calculated for a Wiener model with an integrator are, the delay which can be calculated using the method proposed by Majhi [43] and, the static nonlinearity which will be discussed in the next section.

2.2.2 Nonlinearity Estimation

The nonlinearity is estimated as a polynomial fitting between $v(t)$ and $y(t)$ as in equation (2.6). After identifying the linear subsystem the intermediate signal $v(t)$ is evaluated using (2.9) for any required interval. In this section the equation of $v(t)$ for time interval $t_0 \leqslant t \leqslant t_{01}$ is derived for various cases of roots in the denominator of the linear subsystem.

(i) real roots

From (2.10) and (2.17), $v(t)$ can be written as,

$$v(t) = x(0)\frac{e^{\frac{-t}{T_1}} - e^{\frac{-t}{T_2}}}{T_1 - T_2} + h\frac{T_2 e^{\frac{-t}{T_2}}(1 - 2e^{\frac{t_0}{T_2}}) - T_1 e^{\frac{-t}{T_1}}(1 - 2e^{\frac{t_0}{T_1}})}{T_1 - T_2} - h \tag{2.43}$$

where, $x(0)$ can be calculated from (2.18) as

$$x(0) = h\frac{\left[T_1(1 + e^{\frac{-t_2}{T_1}} - 2e^{\frac{t_0 - t_2}{T_1}}) - T_2(1 + e^{\frac{-t_2}{T_2}} - 2e^{\frac{t_0 - t_2}{T_2}})\right]}{\left(e^{\frac{-t_2}{T_1}} - e^{\frac{-t_2}{T_2}}\right)} \tag{2.44}$$

(ii) complex conjugate roots

Putting the values of T_1 and T_2 from (2.28), the equation of $G(s)$ is modified accordingly as,

$$G(s) = \frac{e^{-\theta s}}{(T_1 s + 1)(T_2 s + 1)} = \frac{\frac{1}{T_1 T_2} e^{-\theta s}}{(s + \frac{1}{T_1})(s + \frac{1}{T_2})} = \frac{(a^2 + b^2)e^{-\theta s}}{(s + a + \mathrm{i}b)(s + a - \mathrm{i}b)}$$

However, the gain term in the numerator, $(a^2 + b^2)$ can be considered along with the nonlin-

earity, hence

$$G(s) = \frac{e^{-\theta s}}{(s+a+\mathrm{i}b)(s+a-\mathrm{i}b)} \tag{2.45}$$

The equation of $v(t)$ for this case can be derived using the modified values of T_1 and T_2 from (2.28) in (2.43). However, it is to be noted that now, (a^2+b^2) should be divided in order to get the actual $v(t)$ hence,

$$v(t) = \frac{x(0)e^{-at}\sin(bt)}{b} - \frac{h}{(a^2+b^2)} - \frac{he^{-at}}{b(a^2+b^2)}\left[a\sin(bt) + b\cos(bt) + 2e^{at_0}\left(a\sin\Big(b(t_0-t)\Big) - b\cos\Big(b(t_0-t)\Big)\right)\right] \tag{2.46}$$

where, $x(0)$ is similarly derived from(2.44) as

$$x(0) = \frac{h\left[be^{at_2} + a\sin(bt_2) + b\cos(bt_2) + 2e^{at_0}\left(a\sin\Big(b(t_0-t_2)\Big) - b\cos\Big(b(t_0-t_2)\Big)\right)\right]}{(a^2+b^2)\sin(bt_2)} \tag{2.47}$$

(iii) repeated roots

The equation for $v(t)$ can be derived by using (2.34) and (2.35) as

$$v(t) = a^2te^{-at}x_2(0) - h\left(1 + e^{-at} - 2e^{a(t_0-t)} + ae^{-at}\left(t - 2(t-t_0)e^{at_0}\right)\right) \tag{2.48}$$

where, $x_2(0)$ can be calculated using (2.36) or (2.37).

(iv) integrating second-order

Considering the modified transfer function $G(s)$ for integrating SOPDT case in (2.40), T_2 should be multiplied in the equation for $v(t)$ in (2.9) i.e.,

$$v(t) = T_2\frac{x_1(t)-x_2(t)}{T_1-T_2} = \frac{x_1(t)-x_2(t)}{\frac{T_1}{T_2}-1} \tag{2.49}$$

However, for integrating SOPDT, $\frac{1}{T_2} \to 0$ which is when substituted in (2.49) gives

$$v(t) = x_2(t) - x_1(t) \tag{2.50}$$

For finding $v(t)$ in time range $t_0 \leqslant t \leqslant t_{01}$, (2.17) is used in (2.50). Then, the limiting condition, $\frac{1}{T_2} \to 0$ is used in the resulting equation which gives the final value of $v(t)$ as

$$v(t) = x(0)(1 - e^{\frac{-t}{T_1}}) + hT_1(1 + e^{\frac{-t}{T_1}} - 2e^{\frac{t_0 - t}{T_1}}) + h(2t_0 - t) \tag{2.51}$$

where, $x(0)$ is similarly calculated using the limiting condition in (2.18) as

$$x(0) = h\frac{T_1(1 + e^{\frac{-t_2}{T_1}} - 2e^{\frac{t_0 - t_2}{T_1}}) + 2t_0 - t_2}{e^{\frac{-t_2}{T_1}} - 1} \tag{2.52}$$

(v) first-order

Substituting $T_2 = 0$ in (2.43) and (2.44) gives the equation to find $v(t)$ for FOPDT system as

$$v(t) = h(e^{\frac{t_2 - t}{T_1}} - 1) \tag{2.53}$$

(vi) integrator

An integrator can be seen as a special case of the integrating SOPDT system where the time constant $T_1 = 0$ in Equation (2.39). Therefore, the intermediate signal $v(t)$ can be derived explicitly from Equation (2.51) by putting $T_1 = 0$ which gives

$$v(t) = h(t_2 - t) \tag{2.54}$$

2.2.3 Linear Structure Identification

A linear model can be identified even if there is no prior knowledge of the system being linear or non-linear in the operating range. Once the intermediate signal $v(t)$ is calculated using the proposed method, the fitted polynomial curve between $v(t)$ and $y(t)$ will automatically tell whether

the system is linear or non-linear. If it is a linear system, the coefficient of the first-degree term i.e, the slope will give the static gain of the system. Without the nonlinearity, this identification scheme of linear models is similar to the previous works of Bajarangbali et al. [44]. However, the expressions of unknown parameters are derived with a more restricted assumptions therefore, less prior knowledge are required. Also, Bajarangbali et al. [44] derived three eqution which are needed to be solved simultaneously for the two time constants and the gain. However, in the proposed work, two equations are solved simultaneously for finding the time constants and the gain is derived from the slope of $v(t)$ and $y(t)$'s graph.

2.3 Mitigation of Measurement Noise

Measurement noise causes relay chattering thereby, as suggested by Åström and Hägglund [14], a relay with hysteresis is used in the identification setup of Figure 2.2. In the mentioned procedure, it can be observed that the correct measurement of switching time t_0 is crucial for all the calculations. The measurement of t_0 is done according to the method mentioned in [43], according to which it is measured as the instant when an abrupt change in 2^{nd} order derivative of the output occurs after the actual relay switching at $t_{\varepsilon p}$. Therefore, a smooth output is required for the derivative to be calculated which motivated the use of a smoothing spline curve fitting technique implemented using [45]. The hysteresis width safe for alleviating the relay chattering is twice greater than the standard deviation (σ) of the noise i.e., $\varepsilon \geq 2\sigma$ [46]. When the standard deviation of the noise is not known, the hysteresis width should be changed heuristically.

A spline of order k is a piece-wise polynomial with degree k. The spline is continuous with continuous derivatives of orders $1, \ldots k-1$, at both of its ends [47]. For $i = \{1, j\}$, given a set of data points (t_i, y_i), which is to be modeled by the relation $y_i = z(t_i)$, the smoothing spline aims at minimizing

$$S(w) = \sum_{i=1}^{j} W_i (y_i - z(t_i))^2 + (1-\lambda) \int_{t_1}^{t_j} \ddot{z}(t)^2 dt \tag{2.55}$$

where,

- W_i are the specified weights.

- z is the spline function.
- λ is the smoothing parameter. $\lambda = 0$ gives a least-squares straight-line fit, while $\lambda = 1$ gives a cubic spline fit.

2.4 Simulation Study

The developed identification method is tested in this section using simulation examples. Various probable cases of the linear subsystem have been considered. While most of the examples are taken from the literature, some examples are novel due to the lack of proper literature on them. Identified systems are validated by calculating ISE using white Gaussian noise as input. The motivation to use white Gaussian noise is derived from Bose [48]'s extended work on Wiener [49]'s original work which says that for any general nonlinear system, a white Gaussian noise is the best probe for it can approximate any given time function arbitrarily closely over any finite time interval. The simulation gives an insight into how the procedure should be implemented. Limitations, drawbacks, and various analyses have also been made in each example.

Eaxmple 1: FOPDT stable

The Wiener model previously studied by Lee et al. [1] is considered for simulation which is given as

$$\textit{Linear subsystem:} \quad G(s) = \frac{e^{-s}}{(5s+1)}$$

$$\textit{Static nonlinearity:} \quad y = 2(1 - e^{-0.693v})$$

With a relay setting of $h = 1$ and $\varepsilon = 0.2$, the time constant is calculated as $T_1 = 5.01$ using (2.41). For a first-order system, the delay measurement does not require finding the derivative as $t_0 = t_1$ in Figure 2.3. Thus, the delay is measured directly from the limit cycle plot as $\theta = t_{\varepsilon p} - t_0 = 1.0002$. Lee et al. [1] also estimated the liner subsystem quite accurately with $T_1 = 5.02$ and $\theta = 1$, however their estimated non-linearity is not as accurate as the proposed method as

shown in Figure 2.4. The polynomial non-linearity is calculated using (2.53) as $y = -0.0292v^4 + 0.1112v^3 - 0.4813v^2 + 1.3887v$ whereas by Lee et al. [1] it is calculated as $y = -0.462v^2 + 1.385v$. The results are tabulated in Table 2.1.

	Linear subsystem: $G(s)$	%error in T_1	Static non-linearity: $f(v)$
Original model	$\frac{e^{-s}}{(5s+1)}$		$2(1-e^{-0.693v}) \simeq -0.0003v^6 + 0.0027v^5 - 0.0192v^4 + 0.1109v^3 - 0.4802v^2 + 1.3860v$
By Lee et al. [1]	$\frac{e^{-s}}{(5.02s+1)}$	0.4%	$-0.462v^2 + 1.385v$
By proposed method	$\frac{e^{-1.0002s}}{(5.01s+1)}$	0.2%	$-0.0292v^4 + 0.1112v^3 - 0.4813v^2 + 1.3887v$

Table 2.1: System identification results of Example 1

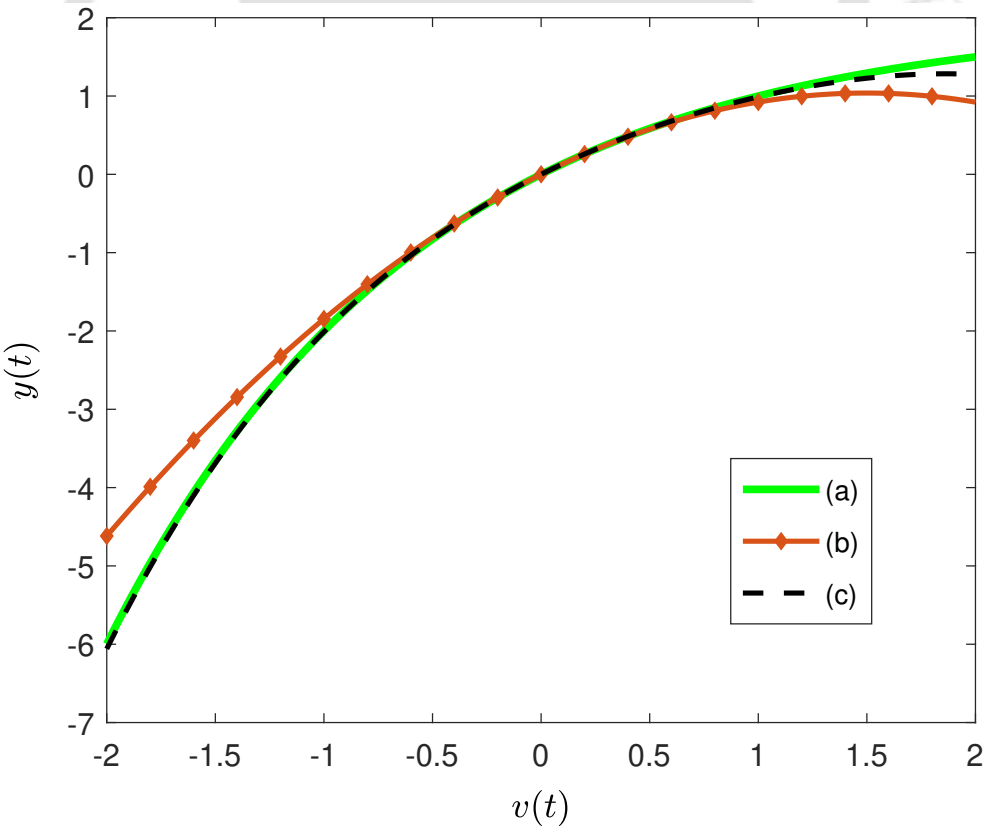

Figure 2.4: Non-linearity of Example 1 : (a) actual nonlinearity, (b) nonlinearity estimated by Lee et al. [1], (c) nonlinearity estimated by the proposed method.

Example 2: FOPDT unstable

An unstable linear FOPDT model studied by Majhi and Atherton [50] has been considered which is given as

$$G(s) = \frac{e^{-0.4s}}{(s-1)} = \frac{-e^{-0.4s}}{(-s+1)}$$

	Linear subsystem: $G(s)$	%error in T_1
Original model	$\frac{e^{-0.4s}}{(s-1)}$	
By Majhi and Atherton [50]	$\frac{-e^{-0.400034s}}{(-1.00013s+1)}$	0.013
By proposed method	$\frac{-1e^{-0.3998s}}{(-1s+1)}$	0

Table 2.2: System identification results of Example 2

A relay setting of $h = 1$ and $\varepsilon = 0.2$ gave a stable limit cycle as shown in Figure 2.5. The measurements are done as $t_0 = 0.582185$ and $t_2 = 2.147355$ which are when used in (2.41) give the exact value of time constant as $T_1 = -1.0$. The delay is measured as $\theta = 0.3998$. For nonlinear static gain, various points of $v(t)$ for time range $t_0 \leqslant t \leqslant t_{01}$ is calculated using (2.53). The calculated points of $v(t)$ is then used to fit a polynomial with $y(t)$ which gave $y = -0.0009v^3 - 0.9999v \simeq -v$, this demonstrate how the prior knowledge of the stability of the system is not required as long as a sustained limit cycle can be induced by the relay. Also, it can be observed that the polynomial is a straight line whose slope is the static gain of the system i.e., prior information about the nonlinearity is also not required. However, an important drawback of the proposed method is that it does not deal with structure detection, i.e., whether the system is Wiener or Hammerstein. A nice work on structure detection using relay feedback has been done by Huang et al. [7]. Majhi and Atherton [50] also estimated the system very close to the real values. The results are presented in Table 2.2.

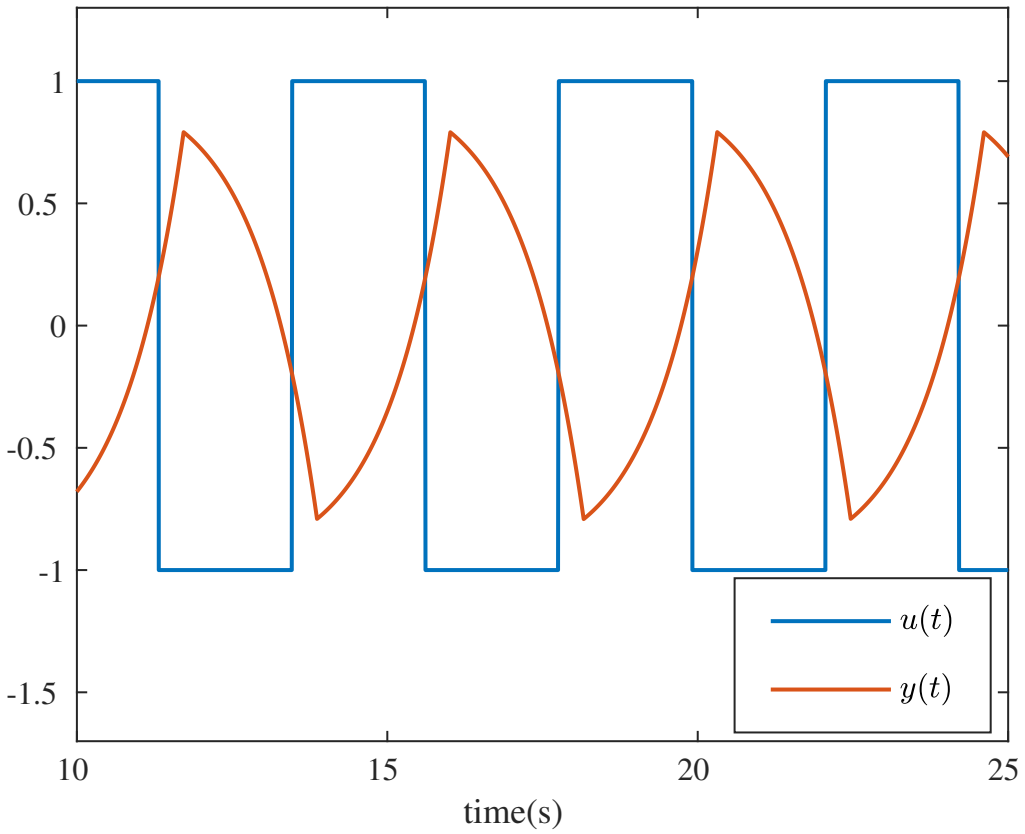

Figure 2.5: Limit cycle oscillation of the unstable FOPDT system in Example 2

Example 3: SOPDT overdamped

A SOPDT model with distinct real roots previously studied by Huang et al. [2] has been considered which is given as

$$\textit{Linear subsystem:} \quad G(s) = \frac{e^{-s}}{(5s+1)(s+1)}$$

$$\textit{Static nonlinearity:} \quad y = 2(1-e^{-0.693v})$$

The relay is set at $h = 3$ and $\varepsilon = 0.2$ for the above system, then using the required time measurements in solving (2.22) and (2.27) gave the values of the two time constants as $T_1 = 4.924$ and $T_2 = 1.007$. The delay is measured as $\theta = 1.0003$. Using (2.43) and (2.44), the intermediate signal for time range $t_0 \leqslant t \leqslant t_{01}$ is calculated which is then used to find the static non-linearity as $y = 0.0031v^5 - 0.0170v^4 + 0.11v^3 - 0.4808v^2 + 1.3865v$. In the work of Huang et al. [2], the

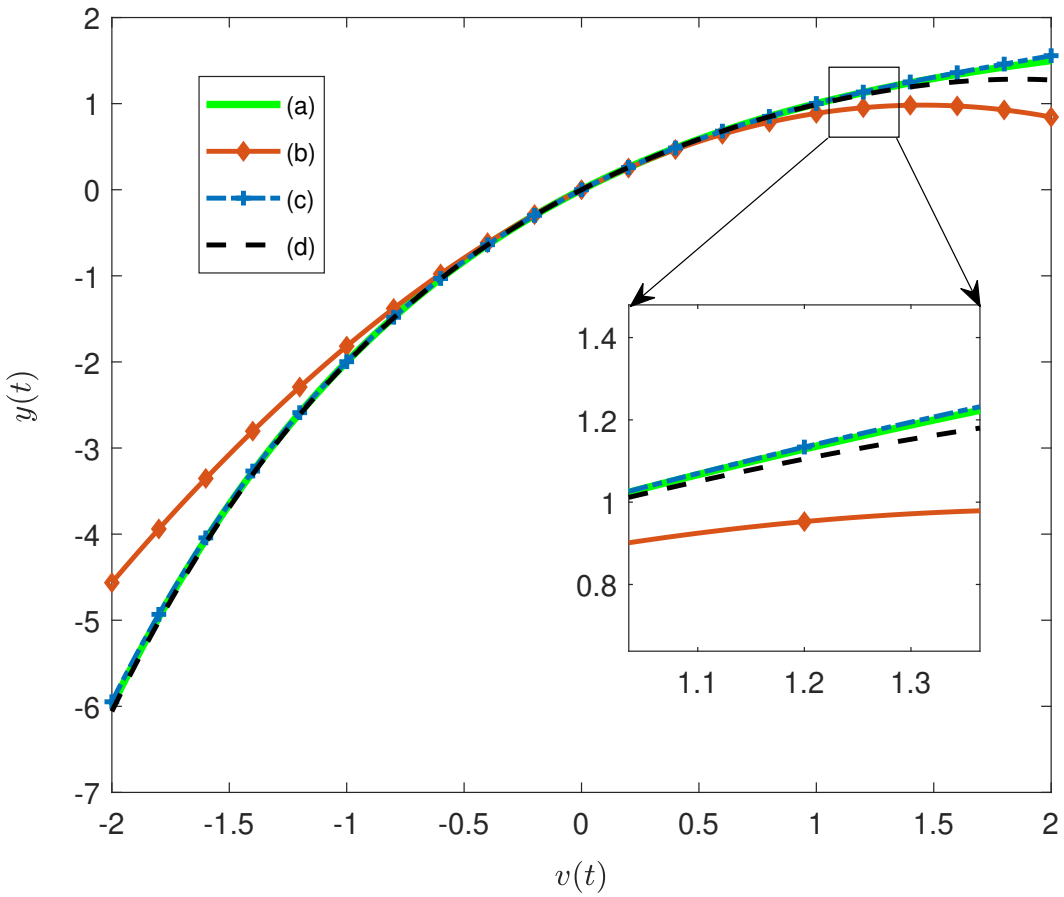

Figure 2.6: Non-linearity of Example 3: (a) actual nonlinearity, (b) nonlinearity estimated by Huang et al. [2], (c) nonlinearity estimated in Example 3, (d) nonlinearity estimated in Example 1

linear system parameters are found as $T_1 = 4.872$, $T_2 = 0.925$ and $\theta = 1.160$ which are not as accurate as the ones calculated using the presented method. From Figure 2.6, it can also be seen that the estimated non-linearity is more accurate than the one estimated by Huang et al. [2], i.e., $y = -0.465v^2 + 1.352v$. Also, the present method is simple and less complex compared to that of Huang et al. [2] which required a two stage relay test and an iterative optimization. The identified model has been compared to Huang et al. [2] using the performance index ISE by giving a zero mean Gaussian white noise input for $100s$ having variance 0.5, the results are tabulated in Table 2.3.

The static non-linearity in this example is the same as the one in Example 1, however, it can be seen in Figure 2.6 that the one estimated in the present example is more accurate than the one estimated previously. The reason for the accuracy is the relay height of $h = 3$, which is higher

	Linear subsystem: $G(s)$	Static non-linearity: $f(v)$	ISE
Original model	$\frac{e^{-s}}{(5s+1)(s+1)}$	$2(1-e^{-0.693v}) \simeq -0.0003v^6 + 0.0027v^5 - 0.0192v^4 + 0.1109v^3 - 0.4802v^2 + 1.3860v$	
Huang et al. [2]	$\frac{e^{-1.160s}}{(4.872s+1)(0.925s+1)}$	$-0.465v^2 + 1.352v$	202.3×10^{-5}
Proposed method	$\frac{e^{-1.0003s}}{(4.924s+1)(1.007s+1)}$	$0.0031v^5 - 0.0170v^4 + 0.11v^3 - 0.4808v^2 + 1.3865v$	2.335×10^{-5}

Table 2.3: System identification results of Example 3

in this example than the previous one at $h = 1$. As the non-linearity is considered monotonic, therefore a higher relay height will give a higher value of $y(t)$ i.e., a longer interval of $t_0 \leqslant t \leqslant t_{01}$ and hence a longer range on the $v \sim y$ curve to find the non-linearity. Thereby, to estimate the nonlinearity for a larger range, only the relay height needs to be increased, there is no need for more than one relay test.

Example 4: SOPDT critically damped

A simulation example for repeated roots has been considered for a linear system which is given as

$$G(s) = \frac{5e^{-s}}{(3s+1)^2}$$

With a relay setting of $h = 1$, $\varepsilon = 0.2$, various measurements on the limit cycles are done. Using (2.38), the time constant is found as $T_1 = 3.0003$ and the time delay is measured as $\theta = 1.0015$. For the static gain, various points of $v(t)$ in time range $t_0 \leqslant t \leqslant t_{01}$ is calculated using (2.48). The calculated points of $v(t)$ is then used to fit a polynomial with $y(t)$ which gave $y = 0.0004v^4 - 0.0003v^2 + 5.0031v \simeq 5.0031v$ i.e, the linear static gain is the slope, 5.0031.

Example 5: integrating SOPDT

A linear integrating SOPDT model previously studied by Majhi [43] has been considered which is given as

$$G(s) = \frac{e^{-1.5s}}{s(5s+1)}$$

Various measurements are done on the limit cycle with the relay set at $h = 1$ and $\varepsilon = 0.2$. Considering a high initial value of $T_2 = 1000$ to solve (2.22) and (2.27) gives $T_1 = 5$ whereas $T_2 \simeq 1000$. The delay is measured as $\theta = 1.503$. The initial state $x(0)$ is calculated using (2.52) as 3.4137. Then, a few points of $v(t)$ for the time range $t_0 \leqslant t \leqslant t_{01}$ is calculated using (2.51) which gave $v = [-1.3120, 0.1963, 1.4088, 2.1731, 2.2577, 1.3118]$, the corresponding values of $y(t)$ are measured as $y = [-1.3120, 0.1963, 1.4088, 2.1730,$
$2.2575, 1.3120]$. When the calculated points are used to fit a polynomial, it gives nearly $y = v$ hence, the static linear gain is 1. Majhi [43] estimated the system as $G(s) = \frac{e^{-1.625s}}{s(5.049s+1)}$. The simulation results are listed in Table 2.4. The error in measurement of the time delay has not been compared as both the work utilises the same technique. The difference in delay measurement is attributed to a higher and hence upgraded version of MATLAB being used in this work (MATLAB 2017).

	Linear System: $G(s)$	% error in T_1
Original model	$\frac{e^{-1.5s}}{s(5s+1)}$	
By Majhi [43]	$\frac{e^{-1.625s}}{s(5.049s+1)}$	0.98
By proposed method	$\frac{e^{-1.503s}}{s(5s+1)}$	0

Table 2.4: System identification results of Example 5

Example 6: SOPDT underdamped

A SOPDT Wiener model with complex conjugate roots has been considered here which is given as

$$\textit{Linear subsystem:} \quad G(s) = \frac{e^{-s}}{(s^2+2s+5)}$$

$$\textit{Static nonlinearity:} \quad y = tan^{-1}v$$

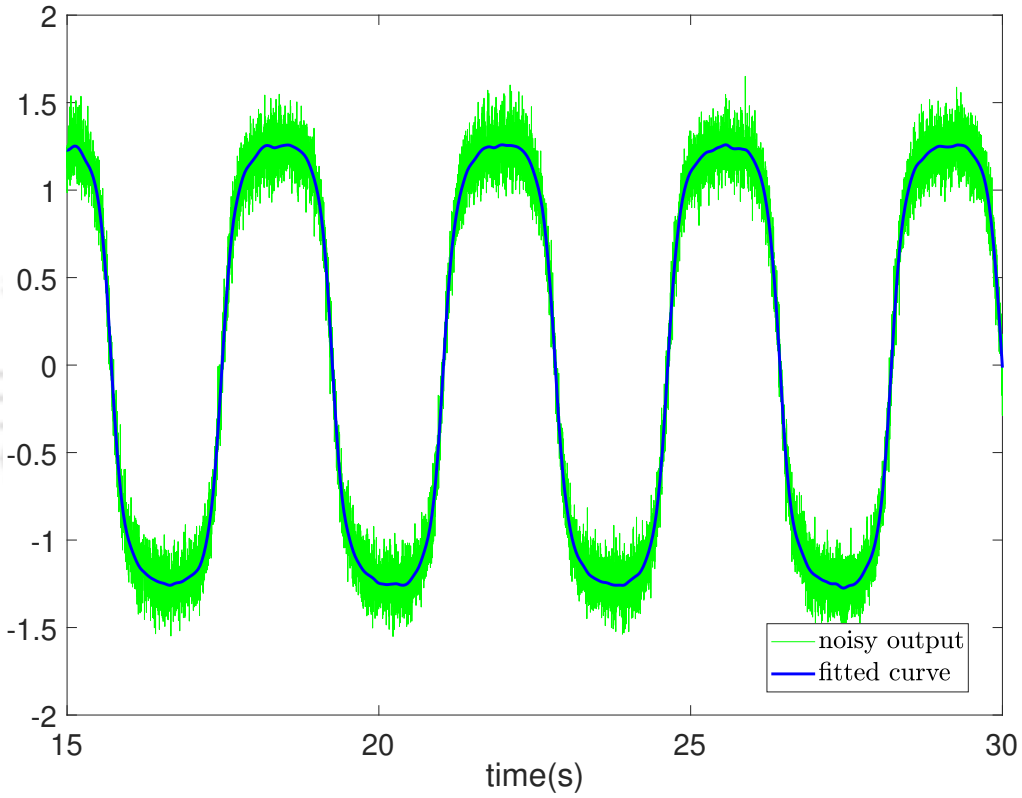

Figure 2.7: Noisy and the retrieved output signal of Example 6

The test is carried out with a relay setting of $h = 10$ and $\varepsilon = 1$ to estimate the system for a larger range of operation as the non-linearity $tan^{-1}v$ looks nearly linear around the origin. The delay is found as $\theta = 1.0005$. The linear system parameters are calculated using (2.29) and (2.30) as $a = 0.992$, $b = 1.9982$. The non-linearity is estimated using (2.46) and (2.47) as $y = -0.0021v^7 + 0.0246v^5 - 0.0020v^4 - 0.1598v^3 - 0.0026v^2 + 0.9157v$. The system is studied under 20dB measurement noise considered to be zero-mean Gaussian. The presumed value of

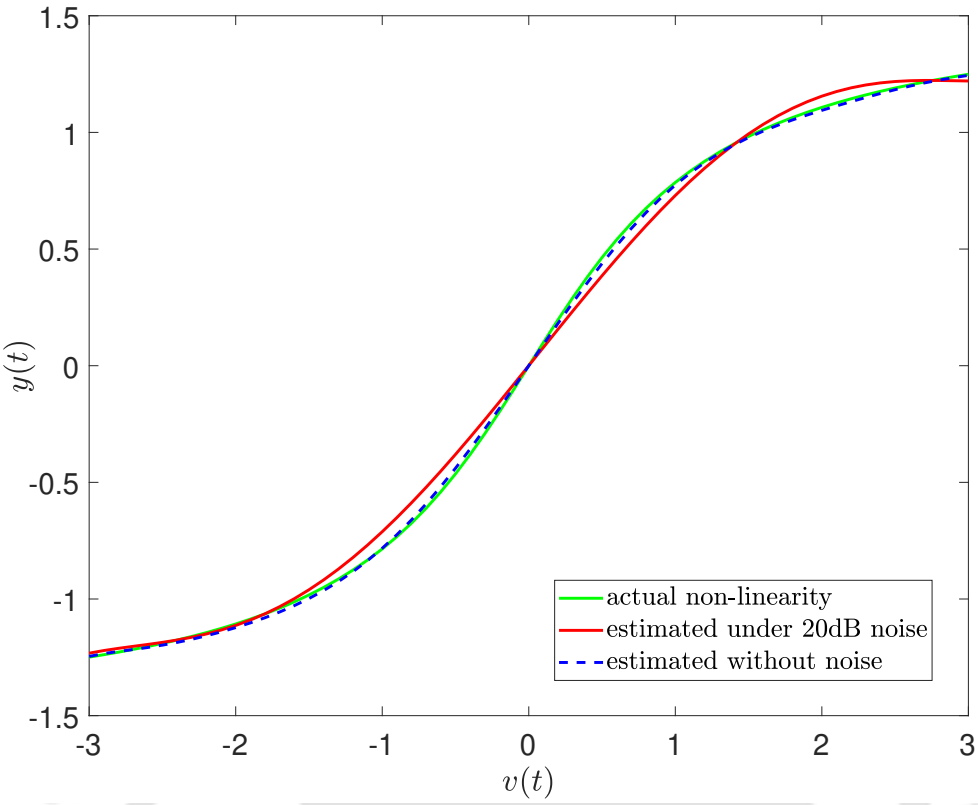

Figure 2.8: Non-linearity of Example 6

	Linear subsystem: $G(s)$	Static non-linearity: $f(v)$	ISE
Original model	$\frac{e^{-s}}{(s^2+2s+5)}$	$tan^{-1}v = -0.143v^7 + 0.2v^5 - 0.333v^3 - 0.0026v^2 + v$	
Without noise	$\frac{e^{-1.0005s}}{(s^2+1.984s+4.977)}$	$-0.0021v^7 + 0.0246v^5 - 0.0020v^4 - 0.1598v^3 - 0.0026v^2 + 0.9157v$	1.066×10^{-3}
With 20dB noise	$\frac{e^{-1.0268s}}{(s^2+1.774s+5.2)}$	$0.0024v^5 - 0.0012v^4 - 0.0633v^3 + 0.0099v^2 + 0.7815v$	6.45×10^{-3}

Table 2.5: System identification results of Example 6

relay width $\varepsilon = 1$ eliminated the chattering in this case, however, it is needed to be adjusted otherwise. The output is extracted from the noisy signal using curve fitting through spline interpolation which is plotted in Figure 2.7. The delay is measured as $\theta = 1.0268$ and the linear parameters under noise are calculated as $a = 0.887$, $b = 2.1$. The non-linearity is calculated as

$y = 0.0024v^5 - 0.0012v^4 - 0.0633v^3 + 0.0099v^2 + 0.7815v$ and is plotted in Figure 2.8 which shows a fair approximation, however, this example doesn't guarantee any consistency in the accuracy of estimation under measurement noise for all Wiener systems. A proper analysis under noise requires the sensitivity and convergence analysis of the entire identification procedure which is beyond the scope of the present work but could be taken up as interesting future work. However, an insight into the convergence of the proposed procedure is given in Sec. 2.5.2. The identification result is tabulated in Table 2.5 where the performance index ISE is calculated by giving a Gaussian noise input for 100s having variance 0.5 and zero mean.

Example 7: SOPDT unstable

A linear SOPDT unstable system previously studied by Ramakrishnan and Chidambaram [51] has been considered here which is given as

$$G(s) = \frac{e^{-0.5s}}{(2s-1)(0.5s+1)}$$

Rearranging the terms of $G(s)$ to bring it in the form of Equation (2.5) gives,

$$G(s) = \frac{-e^{-0.5s}}{(-2s+1)(0.5s+1)}$$

Therefore, the system can be seen as a model with time constants $T_1 = -2$, $T_2 = 0.5$ and linear static gain (-1). A relay setting of $h = 1$ and $\varepsilon = 0.2$ gives various time instances as $t_0 = 0.86538$, $t_1 = 0.86538$, $t_2 = 6.5269$. Utilizing these time instances in Equations (2.22), (2.27) and solving gives the values $T_1 = -2.0016$, $T_2 = 0.5005$. The delay is measured as $\theta = 0.5007$. For the static gain, the value of the intermediate signal $v(t)$ for time range $t_0 \leqslant t \leqslant t_{01}$ is obtained using Equations (2.43), (2.44). The calculated $v(t)$ and the measured $y(t)$ in the interval $t_0 \leqslant t \leqslant t_{01}$ are then used to fit the polynomial which gave $y = -0.0006v^3 - 0.989v \simeq -0.989v$. Therefore, the obtained model is

$$\frac{(-0.989)e^{-0.5007s}}{(-2.0016s+1)(0.5005s+1)}$$

which is when rearranged gives the ultimate identified model as

$$\frac{0.989e^{-0.5007s}}{(2.0016s-1)(0.5005s+1)}$$

The identified parameters are compared to that of Ramakrishnan and Chidambaram [51] in Table 2.6.

	Linear System: $G(s)$	%error in T_1	%error in T_2	%error in θ
Original model	$\frac{e^{-0.5s}}{(2s-1)(0.5s+1)}$			
By Ramakrishnan and Chidambaram [51]	$\frac{e^{-0.52s}}{(1.9999s-1)(0.4837s+1)}$	0.005	3.26	4
By proposed method	$\frac{0.989e^{-0.5007s}}{(2.0016s-1)(0.5005s+1)}$	0.08	0.1	0.14

Table 2.6: System identification results of Example 7

Example 8: integrator

A Wiener model with an integrator is taken as an example with the following dynamics

$$\textit{Linear subsystem:} \quad G(s) = \frac{e^{-s}}{5s}$$

$$\textit{Static nonlinearity:} \quad y = v^3$$

with a relay setting of $h = 1$ and $\varepsilon = 0.5$, the delay is measured as $\theta = 1.001$. The various time instances are measured as $t_1 = 4.96$ and $t_2 = 9.9$. Now, considering it as a FOPDT system and solving equation (2.41) give $T_1 = 1225$ which means $\frac{1}{T_1} \to 0$ hence, it is an integrator. Now, the linear subsystem also has a static gain in $G(s)$ which is $\frac{1}{5} = 0.2$ and can be identified along with the static nonlinearity. Using equation (2.54), the equation for the intermediate signal $v(t)$ in time range $t_0 \leqslant t \leqslant t_{01}$ is calculated as $v = (9.9 - t)$. Now, the value of calculated $v(t)$ and measured $y(t)$ in the time interval $t_0 \leqslant t \leqslant t_{01}$ are used to find the nonlinearity that is calculated as $y = 0.18v^3 + 0.001v$ which is a close approximation to the real static nonlinearity $y = \frac{1}{5}v^3 = 0.2v^3$.

2.5 Discussion

2.5.1 Online Identification and Complexity

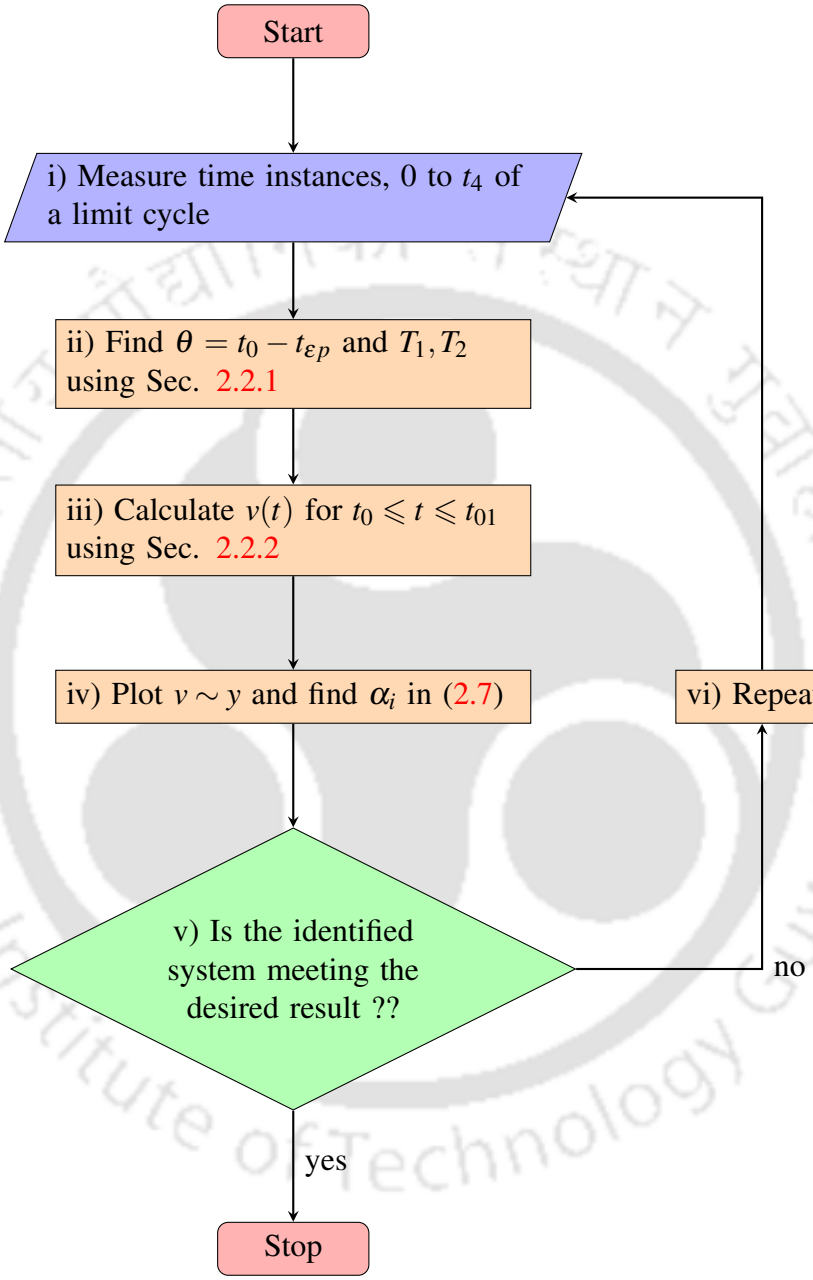

Figure 2.9: Flowchart explaining the steps involved in the Wiener model identification process

The proposed method is straightforward and easy for offline identification, the problem of complexity will arise if considered for an online application. A flowchart describing the entire identification process is shown in Figure 2.9. It consists of only 5 stages. The measurement stage

(i) will not take time, it is the non-linear equation solving stage (ii) which will take a few seconds. Thereafter, the calculation of $v(t)$ and finding the polynomial are also not time-consuming. Therefore, the complexity in identification depends on the method used to solve the non-linear equations in Section 3. However, the FOPDT, linear system, repeated roots case requires only one equation which can be solved efficiently using any numerical or graphical techniques. It is the SOPDT real and complex roots case which is comparatively complex. There are various methods in the literature to find good initial estimates for Wiener models, those can be referred to while using numerical methods. While relay feedback for Wiener system modeling looks easy, it is to be noted that for identification of systems whose parameters vary continuously, it is not very efficient. For such systems, methods that directly use only the input and output without the need for a special set-up/input, are efficient. Having said that, it should also be noted that in system modeling where relay itself is a controller, relay feedback identification may prove more effective. Also, it is efficient for tuning PID like controllers whose parameters don't require continuous tuning.

2.5.2 Existence of Solution and Convergence

The parameters identified in this work are the time constants, delay, and the coefficients of the polynomial nonlinearity. The delay is measured independently using the procedure mentioned in Majhi [43] which is an experimental procedure. According to the method in Majhi [43], it is measured as the instant an abrupt change in 2^{nd} order derivative of the output occurs after the actual relay switching at $t_{\varepsilon p}$. Therefore, the accuracy of measuring the delay depends on the accuracy in calculating the derivative of the output and hence t_0. This is the only crucial use of derivative in the procedure. Looking at all the equations to find the time constants and the nonlinearity (Sec. 2.2.1 and Sec. 2.2.2), it can be observed that no output derivatives are utilized. It is a known fact that calculating derivative under noise is difficult, therefore, a good noise mitigation procedure should be adapted. In the simulation example $2(iv)$, the spline interpolation curve fitting technique worked satisfactorily however, it doesn't guarantee the accuracy in measuring t_0. However, in the FOPDT systems $t_0 = t_1$ i.e., t_0 is the peak of the output hence, no derivatives are required.

For all other cases, the uncertainty in measuring t_0 will affect the uncertainty in calculating the time constants.

To check the existence of solution, let us consider the equation (2.41) to find the time constant of the FOPDT system. For simplicity of calculation, putting $\frac{1}{T_1} = a$ by setting $b = 0$ from (2.28) and rearranging (2.41)

$$F(a) = e^{-at_0}(1 + e^{at_2}) - 2 = 0 \tag{2.56}$$

It is evident that $a = 0$ is a solution to the equation (2.56). Therefore, the curve $F(a)$ will pass through the origin. Now, differentiating $F(a)$ with respect to a

$$\dot{F}(a) = 0 \quad \Rightarrow \quad a^* = \frac{1}{t_2} \ln \left| \frac{t_0}{t_2 - t_0} \right| \tag{2.57}$$

Therefore, a^* is the only critical point of $F(a)$. Now, evaluating the second derivative of $F(a)$ gives

$$\ddot{F}(a) = (t - t_0)^2 e^{a(t_2 - t_0)} + t_0^2 e^{-at_0} \tag{2.58}$$

From (2.58), it can be observed that, irrespective of a, $\ddot{F}(a)$ will always be greater than zero. Therefore, the critical point a^* is the global minimum. As $F(a)$ passes through the origin and has only one global minimum therefore, the minimum peak is either below the $F(a) = 0$ line or touching the origin. If the minimum peak is below the $F(a) = 0$ line, it will cross it again at some value of a which is the unique solution of (2.41). If the minimum peak is touching the origin then $a = 0$ is the only solution that defines a system with a very high time constant as $T_1 = \frac{1}{a}$. The graph plot in Figure 2.10 can be referred to for the said analysis. The graph shows the plot for both stable and unstable systems, the plot will cross the negative real axis for an unstable system. The rate of convergence, however, will depend on the procedure used to solve the non-linear equations for finding the time constants. In this work, the equations are solved in MATLAB by plotting graphs for better accuracy. However, numerical methods are suggested for online applications and application that requires less calculation time.

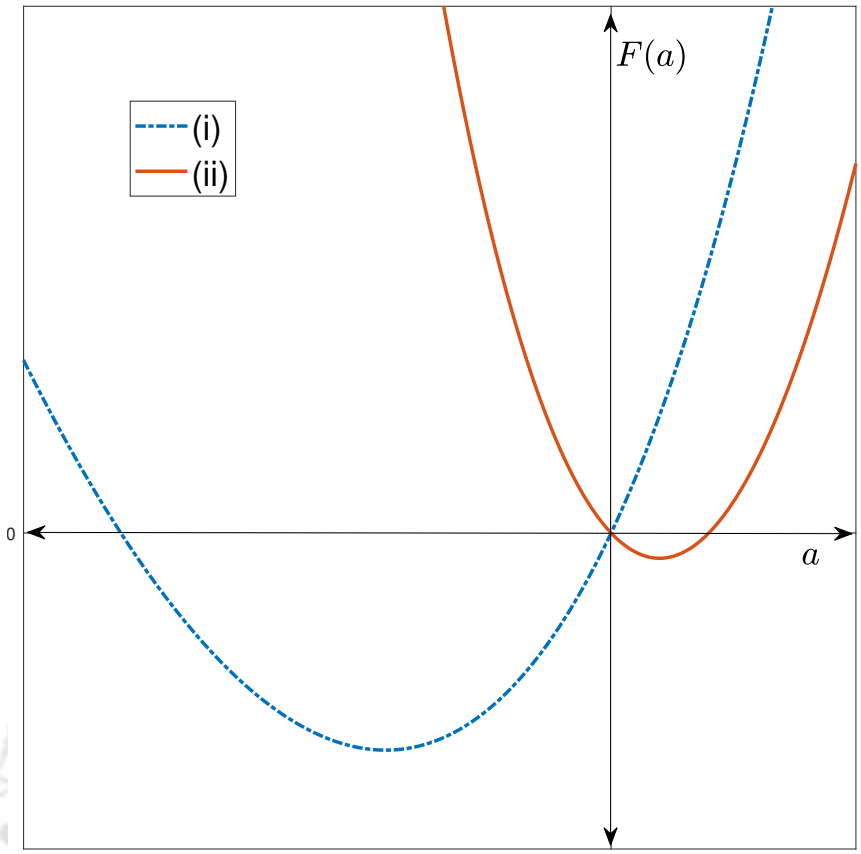

Figure 2.10: Graph of $F(a)$ in (2.53)- (i) of an unstable system. (ii) of a stable system.

Similarly, the existence and uniqueness of all the equations to find T_1 and T_2 can be proved using geometrical analysis. However, analysis for non-linear equations involving two variables (like the set of equations in real roots case and complex conjugate roots case, in Sections 2.2.1 and 2.2.2) requires more mathematical background which has scope for future work.

2.5.3 A discussion on the static nonlinearity

In Section 2.1, it is already mentioned that the static nonlinearity is assumed to be passive and monotonic. In the subsection 2.2.1, it can be noted that finding the peak of the intermediate signal $v(t)$ is essential in the calculation of the time constants. The intermidiate signal $v(t)$ is the output of the linear subsystem whose input is a constant relay height. Therefore, the shape of $v(t)$ will be sinusoidal type (SOPDT and higher order) or triangular type (FOPDT) i.e., with only one peak. The output $y(t)$ is a static function of $v(t)$. The signal $v(t)$ is not measurable therefore, we depend on $y(t)$ for finding the peak of $v(t)$. If the the function $f(v)$ i.e., the static nonlinearity is not

monotonic, it will be difficult to determine the peak of $v(t)$ via $y(t)$. This is why monotonicity is necessary. An example of a nonmonotonic static nonlinearity is the sine function operating beyond $\frac{\pi}{2}$, a input-output graph of which is given in Figure 2.11. It can be seen that it's difficult to find the peak of $v(t)$ looking at $y(t)$ given the nonlinearity is not known. However, in the Hammerstein model identification monotonicity is not a necessacity which will be studied in the next chapter. The monotonicity restriction can be relaxed in Wiener model case if the peak can be found by some other means. Note that the identification procedure in this work is for systems with small time delays as mentioned in Section 2.2 while describing the time instant t_0. A system with large time delay can have ripples even with a monotonic nonlinearity.

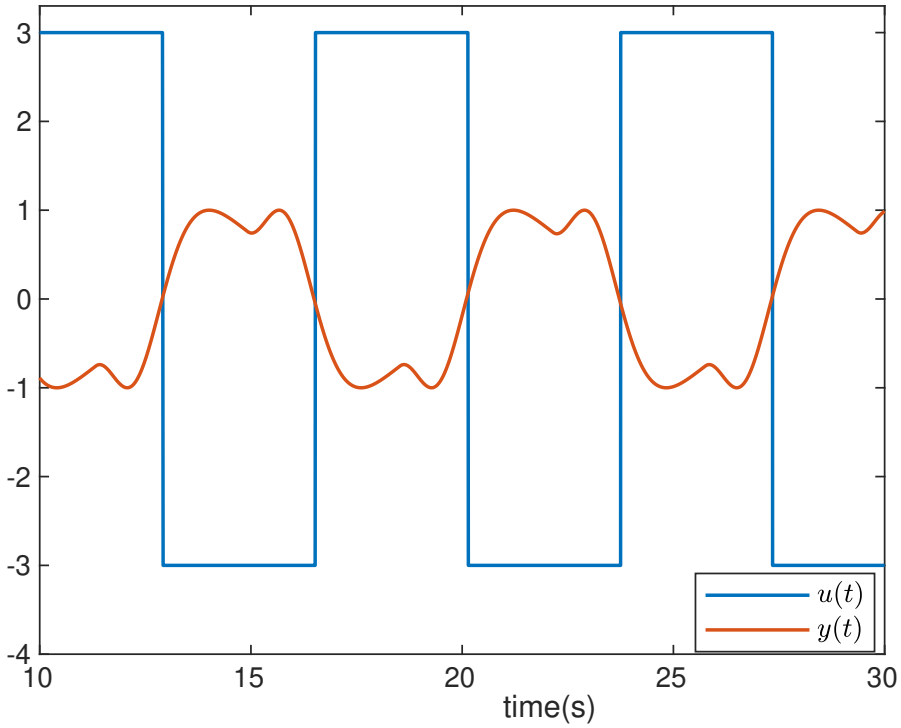

Figure 2.11: Output ripples of a nonmonotonic static nonlinearity.

2.6 Summary

The identification procedure for the Wiener model using relay feedback has been developed and tested in simulation. The procedure is found to be simple, non-iterative, involves feedback, requires less time, thus can be suitable for online identification. The identification method applies to

unstable systems as well. Various probable cases of linear subsystems are discussed, thus widening the application of relay in Wiener system modeling. A discussion on online identification and the existence of a solution has been made. This served as a motivation to further apply relay feedback for Hammerstein modeling.

Chapter 3

Hammerstein Model Identification

Wiener model is developed from the Volterra series, similarly, the Hammerstein model is derived from a class of operator called the Urysohn operator. However, unlike the Wiener model, there is a lack of proper literature on the development of the Hammerstein model from system theory's point of view. Recent work by Poluektov and Polar [52] has tried to fill the gap. A summary from their work is presented here to describe the derivation of the Hammerstein model. We start with the definition of a continuous Urysohn integral operator which transform input $u(t)$ to output $y(t)$ as follows

$$y(t) = \int_0^\infty U(\tau, u(t-\tau))d\tau \tag{3.1}$$

where, $U(\tau, u)$ is known as the kernel of the continuous Urysohn operator. In (3.1), the term $t-\tau$ signifies the causal dependence of output on the input. When it is possible to decompose the Urysohn kernel $U(\tau, u)$, into a product of two different functions $h(\tau)$ and $H(u)$, the Urysohn operator becomes the Hammerstein operator which is given as

$$y(t) = \int_0^\infty h(\tau)H(u(t-\tau))d\tau \tag{3.2}$$

The equation (3.2) represents a system having impulse response $h(\tau)$ with an input which is a function of the original input $u(t)$. When the function $H(u)$ is nonlinear and static, physically (3.2) represents a system with a static nonlinearity followed by a linear subsystem i.e., a Hammerstein model. When the function $H(u)$ is static linear, (3.2) turns into the well known convolution

integral given in (2.1) which represents a linear system. Poluektov and Polar [52] has also shown that Urysohn operator is a special case of the Volterra operator which means the Wiener and Hammerstein models are related.

Narendra and Gallman [53] were first to introduce this model to design a nonlinear system with no-memory input nonlinearities. Narendra and Gallman [53] used a LSE based iterative method for identifying a discrete-time Hammerstein model. Chang and Luus [54] developed a non-iterative LSE based method which includes converting the model into a multi-input single-output (MISO) models in intermediate steps. Afterward, significant works utilizing LSE and Gaussian white input are done by Haist et al. [55], Hsia [56]. Various methods based on correlation analysis and kernel regression estimates are developed by Billings and Fakhouri [57], Stoica and Söderstrom [58], Greblicki and Pawlak [59], Greblicki and Pawlak [60], Krzyzak [61]. The LSE based estimation, correlation analysis, etc are analytic methods that require Gaussian white noise or random binary sequence kinds of stochastic inputs which are easier to implement in algorithms but difficult to implement practically. Therefore, many application oriented methods are developed to identify Hammerstein models which utilizes deterministic signals like an impulse, step, square, sine, etc. Relay feedback is one such method.

As stated in the previous chapter, Luyben and Eskinat [15] were the first to use relay feedback for the identification of the Wiener and Hammerstein models. Their method relied mostly on the experimental solution instead of theoretical analysis. After Luyben and Eskinat [15], Huang et al. [7] proposed an interesting work on structure detection of BONL models. To identify a Hammerstein model using relay feedback, Lee et al. [1] used two separate decoupled methods. The nonlinearity is estimated using an optimization procedure that targets to get a symmetric output. The transfer function of the linear part is identified by making the output behave like that of an integrator-plus-dead-time (IPDT) process. Even though the subsystem identifications are completely decoupled, it is elaborate and hence time-consuming. However, it is convenient for online identification as it doesn't require any change in the identification setup. Park et al. [62] also proposed a decoupled method for the identification of the two subsystems in a Hammerstein model. The linear subsystem is identified using frequency response data of the relay feedback

test, the nonlinearity is identified using a separate triangular input test which further required an open loop activation followed by a closed loop test. It is evident that Park et al. [62]'s method is elaborate, time-consuming and the requirement of open loop activation makes it difficult for online identification. Jeng et al. [37] proposed a method where the nonlinearity estimation follows a lemma that requires the linear subsystem to have an integrator. In the absence of an integrator, an external integrator is added in the feedback loop so that the lemma can be applied. Hence, Jeng et al. [37]'s method is complex for online identification, also it requires tedious resetting of relay too many times. Mehta and Majhi [38] proposed another relay feedback approach to identify Wiener and Hammerstein models which are limited only to second-order critically damped linear subsystems. Juric et al. [63] proposed a frequency response based relay feedback method that requires more experimental run and makes it difficult for online identification.

Similar to the drawbacks noted earlier in case of Wiener model identification using relay feedback, the above mentioned methods in case of Hammerstein model are also limited to mostly FOPDT and critically damped SOPDT models. Although, Jeng et al. [37], Park et al. [62] and Juric et al. [63] did consider more general class of SOPDT models, there are still drawbacks mentioned earlier. The proposed method has developed a simpler identification procedure with wider class of linear subsystem including unstable ones which has not been studied earlier. The procedure also requires relatively less prior knowledge. A general nth order critically damped linear subsystem has also been considered which is first of its kind.

The work in this chapter has been published in [47] and [64].

3.1 Problem Formulation

The setup used for identification is the same as the one in case of Wiener model identification and is shown in Figure 3.1. Similar to the Wiener model, here also a symmetrical relay with hysteresis is used, the detail characteristics of the relay can be found in the previous chapter in Sec. 2.1. The Hammerstein model consist of a static nonlinearity followed by a linear subsystem where $u(t)$, $v(t)$ and $y(t)$ are input signal, immeasurable intermediate signal and the output signal respectively

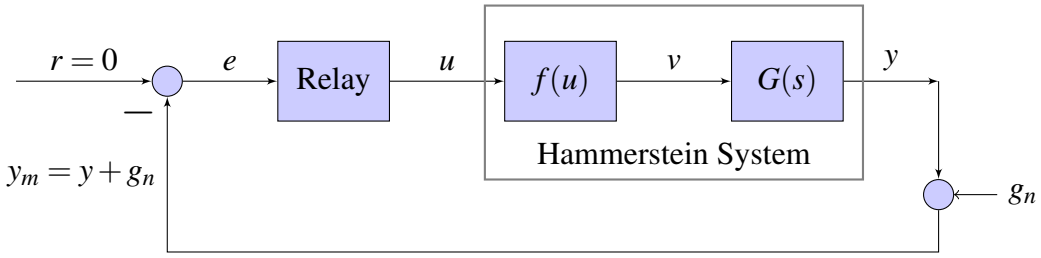

Figure 3.1: Setup used for the identification of Hammerstein model

in Figure 3.1. Sec. 2.1 is recommended for more detail description of the identification setup. A white Gaussian noise input $g_n(t)$ is added at the output to study the effect of measurement noise. The transfer function of the linear subsystem is considered same as the Wiener model case which is

$$G(s) = \frac{e^{-\theta s}}{(T_1 s + 1)(T_2 s + 1)} \tag{3.3}$$

where θ is the time delay and the poles of $G(s)$ i.e., $\frac{-1}{T_1}$ and $\frac{-1}{T_2}$ can be real/complex, both of which cases are treated separately. The system is considered to be stable/unstable depending on the sign of $\frac{-1}{T_1}$ and $\frac{-1}{T_2}$. The DC gain in the transfer function $G(s)$ is assumed one because its effect can be considered along with the static nonlinearity. The static nonlinearity is represented as a polynomial of the form

$$f(u(t)) = \sum_{j=0}^{p} \beta_j u^j(t) \tag{3.4}$$

where β_j's are constants and p is the order of the polynomial. The static nonlinearity is passive as described in Section 2.1 but don't have to be monotonic unlike the Wiener model case. However, the static nonlinearity has to be continuous as discontinuous nonlinearities will not produce limit cycle oscillation and absence of limit cycle oscillation doesn't mean a discontinuity in the nonlinearity. The reason why the proposed identification works for nonmonotonic static nonlinearities as well, will be discussed in the subsection 3.6.3.

As stated earlier in Sec. 1.2 and 2.1, the intermediate signal $v(t)$ may not always be available for measurement. When $v(t)$ is available for measurement, the identification is straight forward and easy. Therefore, considering the worst case, $v(t)$ is assumed to be immeasurable. The overall system dynamics of the Hammerstein system in Figure 3.1 can be written as

$$y(t) = \mathbf{C}\mathbf{X}(t) \tag{3.5}$$

$$\dot{\mathbf{X}}(t) = \mathbf{A}\mathbf{X}(t) + \mathbf{B}v(t-\theta) \tag{3.6}$$

$$v(t) = f(u(t)) \tag{3.7}$$

where,

$$\mathbf{A} = \begin{bmatrix} -\frac{1}{T_1} & 0 \\ 0 & -\frac{1}{T_2} \end{bmatrix}; \qquad \mathbf{B} = \begin{bmatrix} 1 \\ 1 \end{bmatrix}$$

$$\mathbf{C} = \frac{1}{(T_1 - T_2)} \begin{bmatrix} 1 & -1 \end{bmatrix}; \qquad \mathbf{X}(t) = \begin{bmatrix} x_1(t) \\ x_2(t) \end{bmatrix}$$

and subject to the condition that $T_1 \neq T_2$. The critically damped case when $T_1 = T_2$ has been discussed separately.

Considering the set-up in Figure 3.1 and all the assumptions stated above, the final problem is to identify $G(s)$ and $f(u)$ with the knowledge of only $u(t)$ and $y(t)$.

3.2 Hammerstein Model of Second-Order Systems

Similar to the Wiener model identification, here also the process is divided into two stages: linear subsystem identification and nonlinearity estimation. Using the limit cycle data, the transfer function of the linear subsystem i.e., $G(s)$ is evaluated first. Then using the obtained data of the linear subsystem, the nonlinearity is estimated. All the calculations are carried out considering $g_n = 0$ the reason for which is explained in Sec. 2.1. When relay heights are set as h, $-h$, and the hysteresis width as ε, $-\varepsilon$, the typical output of a second or higher order Hammerstein model is given in Figure 3.2. The relay output $u(t)$ is a step signal which switches when $e(t) = -y(t)$ attains $\pm\varepsilon$. The delayed intermediate signal $v(t-\theta)$ is shown instead of $v(t)$ to show the effect of the delay. The nonlinearity being static only changes the amplitude of the relay output which

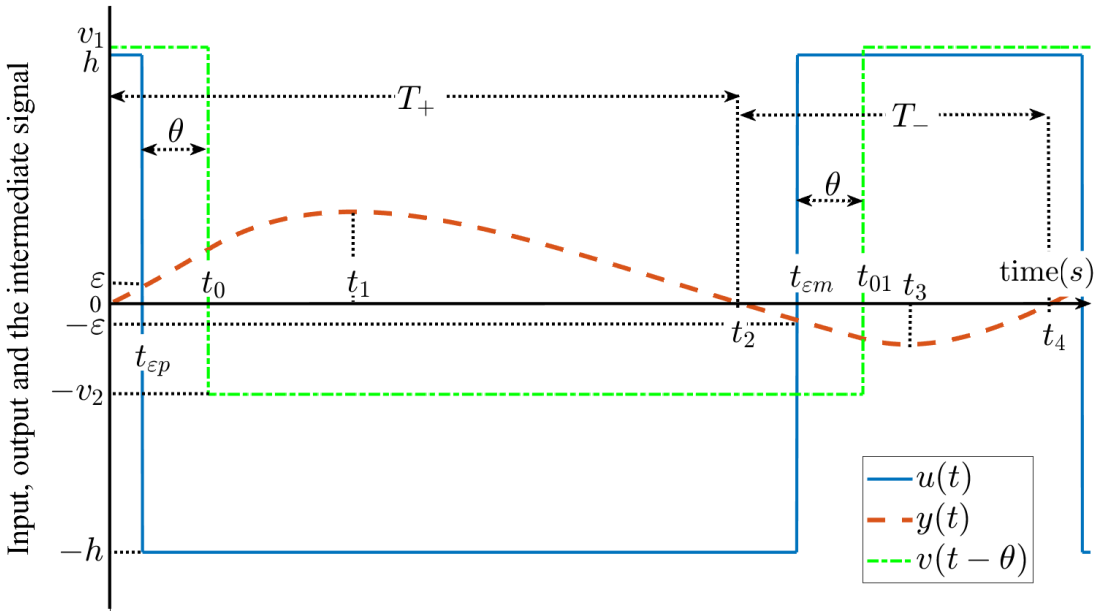

Figure 3.2: Typical output of a Hammerstein model with second or higher order linear subsystem.

makes $v(t)$ also a step signal however with different heights, v_1 in T_1 during which the output is positive and $-v_2$ in T_2 during which the output is negative, see Figure 3.2. Therefore, the linear subsystem with $v(t)$ as input, gives a sinusoidal type output with asymmetric positive and negative half-cycles. The various time instances on the typical output graphs of Figure 3.2 is defined as follows

- $t = 0$ is the beginning of the positive half cycle of the chosen full cycle of $y(t)$ i.e., $y(0) = 0$.
- $t_{\varepsilon p}$ is the time at which $y(t) = \varepsilon$ or the relay output $u(t)$ switches from h to $-h$. In the presence of white noise $g_n(t)$, the denoised output $y(t)$ may not switch exactly at $\pm\varepsilon$. Therefore, $t_{\varepsilon p}$ is measured as the time at which $u(t)$ crosses the time axis. Corresponding to the measured time $t_{\varepsilon p}$, effective ε is measured as the value of the retrieved $y(t)$ at the intersection with $u(t)$.
- t_0 is the time at which the delayed intermediate signal $v(t-\theta)$ crosses the time axis which is not measurable directly. For the measurement of t_0 and hence θ, the procedure mentioned by Majhi [43] is used. If the model is of lower order then the model is usually estimated with its exact order which is assumed to be known. In that case, the time delay θ is measured as the duration from relay switching to the duration at which an abrupt change in nth

order derivative of the output occurs. But higher order systems are usually represented as SOPDT with an effective time delay of θ_E. In such cases, the effective delay is measured as the duration between relay switching to the duration at which the nearby optimum of the second derivative of system output occurs. As mentioned in Section 2.2, the identification procedure considers only systems with small time delays.

- t_1 is the time instance where $y(t)$ attains peak. In the presence of noise, it is taken as the instance where the first derivative of the denoised output crosses the time axis.
- t_2 is the time where the positive half cycle of $y(t)$ ends or $y(t)$ crosses the time axis hence, $y(t_2) = 0$.
- $t_{\varepsilon m}, t_{01}$ and t_3 in the negative half cycle are the same as what $t_{\varepsilon p}, t_0$ and t_1 are in the positive half cycle.
- t_4 is the end of the chosen complete cycle and the beginning of a new one of $y(t)$ and hence, $y(t_4) = 0$.
- T_+ is the time period during which the output is positive and T_- is the time period during which the output is negative.

This typical output plot of Figure 3.2 and various measurements on it serves as the reference for all the proceeding derivations.

3.2.1 Linear Subsystem Identification

Identification of the linear subsystem include only estimation of the time constants T_1 and T_2 of the LTI transfer function, $G(s)$. The calculation of delay has been mentioned in the previous section.

From equation (3.5),

$$x_1(t) - x_2(t) = y(t)(T_1 - T_2) \tag{3.8}$$

$$\Rightarrow \dot{x}_1(t) - \dot{x}_2(t) = \dot{y}(t)(T_1 - T_2) \tag{3.9}$$

Expanding equation (3.6) and subtracting the derivatives of the state vectors,

$$\dot{x}_1(t) - \dot{x}_2(t) = \frac{x_2(t)}{T_2} - \frac{x_1(t)}{T_1} \tag{3.10}$$

Comparing (3.9) and (3.10),

$$-\frac{x_1(t)}{T_1} + \frac{x_2(t)}{T_2} = \dot{y}(t)(T_1 - T_2) \tag{3.11}$$

Solving the two linear equations, (3.8) and (3.11), the expressions of the states in terms of the output can be written as,

$$\mathbf{X}(t) = \begin{bmatrix} x_1(t) \\ x_2(t) \end{bmatrix} = \begin{bmatrix} T_1\Big(y(t) + T_2\dot{y}(t)\Big) \\ T_2\Big(y(t) + T_1\dot{y}(t)\Big) \end{bmatrix} \tag{3.12}$$

Solving equation (3.6) for time range $0 \leqslant t \leqslant t_0$ during which the input to the plant remains piece-wise constant, $v(t-\theta) = v_1$ (refer Figure 3.2),

$$\begin{aligned} \mathbf{X}(t) &= \mathbf{e}^{\mathbf{A}t}\mathbf{X}(0) - (\mathbf{I} - \mathbf{e}^{\mathbf{A}t})\mathbf{A}^{-1}\mathbf{B}v_1 \\ \Rightarrow \begin{bmatrix} x_1(t) \\ x_2(t) \end{bmatrix} &= \begin{bmatrix} e^{\frac{-t}{T_1}}x_1(0) + v_1T_1(1 - e^{\frac{-t}{T_1}}) \\ e^{\frac{-t}{T_2}}x_2(0) + v_1T_2(1 - e^{\frac{-t}{T_2}}) \end{bmatrix} \end{aligned} \tag{3.13}$$

Similarly, solving equation (3.6) for time range $t_0 \leqslant t \leqslant t_{01}$ during which $v(t-\theta) = -v_2$, a piece-wise constant input (refer Figure 3.2) ,

$$\begin{aligned} \mathbf{X}(t) &= \mathbf{e}^{\mathbf{A}(t-t_2)}\mathbf{X}(t_2) + (\mathbf{I} - \mathbf{e}^{\mathbf{A}(t-t_2)})\mathbf{A}^{-1}\mathbf{B}v_2 \\ \Rightarrow \begin{bmatrix} x_1(t) \\ x_2(t) \end{bmatrix} &= \begin{bmatrix} e^{\frac{t_2-t}{T_1}}x_1(t_2) - v_2T_1(1 - e^{\frac{t_2-t}{T_1}}) \\ e^{\frac{t_2-t}{T_2}}x_2(t_2) - v_2T_2(1 - e^{\frac{t_2-t}{T_2}}) \end{bmatrix} \end{aligned} \tag{3.14}$$

Equating the expressions of $\mathbf{X}(t)$ in (3.12) to that in (3.13) for $t = t_{\varepsilon p}$ when $y(t_{\varepsilon p}) = \varepsilon$ and

rearranging,

$$\varepsilon + \dot{y}(t_{\varepsilon p})T_2 - \dot{y}(0)T_2 e^{\frac{-t_{\varepsilon p}}{T_1}} = v_1(1 - e^{\frac{-t_{\varepsilon p}}{T_1}}) \tag{3.15}$$

$$\varepsilon + \dot{y}(t_{\varepsilon p})T_1 - \dot{y}(0)T_1 e^{\frac{-t_{\varepsilon p}}{T_2}} = v_1(1 - e^{\frac{-t_{\varepsilon p}}{T_2}}) \tag{3.16}$$

Dividing (3.15) by (3.16) and solving gives,

$$\begin{aligned}\varepsilon(e^{\frac{-t_{\varepsilon p}}{T_1}} - e^{\frac{-t_{\varepsilon p}}{T_2}}) + \dot{y}(0)(T_1 e^{\frac{-t_{\varepsilon p}}{T_2}} - T_2 e^{\frac{-t_{\varepsilon p}}{T_1}}) + \dot{y}(t_{\varepsilon p})(T_1 e^{\frac{-t_{\varepsilon p}}{T_1}} - T_2 e^{\frac{-t_{\varepsilon p}}{T_2}}) \\ = (T_1 - T_2)\left(\dot{y}(t_{\varepsilon p}) + \dot{y}(0)e^{-t_{\varepsilon p}\left(\frac{1}{T_1}+\frac{1}{T_2}\right)}\right)\end{aligned} \tag{3.17}$$

Case-I: When $t_1 \leq t_0$, equating the expressions of $\mathbf{X}(t)$ in (3.12) to that in (3.13) for $t = t_1$ and solving,

$$y(t_1) - \dot{y}(0)T_2 e^{\frac{-t_1}{T_1}} = v_1(1 - e^{\frac{-t_1}{T_1}}) \tag{3.18}$$

$$y(t_1) - \dot{y}(0)T_1 e^{\frac{-t_1}{T_2}} = v_1(1 - e^{\frac{-t_1}{T_2}}) \tag{3.19}$$

Dividing (3.18) by (3.19) and solving gives,

$$y(t_1)(e^{\frac{-t_1}{T_1}} - e^{\frac{-t_1}{T_2}}) + \dot{y}(0)(T_1 e^{\frac{-t_1}{T_2}} - T_2 e^{\frac{-t_1}{T_1}}) = (T_1 - T_2)\dot{y}(0)e^{-t_1\left(\frac{1}{T_1}+\frac{1}{T_2}\right)} \tag{3.20}$$

Case-II: When $t_1 \geq t_0$, equating the expressions of $\mathbf{X}(t)$ in (3.12) to that in (3.14) for $t = t_1$ and solving,

$$-\left(y(t_1) + \dot{y}(t_2)T_2 e^{\frac{t_2-t_1}{T_1}}\right) = v_2(1 - e^{\frac{t_2-t_1}{T_1}}) \tag{3.21}$$

$$-\left(y(t_1) + \dot{y}(t_2)T_1 e^{\frac{t_2-t_1}{T_2}}\right) = v_2(1 - e^{\frac{t_2-t_1}{T_2}}) \tag{3.22}$$

Dividing (3.21) by (3.22) and solving gives,

$$-y(t_1)(e^{\frac{t_2-t_1}{T_1}} - e^{\frac{t_2-t_1}{T_2}}) + \dot{y}(t_2)(T_1 e^{\frac{t_2-t_1}{T_2}} - T_2 e^{\frac{t_2-t_1}{T_1}}) = (T_1 - T_2)\dot{y}(t_2)e^{(t_2-t_1)\left(\frac{1}{T_1}+\frac{1}{T_2}\right)} \tag{3.23}$$

Now, equations (3.17) and (3.20)/(3.23) will be treated separately for various kinds of roots in the denominator of the linear subsystem.

(i) real roots

When the roots of $G(s)$ are real then the two non-linear equations (3.17) and (3.20)/ (3.23) (depending on the position of t_1), are explicitly used to evaluate T_1 and T_2.

(ii) complex conjugate roots

Let's assume that the roots of $G(s)$ are complex conjugate i.e.,

$$\frac{1}{T_1} = a + \mathrm{i}b \quad \text{and} \quad \frac{1}{T_2} = a - \mathrm{i}b \tag{3.24}$$

The equation of $G(s)$ is modified accordingly as,

$$G(s) = \frac{e^{-\theta s}}{(T_1 s+1)(T_2 s+1)} = \frac{\frac{1}{T_1 T_2} e^{-\theta s}}{(s+\frac{1}{T_1})(s+\frac{1}{T_2})} = \frac{(a^2+b^2)e^{-\theta s}}{(s+a+\mathrm{i}b)(s+a-\mathrm{i}b)}$$

However, the gain term in the numerator, (a^2+b^2) can be considered along with the nonlinearity, hence

$$G(s) = \frac{e^{-\theta s}}{(s+a+\mathrm{i}b)(s+a-\mathrm{i}b)} \tag{3.25}$$

Therefore, putting the values of T_1 and T_2 from (3.24), the equations (3.17) and (3.20)/ (3.23) can be re-written in terms of a and b as,

$$\begin{aligned} \varepsilon(a^2+b^2)\sin(bt_{\varepsilon p}) + a(\dot{y}(t_{\varepsilon p}) - \dot{y}(0))\sin(bt_{\varepsilon p}) + b(\dot{y}(t_{\varepsilon p}) + \dot{y}(0))\cos(bt_{\varepsilon p}) \\ = b\left(\dot{y}(t_{\varepsilon p})e^{at_{\varepsilon p}} + \dot{y}(0)e^{-at_{\varepsilon p}}\right) \end{aligned} \tag{3.26}$$

$$y(t_1)(a^2+b^2)\sin(bt_1) - \dot{y}(0)\Big(a\sin(bt_1) - b\cos(bt_1)\Big) = b\dot{y}(0)e^{-at_1} \tag{3.27}$$

$$y(t_1)(a^2+b^2)\sin\Big(b(t_2-t_1)\Big)+\dot{y}(t_2)\left(a\sin\Big(b(t_2-t_1)\Big)+b\cos\Big(b(t_2-t_1)\Big)\right) = b\dot{y}(t_2)e^{a(t_2-t_1)} \tag{3.28}$$

(iii) repeated roots

For the critically damped linear subsystem the values of the matrices in the state space equations (3.5) and (3.6) are modified as below,

$$\mathbf{A}=\begin{bmatrix}-a & 1\\ 0 & -a\end{bmatrix};\qquad \mathbf{B}=\begin{bmatrix}0\\ 1\end{bmatrix};\qquad \mathbf{C}=a^2\begin{bmatrix}1 & 0\end{bmatrix}$$

where $a=\frac{1}{T_1}$. Using these state matrices in the state equations (3.5) and (3.6) the following expressions are obtained,

$$y(t)=a^2x_1(t) \tag{3.29}$$

$$\dot{x}_1(t)=-ax_1(t)+x_2(t) \tag{3.30}$$

$$\dot{x}_2(t)=-ax_2(t)+v(t-\theta) \tag{3.31}$$

Using equations (3.29) and (3.30) the state vector $\mathbf{X}(t)$ in terms of the output can be expressed as,

$$\mathbf{X}(t)=\begin{bmatrix}x_1(t)\\ x_2(t)\end{bmatrix}=\frac{1}{a^2}\begin{bmatrix}y(t)\\ \dot{y}(t)+ay(t)\end{bmatrix} \tag{3.32}$$

Solving equation (3.6) for time range $0\leqslant t\leqslant t_0$,

$$\mathbf{X}(t)=\begin{bmatrix}x_1(t)\\ x_2(t)\end{bmatrix}=\frac{1}{a^2}\begin{bmatrix}\dot{y}(0)te^{-at}+v_1(1-e^{-at}-ate^{-at})\\ \dot{y}(0)e^{-at}+av_1(1-e^{-at})\end{bmatrix} \tag{3.33}$$

Equating the values of $\mathbf{X}(t)$ in equation (3.32) to that in equation (3.33) for $t = t_{\varepsilon p}$,

$$\varepsilon - \dot{y}(0)t_{\varepsilon p}e^{-at_{\varepsilon p}} = v_1(1 - e^{-at} - ate^{-at}) \tag{3.34}$$

$$-a\varepsilon + \dot{y}(0)e^{-at_{\varepsilon p}} - \dot{y}(t_{\varepsilon p}) = -av_1(1 - e^{-at_{\varepsilon p}}) \tag{3.35}$$

Dividing equations (3.34) by (3.35) and solving gives,

$$a^2\varepsilon t_{\varepsilon p} + \dot{y}(0)(1 - at_{\varepsilon p} - e^{-at_{\varepsilon p}}) = \dot{y}(t_{\varepsilon p})(e^{at_{\varepsilon p}} - at_{\varepsilon p} - 1) \tag{3.36}$$

An alternative derivation:

Repeated root is a special case where, $T_1 = T_2$. Considering $b = 0$ in (3.24) i.e., $\frac{1}{T_1} = a$ and $\frac{1}{T_2} = a + \alpha$ in (3.17) and then letting $\alpha \to 0$ gives the equation to find the repeated root as

$$a^2\varepsilon t_{\varepsilon p} + \dot{y}(0)(1 - at_{\varepsilon p} - e^{-at_{\varepsilon p}}) = \dot{y}(t_{\varepsilon p})(e^{at_{\varepsilon p}} - at_{\varepsilon p} - 1) \tag{3.37}$$

(iv) integrating second-order

This is a special case of SOPDT where one pole tends to zero i.e., $\frac{-1}{T_2} \to 0$. In other term, the time constant T_2 is very high compared to T_1 however, gets canceled with the linear static gain at the numerator of $G(s)$ i.e.,

$$G(s) = \frac{T_2 e^{-\theta s}}{(T_2 s + 1)(T_1 s + 1)} \tag{3.38}$$

but, $T_2 >> 1$

$$\therefore \quad G(s) = \frac{T_2 e^{-\theta s}}{T_2 s(T_1 s + 1)} = \frac{e^{-\theta s}}{s(T_1 s + 1)}$$

Note that this assumption will not affect the actual linear static gain as from the beginning of this section it has been considered with the nonlinear subsystem block. Hence, the value of T_1 can be obtained by solving the non-linear equations (3.17) and (3.20)/ (3.23) considering a very

high initial value of T_2 compared to T_1 as the denominator of $G(s)$ is same as the SOPDT case. It is worth noting that if one intends to reduce equations (3.17) and (3.20)/ (3.23) by limiting $T_2 \to \infty$, the equations reduces to indeterminate forms like $0 = 0$. However, it will be shown in the simulation that considering a relatively high initial value of T_2 compared to T_1 for solving the non-linear equations (3.17) and (3.20)/ (3.23), gives very accurate estimate of T_1 while T_2 comes nearly equal to the considered initial estimate of it.

(v) first-order

A first-order system can be easily detected by studying the shape of the output which will be triangular type. For a FOPDT system, in the typical output plot of Figure 3.2, $t_1 = t_0$ and $T_2 = 0$ in the expression of $G(s)$ in equation (3.3), consequently putting these values in equation (3.17) give the equation for finding the time constant T_1 as,

$$T_1 \dot{y}(t_{\varepsilon p})(e^{\frac{t_{\varepsilon p}}{T_1}} - 1) = \varepsilon \tag{3.39}$$

(vi) integrator

As discussed in Chapter 2, this case can been seen as a special case of integrating SOPDT or the first-order type system. Considering it as a special case of FOPDT type system with $\frac{1}{T_1} \to 0$, $G(s)$ can be re-written as

$$G(s) = \frac{T_1 e^{-\theta s}}{T_1 s + 1} \simeq \frac{T_1 e^{-\theta s}}{T_1 s} = \frac{e^{-\theta s}}{s} \tag{3.40}$$

In another term, the very high time constant T_1 gets canceled with the high linear static gain at the numerator. Hence, No calculations are required to find any time constant. It will be verified in the simulation example that by treating an integrator as a FOPDT system and hence evaluating T_1 using Equation (2.39) gives a very high value. The unknowns required to be calculated for a Hammerstein model with an integrator are, the delay which can be calculated using Majhi [43]'s method and, the static nonlinearity which will be discussed in the next section.

3.2.2 Nonlinearity Estimation

The nonlinearity is estimated as a polynomial fitting between $u(t)$ and $v(t)$ as in equation (3.4). Looking at the Figure 3.2, it can be ascertain that one relay test with a particular relay height gives two points on the polynomial curve $f(u)$ i.e., (h, v_1) and $(-h, -v_2)$. Therefore, it is required to repeat the test half the number of times as the required number of points to be estimated on the polynomial. The relay heights $u(t)$ are taken as Chebyshev nodes to eliminate the effect of Runge's phenomenon of overfitting. A brief detail of Chebyshev nodes is given in section A of the appendix. Note that to estimate the linear subsystem parameters, only one relay test and hence one set of calculations are sufficient however to estimate the nonlinearity, v_1 and v_2 are required to be calculated for each test. In this section, the equations to find the two asymmetric heights, v_1 and v_2 in Figure 3.2 of signal $v(t)$ for various cases of roots in the denominator of the linear subsystem.

(i) real roots

Subtracting (3.15) from (3.16) and solving gives the equation of v_1 as,

$$v_1 = \frac{\dot{y}(t_{\varepsilon p})(T_1 - T_2) - \dot{y}(0)(T_1 e^{\frac{-t_{\varepsilon p}}{T_2}} - T_2 e^{\frac{-t_{\varepsilon p}}{T_1}})}{(e^{\frac{-t_{\varepsilon p}}{T_1}} - e^{\frac{-t_{\varepsilon p}}{T_2}})} \tag{3.41}$$

Equating the expressions of $\mathbf{X}(t)$ in (3.13) to that in equation (3.14) for $t = t_{\varepsilon m}$ and solving,

$$\varepsilon + \dot{y}(t_{\varepsilon m})T_2 - \dot{y}(t_2)T_2 e^{\frac{t_2 - t_{\varepsilon m}}{T_1}} = v_2(1 - e^{\frac{t_2 - t_{\varepsilon m}}{T_1}}) \tag{3.42}$$

$$\varepsilon + \dot{y}(t_{\varepsilon m})T_1 - \dot{y}(t_2)T_1 e^{\frac{t_2 - t_{\varepsilon m}}{T_2}} = v_2(1 - e^{\frac{t_2 - t_{\varepsilon m}}{T_2}}) \tag{3.43}$$

Subtracting (3.43) from (3.42) and solving gives the equation for v_2 as,

$$v_2 = \frac{\dot{y}(t_{\varepsilon m})(T_1 - T_2) - \dot{y}(t_2)(T_1 e^{\frac{t_2 - t_{\varepsilon m}}{T_2}} - T_2 e^{\frac{t_2 - t_{\varepsilon m}}{T_1}})}{(e^{\frac{t_2 - t_{\varepsilon m}}{T_1}} - e^{\frac{t_2 - t_{\varepsilon m}}{T_2}})} \tag{3.44}$$

(ii) complex conjugate roots

When the roots are complex conjugates, note that in the modified expression of $G(s)$ in (3.25), (a^2+b^2) is multiplied which although doesn't affect the equations to find a and b while converting from real roots case to complex conjugates case, however, will affect $v(t)$. Therefore, while converting the equation of $v(t)$ in real roots case to complex conjugates case, (a^2+b^2) need to be multiplied. Hence, putting the values of T_1 and T_2 for complex conjugate case from (3.24) in (3.41) and (3.44)

$$v_1 = \frac{\dot{y}(t_{\varepsilon p})be^{at_{\varepsilon p}} + \dot{y}(0)\Big(a\sin(bt_{\varepsilon p}) - b\cos(bt_{\varepsilon p})\Big)}{\sin(bt_{\varepsilon p})} \tag{3.45}$$

$$v_2 = \frac{-\dot{y}(t_{\varepsilon m})be^{a(t_{\varepsilon m}-t_2)} + \dot{y}(t_2)\left(a\sin\Big(b(t_2-t_{\varepsilon m})\Big) + b\cos\Big(b(t_2-t_{\varepsilon m})\Big)\right)}{\sin\Big(b(t_2-t_{\varepsilon m})\Big)} \tag{3.46}$$

(iii) repeated roots

From equation (3.35) the equation for finding v_1 can be derived as the following,

$$v_1 = \frac{\varepsilon a + \dot{y}(t_{\varepsilon p}) - \dot{y}(0)e^{-at_{\varepsilon p}}}{a(1-e^{-at_{\varepsilon p}})} \tag{3.47}$$

Solving equation (3.6) for time range $t_0 \leqslant t \leqslant t_{01}$,

$$\mathbf{X}(t) = \frac{1}{a^2}\begin{bmatrix} -\dot{y}(t_2)(t-t_2)e^{a(t_2-t)} - v_2(1-e^{a(t_2-t)} - a(t-t_2)e^{a(t_2-t)}) \\ -\dot{y}(t_2)e^{-at} + av_2(1-e^{a(t_2-t)}) \end{bmatrix} \tag{3.48}$$

Equating $x_2(t_{\varepsilon m})$ from equation (3.32) to that in equation (3.48) gives the value of v_2 as the following,

$$v_2 = \frac{a\varepsilon + \dot{y}(t_{\varepsilon m}) - \dot{y}(t_2)e^{a(t_2-t_{\varepsilon m})}}{a(1-e^{a(t_2-t_{\varepsilon m})})} \tag{3.49}$$

An alternative derivation:

The equations of v_1, v_2 for repeated root case can be calculated alternatively by assuming $\frac{1}{T_1} = a$ and $\frac{1}{T_2} = a + \alpha$ in (3.41), (3.44) and then letting $\alpha \to 0$,

$$v_1 = \frac{\varepsilon a + \dot{y}(t_{\varepsilon p}) - \dot{y}(0)e^{-at_{\varepsilon p}}}{a(1 - e^{-at_{\varepsilon p}})} \tag{3.50}$$

$$v_2 = \frac{\varepsilon a + \dot{y}(t_{\varepsilon m}) - \dot{y}(t_2)e^{a(t_2 - t_{\varepsilon m})}}{a(1 - e^{a(t_2 - t_{\varepsilon m})})} \tag{3.51}$$

(iv) integrating second-order

In the modified expression of $G(s)$ considered for the case of integrating SOPDT i.e., in equation (3.38), an extra gain T_2 is multiplied in order to get the required model. This doesn't affect the equations for finding T_1 and T_2 as the denominator is unchanged, however it will affect the expressions of v_1 and v_2. Therefore, in (3.41), assuming $T_2 >> T_1$ and dividing the final expression by T_2, similarly solving (3.43) gives the ultimate equations of v_1 and v_2 as,

$$v_1 = \frac{\dot{y}(0)e^{\frac{-t_{\varepsilon p}}{T_1}} - \dot{y}(t_{\varepsilon p})}{(e^{\frac{-t_{\varepsilon p}}{T_1}} - 1)} \tag{3.52}$$

$$v_2 = \frac{\dot{y}(t_2)e^{\frac{t_2 - t_{\varepsilon m}}{T_1}} - \dot{y}(t_{\varepsilon m})}{(e^{\frac{t_2 - t_{\varepsilon m}}{T_1}} - 1)} \tag{3.53}$$

(v) first-order

In the expressions of v_1 and v_2 i.e., (3.41) and (3.44), putting $T_2 = 0$ give the equations for first-order system as,

$$v_1 = T_1\dot{y}(t_{\varepsilon p})e^{\frac{t_{\varepsilon p}}{T_1}} \tag{3.54}$$

$$v_2 = T_1\dot{y}(t_{\varepsilon m})e^{\frac{t_{\varepsilon m}}{T_1}} \tag{3.55}$$

(vi) integrator

In the previous subsection 3.2.1, an integrator is shown to be a special case of the FOPDT system with a very high static linear gain T_1. Although, this did not affect the calculation of the time constant (which is always 1 in this case), it will affect the static nonlinearity. Therefore, to derive the equations of the intermediate signal $v(t)$, the assumed linear static gain T_1 is divided in Equations (3.54) and (3.55). This gives a direct measurement of $v(t)$ therefore, for a Hammerstein model with an integrator, no calculations are required.

$$v_1 = \dot{y}(t_{\varepsilon p}) \tag{3.56}$$

$$v_2 = \dot{y}(t_{\varepsilon m}) \tag{3.57}$$

3.2.3 Linear Structure Identification

A linear system can be thought of as a special case of a Hammerstein non-linear model where the polynomial nonlinearity is simply a straight line passing through the origin i.e., $v = f(u) = ku$. The linear subsystem identification part of the mentioned procedure is independent of the static nonlinearity hence it can be used for any linear system identification without any modifications. However, unlike the nonlinearity which requires to repeat the test more than one time to get more points on the $u \sim v$ graph for curve fitting, the linear system identification requires only one test to find all unknown parameters. After finding the time constants and the time delay, the value of $\frac{v_1}{h}$ or $\frac{v_2}{h}$ will give the static gain k as for a linear system the limit cycle output is symmetric therefore, $v_1 = v_2$. Few examples are taken in the simulation to address the application of the proposed procedure to linear systems as well.

It is to be noted that a linear system can be identified either as a Wiener or Hammerstein model. However, the equations for parameter estimation are different. Again, these procedures are similar to the work of Bajarangbali et al. [44] as mentioned before in section 2.2.3.

3.3 Hammerstein Model of *n*th Order Systems

Sometimes, for simplification, higher order linear systems (mostly, when the system is over damped) are represented with dominating pole having pole multiplicity. Therefore, it gives rise to a specific class of linear system with the following transfer function

$$G(s) = \frac{e^{-\theta s}}{(T_1 s + 1)^n} \tag{3.58}$$

where n is the order of the system. This section deals with identification of Hammerstein model with the above type of linear subsystem. The nonlinearity is considered as before, static and monotonic, represented as a polynomial as in (3.4). The setup used is the same as shown in Figure 3.1 therefore the overall dynamics of the Hammerstein system are also the same three equations i.e., (3.5), (3.6) and (3.7). However, due to the change in $G(s)$ the new state matrices are given as

$$\mathbf{A} = \begin{bmatrix} a & 1 & 0 & \cdots & \cdot & 0 \\ 0 & a & 1 & \cdots & \cdot & 0 \\ 0 & 0 & a & \cdots & \cdot & 0 \\ \vdots & \vdots & \vdots & \ddots & \cdots & \vdots \\ \cdot & \cdot & \cdot & \cdots & a & 1 \\ 0 & 0 & \cdots & 0 & 0 & a \end{bmatrix}; \quad \mathbf{B} = \begin{bmatrix} 0 \\ 0 \\ 0 \\ \vdots \\ 0 \\ (-1)^n \end{bmatrix}; \quad \mathbf{X} = \begin{bmatrix} x_1(t) \\ x_2(t) \\ x_3(t) \\ \vdots \\ \cdot \\ x_n(t) \end{bmatrix}$$

$$\mathbf{C} = a^n \begin{bmatrix} 1 & 0 & 0 & \cdots & \cdot & 0 \end{bmatrix}; \qquad \text{where,} \quad a = \frac{-1}{T_1}.$$

Similar to the previous case, the identification procedure consists of two stages, linear subsystem identification, and the nonlinearity estimation. A typical graph of various signals during the identification is shown in Figure 3.3. All time instances in Figure 3.3 is the same as the ones described in the previous section i.e., Sec. 3.2. However, some changes are made which are described below

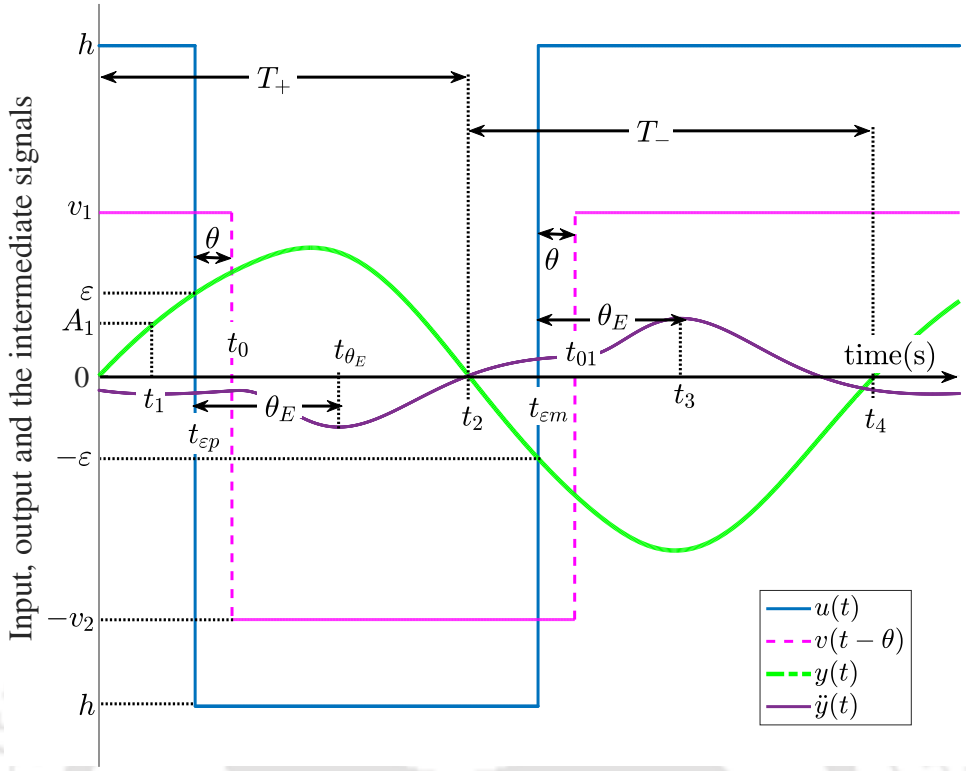

Figure 3.3: Typical output of a Hammerstein model with order $n \geq 1$.

- t_1 is any randomly chosen time instance between $0 \leqslant t \leqslant t_{\varepsilon p}$ and A_1 is $y(t_1)$. Earlier, in Sec. 3.2, t_1 was the peak of $y(t)$ however, in the subsequent derivation for this case, the peak of the output is not used hence the said changes are done.

- t_{θ_E} is the time instance where optimum of the second derivative of the output nearest to $t_{\varepsilon p}$ occurs. This time instance is used to measure the time delay using the proposed method by [43]. For a higher order system, the effective time delay is measured as the duration between relay switching to the duration at which the nearby optimum of the second derivative of system output occurs.

The newly defined matrices, time instances, and the graph of Figure 3.3 will be used in the subsequent section for all the required derivation.

3.3.1 Linear Subsystem Identification

Linear subsystem identification includes identification of $G(s)$ where the only two unknowns are θ and time constant T_1. It is to be noted that the order of the system is assumed to be known. However, it is also applicable to cases where the order is unknown but very high and the estimation is done using smaller (say first/second/third) orders. While the measurement of delay has been mentioned in the previous section, this section contains only the derivations required to find the time constant T_1.

Solving (3.5),

$$x_1(t) = \frac{y(t)}{a^n} \tag{3.59}$$

Expanding (3.6),

$$\begin{aligned} \dot{x_1}(t) &= ax_1(t) + x_2(t) \\ \dot{x_2}(t) &= ax_2(t) + x_3(t) \\ &\vdots \\ &\vdots \\ \dot{x}_{n-1}(t) &= ax_{n-1}(t) + x_n(t) \\ \dot{x_n}(t) &= ax_n(t) + (-1)^n v(t-\theta) \end{aligned} \tag{3.60}$$

Using (3.59) and the first equation from (3.60),

$$x_2(t) = \frac{1}{a^n}[\dot{y}(t) - ay(t)] \tag{3.61}$$

Using (3.61) and the second equation from (3.60),

$$x_3(t) = \frac{1}{a^n}[\ddot{y}(t) - 2a\dot{y}(t) + a^2 y(t)] \tag{3.62}$$

Similarly, any state can be written in terms of the output $y(t)$ as

$$x_n(t) = \frac{1}{a^n}\sum_{k=0}^{n-1}\binom{n-1}{k}\frac{d^{(n-1-k)}y(t)}{dt^{(n-1-k)}}(-a)^k \qquad \text{for all} \quad n \geq 1. \tag{3.63}$$

Therefore the state matrix can be written in the general form as,

$$\mathbf{X}(t) = \begin{bmatrix} \dfrac{y(t)}{a^n} \\ \dfrac{1}{a^n}[\dot{y}(t) - ay(t)] \\ \vdots \\ \vdots \\ \dfrac{1}{a^n}\displaystyle\sum_{k=0}^{n-1} \binom{n-1}{k} \frac{d^{(n-1-k)}y(t)}{dt^{(n-1-k)}}(-a)^k \end{bmatrix} \tag{3.64}$$

Solving (3.6) for time range $0 \leqslant t \leqslant t_0$ during which the input to the plant remains piece-wise constant, $v(t-\theta) = v_1$ (refer Figure 3.3),

$$\mathbf{X}(t) = \mathbf{e}^{\mathbf{A}t}\mathbf{X}(0) - (\mathbf{I} - \mathbf{e}^{\mathbf{A}t})\mathbf{A}^{-1}\mathbf{B}v_1 \tag{3.65}$$

Putting the value of $\mathbf{X}(0)$ using (3.64) in (3.65), the value of $x_1(t)$ for time range $0 \leqslant t \leqslant t_0$ can be written as

$$x_1(t) = \frac{1}{a^n}\left\{\left[1 - e^{at}\sum_{i=0}^{n-1}\frac{(-at)^i}{i!}\right]v_1 + e^{at}\sum_{i=1}^{n-1}\sum_{k=0}^{i}\frac{t^i}{i!}\binom{i}{k}\frac{d^{(i-k)}y(0)}{dt^{(i-k)}}(-a)^k\right\} \tag{3.66}$$

From Figure 3.3,

$$\begin{aligned} y(t_{\varepsilon p}) &= \varepsilon \\ \Rightarrow a^n x_1(t_{\varepsilon p}) &= \varepsilon \end{aligned} \tag{3.67}$$

Using (3.66) in (3.67),

$$\left[1 - e^{at_{\varepsilon p}}\sum_{i=0}^{n-1}\frac{(-at_{\varepsilon p})^i}{i!}\right]v_1 = \varepsilon - e^{at_{\varepsilon p}}\sum_{i=1}^{n-1}\sum_{k=0}^{i}\frac{t_{\varepsilon p}^i}{i!}\binom{i}{k}\frac{d^{(i-k)}y(0)}{dt^{(i-k)}}(-a)^k \tag{3.68}$$

Again from Figure 3.3,

$$\begin{aligned} y(t_1) &= A_1 \\ \Rightarrow a^n x_1(t_1) &= A_1 \end{aligned} \tag{3.69}$$

Using (3.66) in (3.69),

$$\left[1 - e^{at_1}\sum_{i=0}^{n-1}\frac{(-at_1)^i}{i!}\right]v_1 = A_1 - e^{at_1}\sum_{i=1}^{n-1}\sum_{k=0}^{i}\frac{t_1^i}{i!}\binom{i}{k}\frac{d^{(i-k)}y(0)}{dt^{(i-k)}}(-a)^k \tag{3.70}$$

Dividing (3.68) by (3.70) gives the equation to find a and hence T_1 as

$$\frac{1 - e^{at_{\varepsilon p}}\sum_{i=0}^{n-1}\frac{(-at_{\varepsilon p})^i}{i!}}{1 - e^{at_1}\sum_{i=0}^{n-1}\frac{(-at_1)^i}{i!}} = \frac{\varepsilon - e^{at_{\varepsilon p}}\sum_{i=1}^{n-1}\sum_{k=0}^{i}\frac{t_{\varepsilon p}^i}{i!}\binom{i}{k}\frac{d^{(i-k)}y(0)}{dt^{(i-k)}}(-a)^k}{A_1 - e^{at_1}\sum_{i=1}^{n-1}\sum_{k=0}^{i}\frac{t_1^i}{i!}\binom{i}{k}\frac{d^{(i-k)}y(0)}{dt^{(i-k)}}(-a)^k} \tag{3.71}$$

3.3.2 Nonlinearity Estimation

Similar to the Wiener model case in Chapter 2 and the previous Hammerstein model identification in Section 3.2, the nonlinearity has been estimated as a polynomial as in equation 3.4. One relay test gives two points on the polynomial curve $u \sim v$ (see Figure 3.3) therefore, as stated in Sec. 3.2.2, the test is repeated according to the requirement with the relay heights taken as Chebyshev nodes. This section presents the derivation of the intermediate signal $v(t)$ i.e., v_1 and v_2 in Figure 3.3.

From (3.68), the equation for v_1 can be written as

$$v_1 = \frac{\varepsilon - e^{at_{\varepsilon p}}\sum_{i=1}^{n-1}\sum_{k=0}^{i}\frac{t_{\varepsilon p}^i}{i!}\binom{i}{k}\frac{d^{(i-k)}y(0)}{dt^{(i-k)}}(-a)^k}{1 - e^{at_{\varepsilon p}}\sum_{i=0}^{n-1}\frac{(-at_{\varepsilon p})^i}{i!}} \tag{3.72}$$

The equation for v_1 can also be found from (3.70) as

$$v_1 = \frac{A_1 - e^{at_1}\sum_{i=1}^{n-1}\sum_{k=0}^{i}\frac{t_1^i}{i!}\binom{i}{k}\frac{d^{(i-k)}y(0)}{dt^{(i-k)}}(-a)^k}{1 - e^{at_1}\sum_{i=0}^{n-1}\frac{(-at_1)^i}{i!}} \tag{3.73}$$

Solving (3.6) for time range $t_0 \leqslant t \leqslant t_{01}$,

$$\mathbf{X}(t) = \mathbf{e}^{\mathbf{A}(t-t_2)}\mathbf{X}(t_2) + (\mathbf{I} - \mathbf{e}^{\mathbf{A}(t-t_2)})\mathbf{A}^{-1}\mathbf{B}v_2 \tag{3.74}$$

Putting the value of $\mathbf{X}(t_2)$ using (3.64) in (3.74), the value of $x_1(t)$ for time range $t_0 \leqslant t \leqslant t_{01}$ can be written as

$$\begin{aligned} x_1(t) = \frac{1}{a^n}\Bigg\{ & \left[1 - e^{a(t-t_2)}\sum_{i=0}^{n-1}\frac{(-a(t-t_2))^i}{i!}\right]v_2 \\ & + e^{a(t-t_2)}\sum_{i=1}^{n-1}\sum_{k=0}^{i}\frac{(t-t_2)^i}{i!}\binom{i}{k}\frac{d^{(i-k)}y(t_2)}{dt^{(i-k)}}(-a)^k\Bigg\} \end{aligned} \tag{3.75}$$

From Figure 3.3,

$$\begin{aligned} y(t_{\varepsilon m}) &= -\varepsilon \\ \Rightarrow a^n x_1(t_{\varepsilon m}) &= -\varepsilon \end{aligned} \tag{3.76}$$

Using (3.75) in (3.76), v_2 can be found as

$$v_2 = \frac{\varepsilon + e^{a(t_{\varepsilon m}-t_2)}\sum_{i=1}^{n-1}\sum_{k=0}^{i}\frac{(t_{\varepsilon m}-t_2)^i}{i!}\binom{i}{k}\frac{d^{(i-k)}y(t_2)}{dt^{(i-k)}}(-a)^k}{1 - e^{a(t_{\varepsilon m}-t_2)}\sum_{i=0}^{n-1}\frac{(-a(t_{\varepsilon m}-t_2))^i}{i!}} \tag{3.77}$$

Note that in the absence of the static nonlinearity, this identification procedure is similar to the one proposed by Pandey et al. [65] for linear systems. However, Pandey et al. [65] have considered a zero in their linear model.

3.4 Mitigation of Measurement Noise

To test the usefulness of the procedure in realistic conditions, random Gaussian noise is added to the system output. Relay chattering occurs as a result of incorporating noise. As suggested in [14], hysteresis is used to prevent chattering which proved effective in the simulation example discussed however, it is not proven theoretically. A safe range for choosing the width of hysteresis is twice greater than the standard deviation (σ) of the noise i.e., $\varepsilon \geq 2\sigma$ [46]. When the standard deviation of the noise is not known, the hysteresis width should be changed heuristically.

It can be observed from the previous sections that the peak of the output signal is crucial to select the equations for calculation of time constant. Denoising a corrupted signal using conventional Fourier transform smooths out its sharp features like peak, especially in FOPDT systems which gives a triangular type output. Therefore, to preserve the shape of the original signal, the wavelet transform based denoising technique has been opted. The continuous wavelet transform (CWT) of a function $y(t)$ (assuming that $y \in L^2(\mathbf{R})$, where $L^2(\mathbf{R})$ is the space of functions whose L^2 norm is finite) is expressed as:

$$Y(F,H) = \frac{1}{\sqrt{F}} \int_{-\infty}^{\infty} \phi\left(\frac{t-H}{F}\right) y(t)dt \tag{3.78}$$

where, $\phi(t)$ the mother wavelet is a basis function of $L^2(\mathbf{R})$. The dilation parameter F corresponds to information about frequency whereas the translation parameter H corresponds to time domain information. The integral in equation (3.78) is simply a convolution operation of the signal and the mother wavelet, $\phi(t)$. Unlike the Fourier transform where the basis function is only $e^{i\omega t}$, in the wavelet transform there are numerous choices for $\phi(t)$. The choice of wavelet, $\phi(t)$ depends on the shape and the properties of the signal to be denoised. For a particular wavelet, the number of vanishing/zero moments is equal to half of all coefficients. The vanishing moment of a wavelet determines its ability to depict the polynomial contents of a signal. For example, db2 (Haar wavelet), which has one vanishing moment, represents polynomials of one coefficient i.e., constant signals. Likewise, db4 (Daubechies-4 wavelet) represents polynomials with two coefficients which are, constant and linear signals. For instance, when the output of the system is

triangular type as in FOPDT, it can be represented better by a first degree polynomial, hence the db4 wavelet is used [66]. The choice of mother wavelet is dependent on the shape of the output waveform.

3.5 Simulation Study

Various examples mostly from the literature have been taken to test the method in simulation. Similar to the Wiener model case, all probable cases of the linear subsystem are discussed. Notes on the implementation procedure, analysis, and comparisons are made at the end of each example. Validation is done by calculating ISE using random white Gaussian noise as input. A case of measurement noise has also been considered.

Example 1: FOPDT stable

A FOPDT Hammerstein system studied previously by Juric et al. [63] is considered here which is given as,

$$\textit{Static nonlinearity:} \quad f(u) = \tan^{-1} u$$
$$\textit{Linear subsystem:} \quad G(s) = \frac{e^{-0.5s}}{2s+1}$$

Several tests are done using different relay heights, the results are tabulated in Table 3.2. The time constant is found for each test using (3.39) and the average of them is considered as the ultimate estimate which is $T_1 = 2.00126$. Similarly, the delay is found to be $\theta = 0.50042$ using Majhi [43]'s method. Various points on the static non-linear curve are estimated using (3.54),(3.55) and listed in Table 3.2. Observing the "% error" columns of Table 3.2, there is a significant improvement in the estimation compared to that of Juric et al. [63]. By the proposed method the estimated relative error stayed within 0.1% whereas, in case of Juric et al. [63]'s method, it stayed within 1.5%. The linear subsystem results are tabulated in Table 3.1 .

	Linear subsystem: $G(s)$	%error in T_1	%error in θ
Original model	$\frac{e^{-0.5s}}{(2s+1)}$		
By Juric et al. [63]	$\frac{e^{-0.5071s}}{(2.2039s+1)}$	10.195	1.42
By proposed method	$\frac{e^{-0.50042s}}{(2.00126s+1)}$	0.063	0.084

Table 3.1: Linear subsystem identification results of Example 1

Expt.	h	$f(h)$ (original)	$f(h)$ (calculated)	% error	$f(h)$ (by Juric et al. [63])	% error
1	0.2	0.1974	0.1975	0.05	0.2002	1.42
2	0.5	0.4636	0.4640	0.09	0.4698	1.34
3	0.8	0.6747	0.6753	0.09	0.6835	1.30
4	1.1	0.8330	0.8336	0.07	0.8430	1.20
5	1.5	0.9828	0.9835	0.07	0.9959	1.33
6	2	1.1072	1.1079	0.06	1.1216	1.30
7	3	1.2491	1.2499	0.06	1.2638	1.18
8	5	1.3734	1.3743	0.07	1.3917	1.33
9	8	1.4464	1.4474	0.07	1.4656	1.33
10	10	1.4711	1.4721	0.07	1.4887	1.19

Table 3.2: Comparison of estimated nonlinearity for Example 1

Example 2: FOPDT unstable

An unstable FOPDT linear system previously studied by Majhi and Atherton [50] having the following transfer function which is rewritten in the form assumed for the proposed procedure as:

$$G(s) = \frac{e^{-0.4s}}{s-1} = \frac{(-1)e^{-0.4s}}{(-s+1)}$$

With a relay setting of $h = 0.588$ and $\varepsilon = 0.2$ gives $t_{\varepsilon p} = 0.29324$ and $t_0 = 0.69307$. A linear system gives symmetric limit cycle oscillation hence, $\dot{y}(t_{\varepsilon p}) = \dot{y}(t_{\varepsilon m}) = 0.78784$. Using these measurements, the delay $\theta = t_0 - t_{\varepsilon p} = 0.39983$. Using (3.39), the time constant is calculated as $T_1 = -1.00050$ which is when substituted in (3.54), (3.55) gives $v_1 = v_2 = -0.58823$. Then, the static gain is given as $\frac{v_1}{h} = -1.00040$. This example illustrates that the procedure doesn't require to know a prior whether the system is stable or unstable, the equations used for parameter estimations automatically gives the sign of the time constant and gain accordingly. It is worthy to note that this example has been studied in the Wiener model case as well in Example 1 of Section 2.4 where a polynomial fitting is required to find the static gain whereas here it can be calculated more directly. Comparing both the methods, it can be observed that the identification of a linear system considering it as a Hammerstein model is easier compared to considering it as a Wiener model. The overall result is tabulated in Table 3.3.

	Linear subsystem: $G(s)$	%error in T_1
Original model	$\frac{e^{-0.4s}}{(s-1)} = \frac{(-1)e^{-0.4s}}{(-s+1)}$	
By Majhi and Atherton [50]	$\frac{-e^{-0.400034s}}{(-1.00013s+1)}$	0.013
By proposed method as Wiener model	$\frac{-1e^{-0.3998s}}{(-1s+1)}$	0
By proposed method as Hammerstein model	$\frac{-1.0004e^{-0.39983s}}{(-1.0005s+1)}$	0.05

Table 3.3: System identification results of Example 2

Example 3: SOPDT overdamped

A Hammerstein model with two real and distinct roots of the linear subsystem is considered for analysis which was previously studied by Juric et al. [63] and is given as,

$$\textit{Static nonlinearity:} \quad f(u) = u + |\frac{u}{2}|$$
$$\textit{Linear subsystem:} \quad G(s) = \frac{e^{-0.5s}}{2s^2+3s+1}$$

For various relay heights the measurements are taken and the estimation result for the nonlinearity is tabulated in Table 3.5. The time constants averaging over all the five tests are found as $T_1 = 1.95044$, $T_2 = 1.02520$ using (3.17), (3.20) and the delay as $\theta = 0.50025$. The linear subsystem identification results are tabulated in Table 3.4. The intermediate signal $v(t)$ is found using (3.41) and (3.44). Observing the two "% error" rows in Table 3.5, it is evident that there is significant improvement by proposed method over Juric et al. [63]'s results.

	Linear subsystem: $G(s)$	%error in coefficients of s^2 and s	%error in θ
Original model	$\frac{e^{-0.5s}}{(2s^2+3s+1)}$		
By Juric et al. [63]	$\frac{e^{-0.4849s}}{(2.2263s^2+3.0615s+1)}$	11.315 2.05	3.02
By proposed method	$\frac{e^{-0.500025s}}{(1.9996s^2+2.97564s+1)}$	0.02 0.812	0.005

Table 3.4: Linear subsystem identification results of Example 3

Expt.		1	2	3	4	5
h		1	2	3	4	5
$f(h)$	original	1.5	3	4.5	6	7.5
	by Juric et al. [63]	1.4050	2.8100	4.2173	5.6200	7.0250
	calculated	1.4890	2.9780	4.4670	5.9559	7.4450
% error	by Juric et al. [63]	6.33	6.33	6.28	6.33	6.33
	calculated	0.73	0.73	0.73	0.74	0.73
$f(-h)$	original	-0.5	-1	-1.5	-2	-2.5
	by Juric et al. [63]	-0.5169	-1.0339	-1.5506	-2.0677	-2.5847
	calculated	-0.5003	-1.0005	-1.4944	-1.9972	-2.5014
% error	by Juric et al. [63]	3.38	3.39	3.37	3.39	3.39
	calculated	0.06	0.05	0.37	0.14	0.06

Table 3.5: Comparison of estimated nonlinearity for Example 3

Example 4: integrating SOPDT

An integrating SOPDT linear system previously studied by Majhi [43] has been studied which has the following transfer function,

$$G(s) = \frac{e^{-1.5s}}{s(5s+1)}$$

With a relay setting of $h = 0.951$ and $\varepsilon = 0.2$, measurements are made on the limit cycle. The initial estimates were taken as $T_1 = 0.1$ and $T_2 = 10000$ which when used to solve equations (3.17) and (3.20), gave $T_1 = 5$ and $T_2 = 9981.2$. The time delay θ is measured using the sharp change in the second derivative plot at t_0 as $\theta = t_0 - t_{\varepsilon p} = 1.80326 - 0.30301 = 1.50025$. Using (3.52) and (3.53), the value of v_1 is calculated as $v_1 = 0.95080$ which is also the value of v_2 for the

symmetry of limit cycle in case of a linear system. Hence the static gain $\frac{v_1}{h}$ gives 0.99980. The estimated values are more accurate compared to that of Majhi [43] which estimated $\theta = 1.62500$ and $T_1 = 5.04900$. This example has been studied in the Wiener model case as well in Example 5. Therefore, it can be observed again that for a linear system, considering the static gain before the system i.e., as a Hammerstein model, makes identification easier compared to considering it after the linear system as in Wiener model. Also, note that it is not necessary to know beforehand if a system is linear or not. A few numbers of tests should be performed with different relay heights. If the intermediate signal $v(t)$ turns out to be symmetric and $v(t)/h$ has the same values for each test then it is a linear system.

Example 5: SOPDT underdamped

A Hammerstein system with complex linear subsystem roots is also considered for the study of complex roots which is taken as,

$$\textit{Static nonlinearity:} f(u) = 2(1 - e^{-0.693u})$$
$$\textit{Linear subsystem:} G(s) = \frac{e^{-s}}{s^2 + 2s + 5}$$

The nonlinearity is estimated for the interval $(-2, 2)$ with 7 Chebyshev nodes i.e., three relay tests were performed as the known point 0 is also one of the Chebyshev nodes. Hence, the relay heights are $h = 0.86777, 1.56366, 1.94985$ and the width taken as $\varepsilon = 0.1, 0.2, 0.2$ respectively. Averaging the estimated values in each test gives $a = 1.02$ and $b = 2.01$ which are then used to find $v(t)$. The delay is measured for the 3 tests and averaged as $\theta = 1.002$. The nonlinearity is fitted as $v(t) = 1.4337u - 0.4784u^2 + 0.1097u^3 - 0.0229u^4 + 0.0031u^5$. The number of Chebyshev nodes is chosen randomly in this work however, one should choose it based on their need for accuracy and availability of time.

The system is estimated under 20dB measurement noise (zero-mean Gaussian). The noisy output, $y_m(t)$ is retrieved through wavelet transform as shown in Figure 3.4 using MATLAB's Wavelet Toolbox [67]. The same three relay settings are used to identify the system under noise,

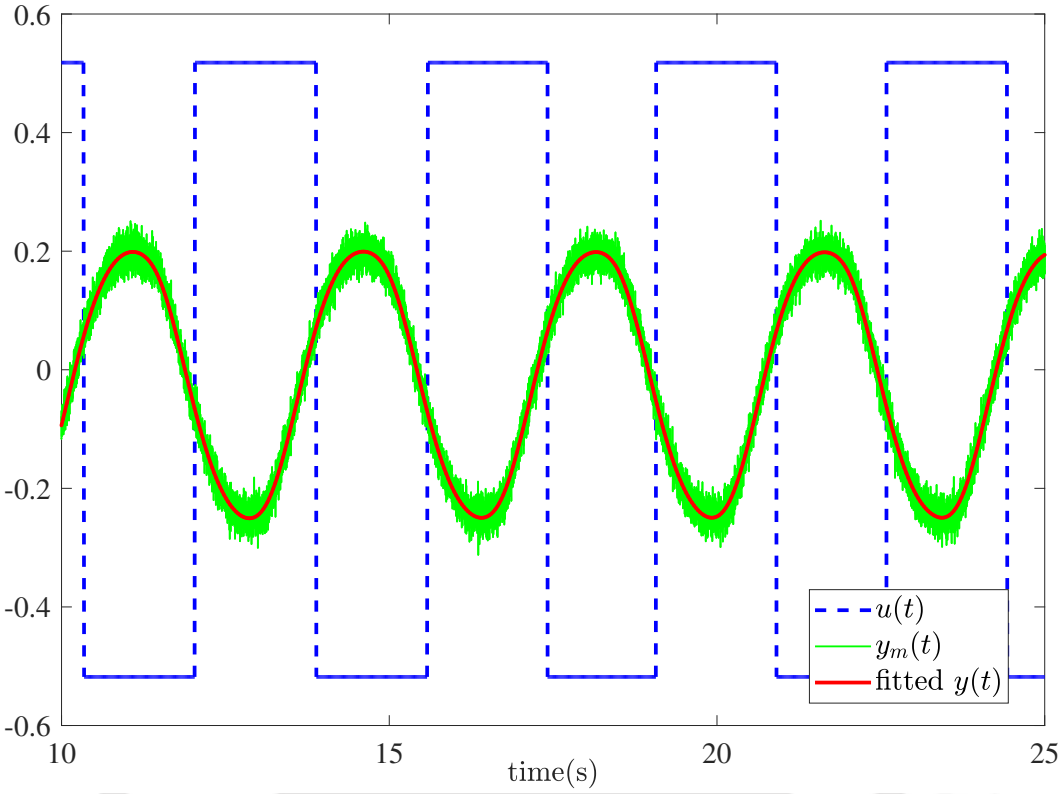

Figure 3.4: Noisy and the retrieved output signal of Example 5

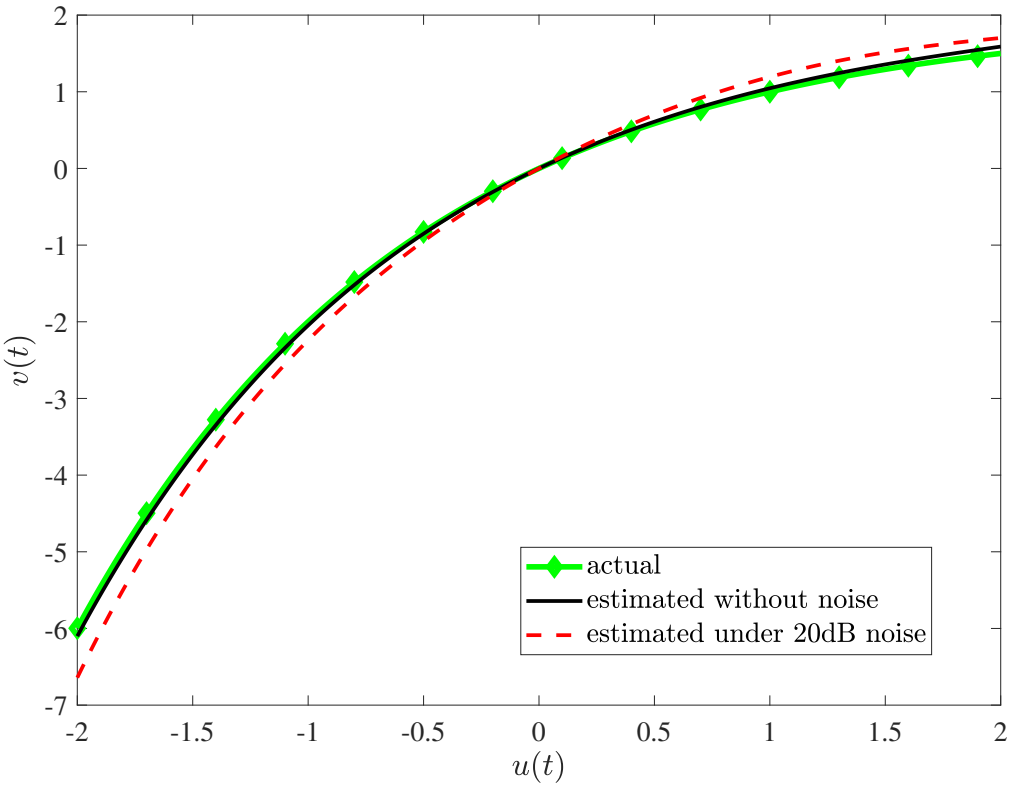

Figure 3.5: Nonlinearity of Example 5

however, as the relay switching under noise is not exactly at ε therefore, the magnitude of $y(t)$ at the switching instant is measured and substituted in place of ε in the equations to find the a and b. For this example, the presumed hysteretic widths eliminated chattering, in cases where it doesn't, the hysteretic width (ε) should be changed accordingly. The different system parameters are found as $a = 1.0827$, $b = 2.0448$, $\theta = 1.1067$ and the nonlinearity calculated as $v(t) = 1.6255u - 0.4906u^2 + 0.0841u^3 - 0.0328u^4 + 0.0078u^5$. The estimated nonlinearity is plotted in Figure 3.5 which shows that the nonlinearity under noise didn't drift apart much from the actual one. However, this example doesn't guarantee a consistent accuracy of estimation under measurement noise for all Hammerstein systems. Proper analysis of the effect of measurement noise can be studied by sensitivity and convergence analysis of the equations involved in finding the time constants and the intermediate signal $v(t)$ (for all cases of linear subsystems) which is not under the scope of the present work. The model validation is done using ISE by giving a zero-mean Gaussian noise input for $100s$ with variance 0.5. The result is tabulated in Table 3.6. It can be seen that the ISE is high for the model estimated under noise therefore, the proposed method under noise needs more analysis in future works.

	Static non-linearity: $f(u)$	Linear subsystem: $G(s)$	ISE
Original model	$2(1-e^{-0.693u}) \simeq$ $-0.0003u^6 + 0.0027u^5 - 0.0192u^4 +$ $0.1109u^3 - 0.4802u^2 + 1.3860u$	$\frac{e^{-s}}{(s^2+2s+5)}$	
By proposed method	$1.4337u - 0.4784u^2 + 0.1097u^3 -$ $0.0229u^4 + 0.0031u^5$	$\frac{e^{-1.002s}}{(s^2+2.04s+5.08)}$	$0.3842 \times$ 10^{-3}
Under 20dB noise	$1.6255u - 0.4906u^2 + 0.0841u^3 -$ $0.0328u^4 + 0.0078u^5$	$\frac{e^{-1.1067s}}{(s^2+2.16s+5.35)}$	$26.67 \times$ 10^{-3}

Table 3.6: System identification results of Example 5

Example 6: SOPDT unstable

The same linear unstable system studied in Chapter 2 has been studied here which was earlier studied by Ramakrishnan and Chidambaram [51] and is given as

$$G(s) = \frac{e^{-0.5s}}{(2s-1)(0.5s+1)}$$

Rearranging $G(s)$ to bring it in the form of (3.3) gives

$$G(s) = \frac{(-1)e^{-0.5s}}{(-2s+1)(0.5s+1)}$$

With a relay setting of $\varepsilon = 0.2$ and $h = 1$, the system gives a sustained oscillation which is shown in Figure 3.6. The delay is measured as $\theta = 0.5004$ using Majhi [43]'s method. The various time instances, amplitudes and derivatives are measured. Using Equations (3.17), (3.23) the time constants are calculated as $T_1 = -1.998$, $T_2 = 0.486$ which are a close approximation of the modified $G(s)$'s time constants, -2, 0.5. The intermediate signal's amplitudes are measured as $v_1 = -0.9998$ and $v_2 = -1.0005$, taking the average gives -1.00015. As described in Section 3.3, the static gain is calculated as $\frac{v_1}{h}$ or $\frac{v_2}{h}$ which on averaging gives -1.00015. Therefore the estimated model is

$$G(s) = \frac{(-1.00015)e^{-0.5004s}}{(-1.998s+1)(0.486s+1)}$$

which is when rearranged gives the identified model in the required form as

$$G(s) = \frac{(1.00015)e^{-0.5004s}}{(1.998s-1)(0.486s+1)}$$

Ramakrishnan and Chidambaram [51] used a method that utilizes both time and frequency domain calculations which is elaborate. The proposed method is straight forward, requires fewer measurements and calculations. A comparison of estimated values by both the methods are listed in Table 3.7.

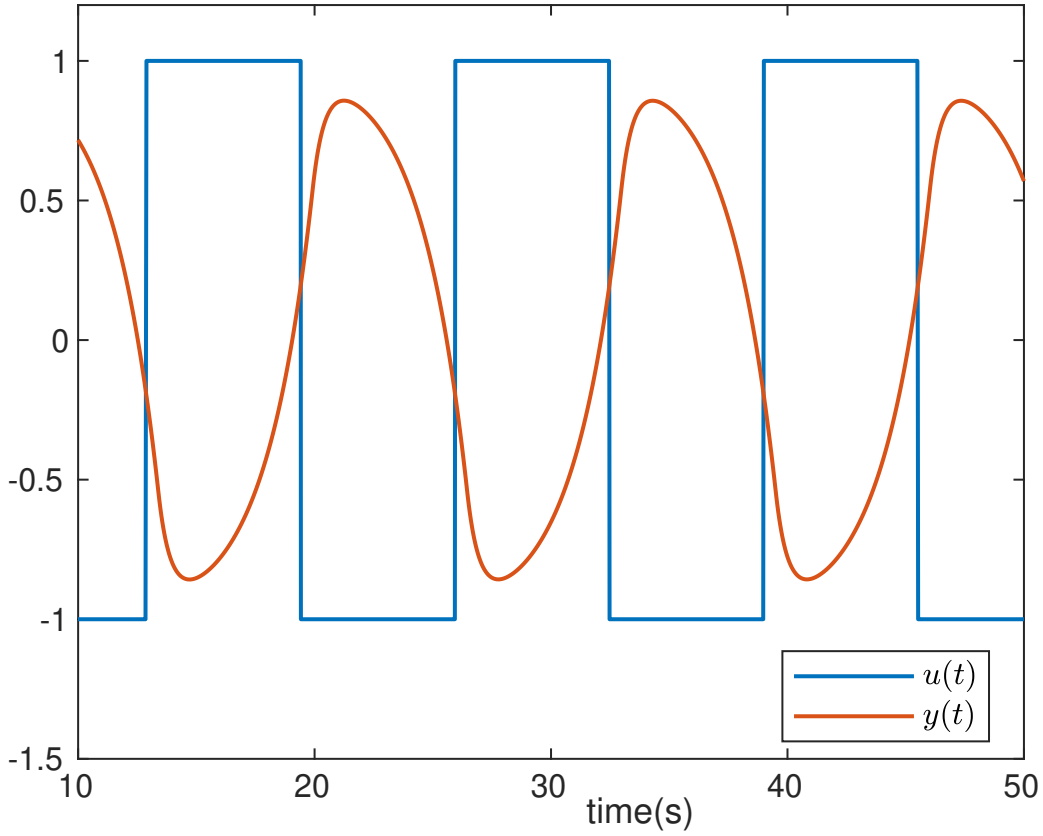

Figure 3.6: Limit cycle oscillation of unstable SOPDT system in Example 6

	Linear System: $G(s)$	%error in T_1	%error in T_2	%error in θ
Original model	$\frac{e^{-0.5s}}{(2s-1)(0.5s+1)}$			
By Ramakrishnan and Chidambaram [51]	$\frac{e^{-0.52s}}{(1.9999s-1)(0.4837s+1)}$	0.005	3.26	4
By proposed method	$\frac{(1.00015)e^{-0.5004s}}{(1.998s-1)(0.486s+1)}$	0.1	2.8	0.08

Table 3.7: System identification results of Example 6

Example 7: integrator

A Hammerstein model with an integrator is taken as an example with the following dynamics

$$\textit{Static nonlinearity:} \quad v = \frac{3u}{u^2+1}$$

$$\textit{Linear subsystem:} \quad G(s) = \frac{e^{-s}}{5s}$$

With a relay height $h = \pm 1$ and width $\varepsilon = \pm 0.2$, the required time instances on the limit cycle are measured as $t_{\varepsilon p} = 0.667, t_1 = 1.66745$. The required amplitudes are measured as $\dot{y}(t_{\varepsilon p}) = \dot{y}(t_{\varepsilon m}) = 0.3$. As proposed in subsection 3.2.1, the time constant in solving the Equation (3.39) of the FOPDT case gives a very high value of $T_1 = -785$. The result is in accordance to the assumption proposed in subsection 3.2.1 in the integrator case.

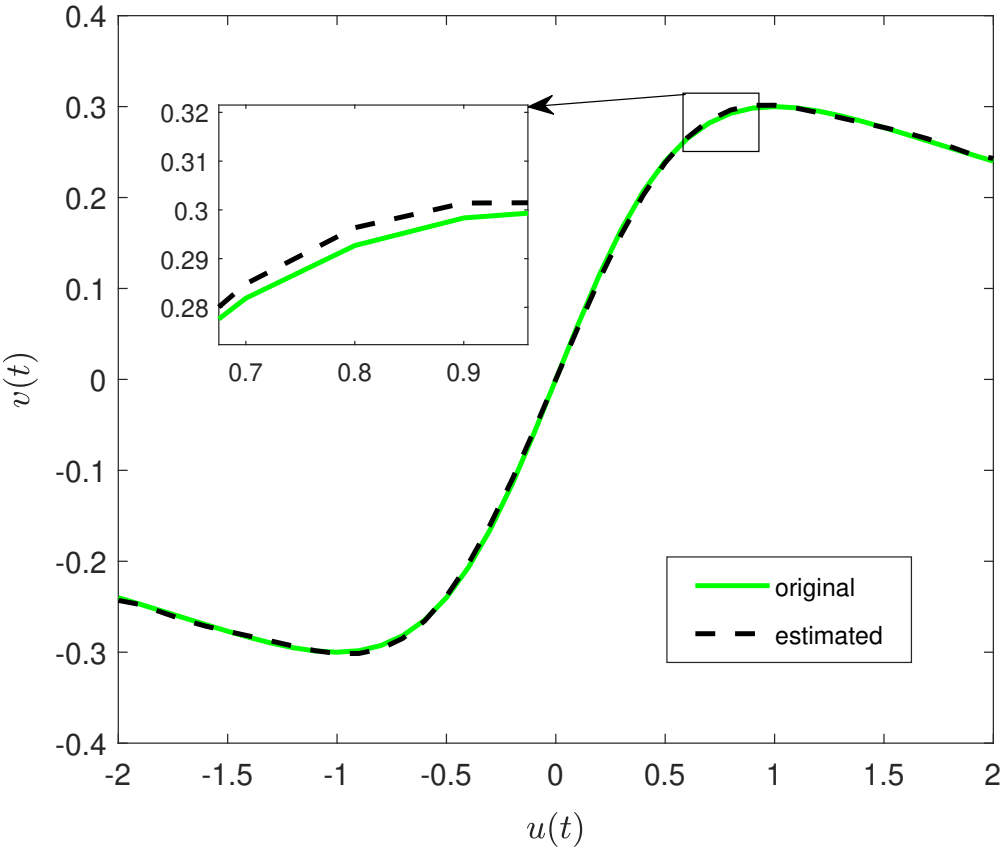

Figure 3.7: Nonlinearity of Example 7

The static nonlinearity is estimated by setting the relay heights to Chebyshev nodes with $l = 5$. Therefore, 11 numbers of interpolating points on the nonlinear curve are calculated or in this case simply measured as $v_1 = \dot{y}(t_{\varepsilon p})$, $v_2 = \dot{y}(t_{\varepsilon m})$ from Equations (3.56), (3.57). The various relay height inputs were $h = [-1.98, -1.82, -1.52, -1.08, -0.56, 0, 0.56, 1.08, 1.52, 1.82, 1.98]$ and the corresponding intermediate signal is measured as $v = [-0.2414, -0.2532, -0.2755, -0.2991, -0.2558, 0, 0.2558, 0.2991, 0.2755, 0.2532, 0.2414]$. The nonlinearity is plotted in Figure 3.7. Note that the static linear gain $\frac{1}{5} = 0.2$ is included in the nonlinearity, it is not calculated separately. The performance of the identified system is measured by giving a Gaussian white

input for 100 seconds having 0.5 variance and measuring the corresponding ISE. The result is tabulated in Table 3.8.

It can be noted that the nonlinearity in this example is not monotonic. Each identification step with a perticular relay height gives two points of the nonlinearity. The changing slope of the nonlinearity doesn't affect the identification procedure as the typical output graph used for all calculation in Figure 3.2 stays unchanged. Therefore, the proposed identification method works for nonmonotonic nonlinearity as well.

	Static non-linearity: $f(u)$	Linear subsystem: $G(s)$	ISE
Original model	$\frac{3u}{u^2+1} \simeq -0.0090u^{11} + 0.0563u^9 - 0.1910u^7 + 0.3931u^5 - 0.5459u^3 + 0.5955u$	$\frac{e^{-s}}{5s}$	
By proposed method	$0.0030u^9 - 0.0361u^7 + 0.1689u^5 - 0.4014u^3 + 0.5671u$	$\frac{e^{-1.00045s}}{s}$	0.01836

Table 3.8: System identification results of Example 7

Example 8: nth order system

A $5th$ order Hammerstein model studied in this example is the one previously studied by Lee et al. [1] which is given as

$$\textit{Static nonlinearity:} f(u) = 1.5(1 - e^{-0.5u}) \mid u \mid$$

$$\textit{Linear subsystem:} G(s) = \frac{e^{-s}}{(s+1)^2(2s+1)^3}$$

The fifth order system is identified as a repeated second-order as well as a repeated third order model as in equation (3.58). Therefore, the method described in Section 3.3 is used for the identification. The identification is done for the operating range $u \in (-1,1)$ with 7 Chebyshev nodes i.e., with relay heights $h = \{\pm 0.433885, \pm 0.78133, \pm 0.975\}$. For model order $n = 2$, the

equation for calculating $T_1 = -\frac{1}{a}$ is derived from (3.71) as

$$\frac{1-e^{at_{\varepsilon p}}(1-at_{\varepsilon p})}{1-e^{at_1}(1-at_1)} = \frac{\varepsilon - t_{\varepsilon p}\dot{y}(0)e^{at_{\varepsilon p}}}{A_1 - t_1\dot{y}(0)e^{at_1}} \tag{3.79}$$

Using the various measurements on the obtained limit cycles in above equation, the time constant is found as $T_1 = 2.5$ and the delay is measured as $\theta = 3.95$. Similarly, for model order $n = 3$, the equation for calculating T_1 is derived from (3.71) as

$$\frac{1-e^{at_{\varepsilon p}}\left(1-at_{\varepsilon p}+\frac{(at_{\varepsilon p})^2}{2}\right)}{1-e^{at_1}\left(1-at_1+\frac{(at_1)^2}{2}\right)} = \frac{\varepsilon - e^{at_{\varepsilon p}}\left(\dot{y}(0)t_{\varepsilon p}+\frac{t_{\varepsilon p}^2}{2}\left(\ddot{y}(0)-2\dot{y}(0)a\right)\right)}{A_1 - e^{at_1}\left(\dot{y}(0)t_1+\frac{t_1^2}{2}\left(\ddot{y}(0)-2\dot{y}(0)a\right)\right)} \tag{3.80}$$

Using the various measurements from the limit cycles in above equation, the time constant is found as $T_1 = 1.8868$ and the delay is measured as $\theta = 2.388$. The equations to find v_1 and v_2 for $n = 2$ are derived using Equations (3.72) and (3.77) as

$$v_1 = \frac{\varepsilon - t_{\varepsilon p}\dot{y}(0)e^{at_{\varepsilon p}}}{1-e^{at_{\varepsilon p}}(1-at_{\varepsilon p})} \tag{3.81}$$

$$v_2 = \frac{\varepsilon + (t_{\varepsilon m}-t_2)\dot{y}(t_2)e^{a(t_{\varepsilon m}-t_2)}}{1-e^{a(t_{\varepsilon m}-t_2)}\left(1-a(t_{\varepsilon m}-t_2)\right)} \tag{3.82}$$

Similarly for $n = 3$, the equations to find v_1 and v_2 are derived as

$$v_1 = \frac{\varepsilon - e^{at_{\varepsilon p}}\left(\dot{y}(0)t_{\varepsilon p}+\frac{t_{\varepsilon p}^2}{2}\left(\ddot{y}(0)-2\dot{y}(0)a\right)\right)}{1-e^{at_{\varepsilon p}}\left(1-at_{\varepsilon p}+\frac{(at_{\varepsilon p})^2}{2}\right)} \tag{3.83}$$

$$v_2 = \frac{\varepsilon + e^{a(t_{\varepsilon m}-t_2)}\left(\dot{y}(0)(t_{\varepsilon m}-t_2)+\frac{(t_{\varepsilon m}-t_2)^2}{2}\left(\ddot{y}(t_2)-2\dot{y}(t_2)a\right)\right)}{1-e^{a(t_{\varepsilon m}-t_2)}\left(1-a(t_{\varepsilon m}-t_2)+\frac{\left(a(t_{\varepsilon m}-t_2)\right)^2}{2}\right)} \tag{3.84}$$

The various points of the intermediate signal for $n = 2$ is calculated as $v = \{-0.9,$

$-0.5506, -0.158, 0, 0.129, 0.387, 0.58\}$ using Equations (3.81) and (3.82). Similarly, for $n = 3$ using Equations (3.83) and (3.84), $v = \{-0.9, -0.537234, -0.1526, 0, 0.124854, 0.3695, 0.5655\}$. It is interesting to note that the intermediate signal stays unchanged for any change in the model order, n. The identified system is validated using random Gaussian noise with variance 0.5 as test signal applied for 100 seconds. All results are tabulated in Table 3.9. It can be noted in this case that a second-order plus dead time linear subsystem is a better fit than a third order plus dead time.

	Static non-linearity ($f(u)$)	Linear subsystem ($G(s)$)	ISE
Original model	$1.5(1-e^{-0.5u})\|u\| \simeq$ $0.1580u - 0.0531u^2 + 0.9083u^3 +$ $+0.1874u^4 - 0.2885u^5 + 0.0486u^6$	$\frac{e^{-s}}{(s+1)^2(2s+1)^3}$	
By Lee et al. [1]	$0.266u - 0.038u^2 + 0.511u^3 - 0.163u^4$	$\frac{e^{-3.82s}}{(2.74s+1)(2.63s+1)}$	0.481
By proposed method with $n = 2$	$0.1850u - 0.0465u^2 + 0.8163u^3 -$ $0.1706u^4 - 0.2235u^5 + 0.0447u^6$	$\frac{e^{-3.95s}}{(2.5s+1)^2}$	0.051
By proposed method with $n = 3$	$0.1865u - 0.0396u^2 + 0.7359u^3 -$ $0.1901u^4 - 0.1488u^5 + 0.0492u^6$	$\frac{e^{-2.38s}}{(1.88s+1)^3}$	0.161
By proposed method in Section 3.2.1	$0.1844u - 0.0447u^2 + 0.8149u^3 -$ $0.1993u^4 - 0.2328u^5 + 0.06u^6$	$\frac{e^{-2.95s}}{(2.45s+1)^2}$	0.066

Table 3.9: System identification results of the Hammerstein model in Example 8.

For a cross-check, using the same limit cycle measurements, the system is identified using the repeated root case described in Section 3.2.1. It can be observed in the Table 3.9 that both the proposed methods gives close estimates, while Section 3.2 is specific only to second-order systems, Section 3.3 is for generalised nth order systems. This result further validates the accuracy of both methods.

3.6 Discussion

3.6.1 Online Identification and Complexity

A flowchart describing the entire identification procedure of Section 3.2 is shown in Figure 3.8. Unlike the identification of the Wiener model, identifying the Hammerstein model requires more than one relay test. However, the relay heights can be preset to Chebyshev nodes (see Appendix A) which makes it convenient for online application. Looking at the flowchart in Figure 3.8, the complexity in identification may arise while solving the nonlinear equations to find the time constants in stage (iii). In this work, the graphical method is used to solve the nonlinear equations however other methods should be chosen when time is an essential factor. Also, one can get rid of calculating the time constant for every relay test when time constraint is more essential than accuracy. Comparing the flowchart of Figure 2.9 to that in Figure 3.8, identifying the Hammerstein model is more elaborate compared to identifying the Wiener model however, the complexity remains almost the same.

3.6.2 Existence of Solution and Convergence

The various parameters of the Hammerstein model that has been identified are delay, time constants, and the coefficients of the polynomial nonlinearity. As stated in Section 3.2, the delay is measured independently using the experimental method of Majhi [43]. While in Wiener model identification, the derivative of output was required only to calculate delay here in identifying Hammerstein model derivatives are required for calculating the time constants as well which is a major drawback in presence of noise. Therefore a good noise removal technique is needed. While wavelet transform based denoising worked fine in the simulation examples, it is advised to select a good denoising technique according to specific applications.

For checking the existence of solution, let us consider the equation for finding time constant in the first-order case i.e., (3.39). To simplify the calculation, let us put $\frac{1}{T_1} = a$ by setting $b = 0$ in

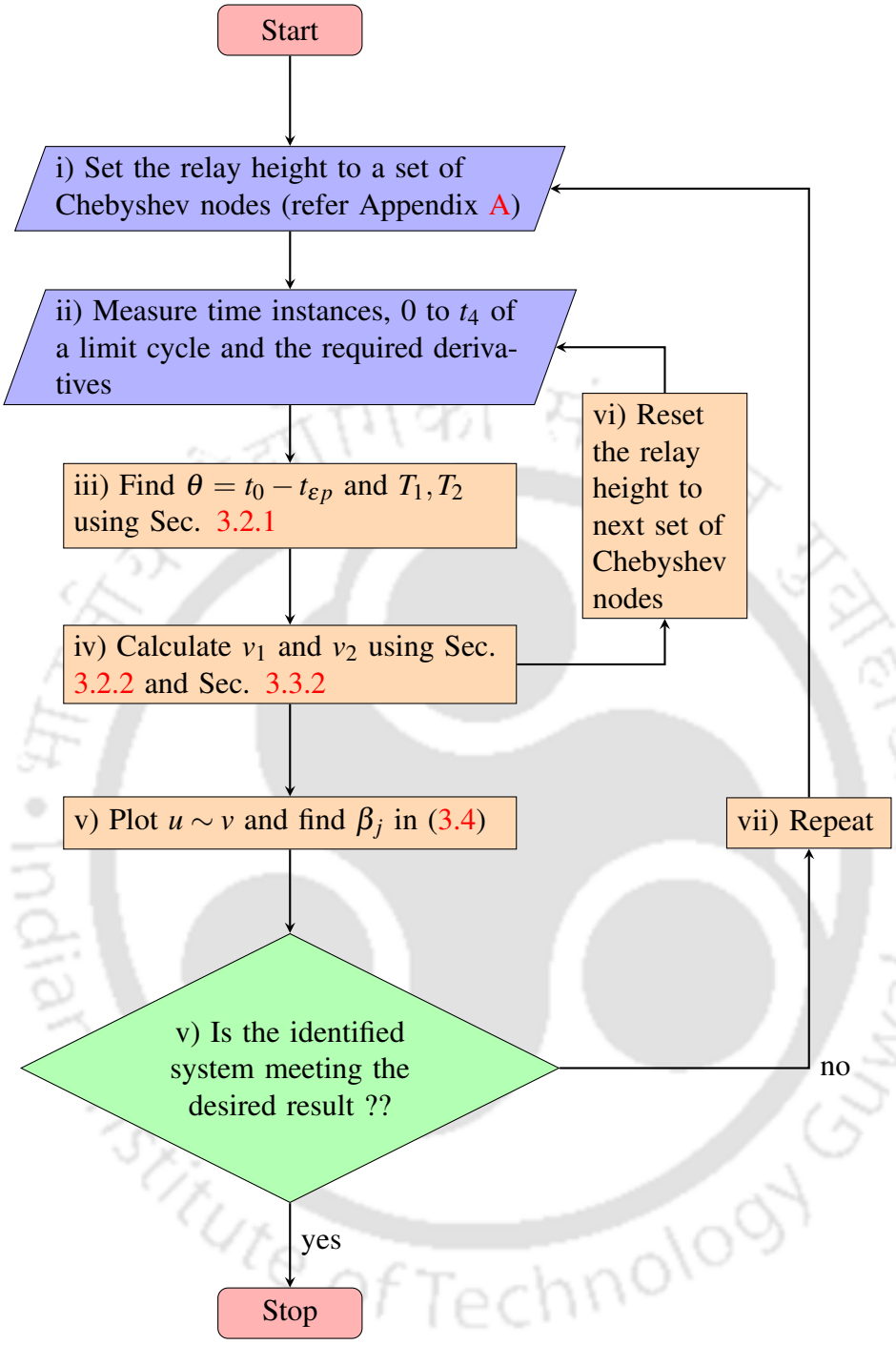

Figure 3.8: Flowchart explaining the steps involved in the Hammerstein model identification process

(3.24) and then rearranging (3.39) accordingly

$$F(a) = e^{at_{\varepsilon p}} - \left(1 + \frac{\varepsilon a}{\dot{y}(t_{\varepsilon p})}\right) = 0 \tag{3.85}$$

It is evident that $a = 0$ is a solution of (3.85) therefore, the curve $F(a)$ will pass through the origin. Now, differentiating $F(a)$ with respect to a,

$$\dot{F}(a) = 0 \qquad \Rightarrow \qquad a^* = \frac{1}{t_{\varepsilon p}} \ln \left| \frac{\varepsilon}{t_{\varepsilon p} \dot{y}(t_{\varepsilon p})} \right| \tag{3.86}$$

Therefore, a^* is the only critical point of $F(a)$. Now, evaluting the second derivative of $F(a)$,

$$\ddot{F}(a) = t_{\varepsilon p}^2 e^{a t_{\varepsilon p}} \tag{3.87}$$

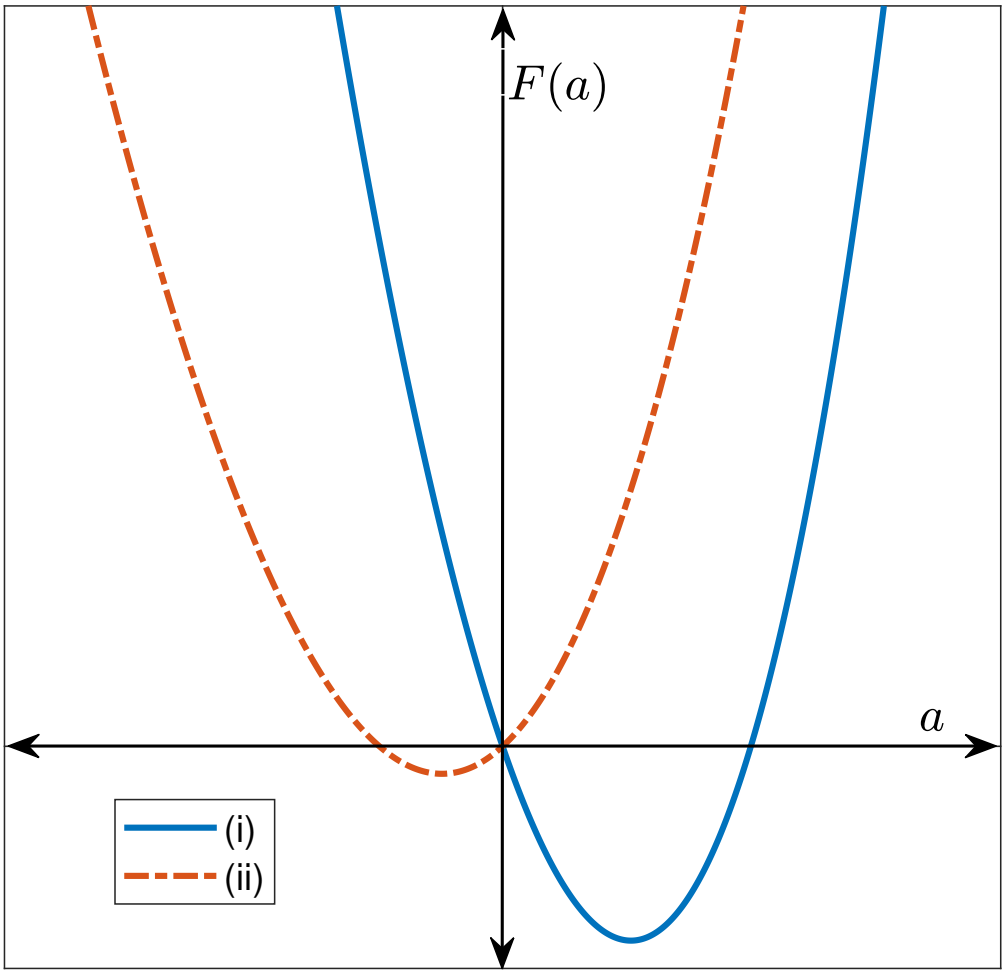

Figure 3.9: Graph of $F(a)$ in (3.85) - (i) of an stable system. (ii) of a unstable system.

Therefore, the second derivative in Equation (3.87) will be positive for all values of a hence the critical point a^* is a global minimum. Going by the similar arguments made in Subsection

2.5.2, there are only two possible solutions for $F(a) = 0$: first, when the minimum peak is below $F(a) = 0$, the curve will intersect it somewhere other than the origin which will be the solution, second, when the minimum peak is touching the origin then $a = 0$ is the only solution which defines a system with a very high time constant. The graph plot in Figure 3.9 can be referred to for the analysis. The graph shows the plot for both stable and unstable systems. However, the rate of convergence will depend on the procedure used to solve the non-linear equations to find the time constants. In this work, the equations are solved in MATLAB by plotting graphs for better accuracy. However, numerical methods are suggested for online applications and applications with time constraints. A similar geometrical analysis can be done to prove the existence and uniqueness of equations to find time constants for all other cases as well.

3.6.3 A discussion on the static nonlinearity

For a Hammerstein model, the static nonlinearity comes just after the relay which means it simply acts as a relay bias. Therefore, the limit cycle oscillation at the output as shown in Figure 3.2 will be unaffected by the slope change of the input nonlinearity. Figure 3.2 is the key upon which the entire identification procedure relies and it stays unchanged with the changing slope of the nonlinearity. Therefore, as long as the static nonlinearity is continuous and passive, the identification procedure will work. Hence, monotonicity is not a necessity. However, it is true only for small time delay systems as the limit cycle in Figure 3.2 may have ripples with large time delay.

3.7 Summary

Following the identification procedure for the Wiener model, a very similar procedure for the Hammerstein model has also been developed. Similar to the Wiener model case, first a Hammerstein model with SOPDT linear subsystem has been identified. The method is then extended into a somewhat generalized nth order linear subsystem case. Various examples are from the literature that is simulated and the results are analyzed. A brief discussion on online identification

and the existence of a solution has also been done. A linear system is a special case of both the Wiener and the Hammerstein model, can also be identified with the same procedures developed for both the models. However, it is found that identifying a Linear system as a Hammerstein model is more convenient than identifying it as a Wiener model as it requires fewer calculations and measurements.

Chapter 4

Hammerstein Model of a Buck Converter

This chapter is an attempt at discussing the practical applicability of the developed method in Chapter 3 in which various Hammerstein models are identified. It is well known that power electronic switching converters display nonlinear behaviors. Therefore, a non-ideal buck converter has been taken as an example. The Hammerstein model consists of a static non-linearity succeeded by a linear subsystem. In a buck converter, the PWM (pulse width modulating) generator, MOSFET, and the diode are the main sources of non-linearities. As these components immediately follow after the gate signal which is considered as the control input, it is heuristically assumed that a Hammerstein model would be a better choice. Also, this assumption is partly influenced by the previous works of Balestrino et al. [68] and Alonge et al. [69]. The purpose of the implementation of a non-ideal buck converter is to show the possible practical applicability aspects of an alternative approach of identification proposed in this work. It is stressed here that the authors are refraining from concluding anything on the non-linear behavior of converters in general or any comparisons to the vast numbers of identification approaches that have been developed in the literature.

There is a vast literature for various circuit oriented averaging models of switching converters since the elemental work of Wester and Middlebrook [70]. Middlebrook and Cuk [71] worked on unifying the state space based averaging approach developed by Wester and Middlebrook [70]. Further advance works on averaging techniques are carried out by Hsu et al. [72], Pietkiewicz and Tollik [73], Czarkowski and Kazimierczuk [74], Davoudi et al. [75]. These models have

the drawback that they are linearized and hence assumes lots of restrictions on the operating conditions due to which non-linear modeling approaches are developed. Some significant works on nonlinear modeling of the buck converter are done by Tymerski et al. [76], Hamill et al. [77], Tse and Adams [78], Balestrino et al. [68], Alonge et al. [69].

Balestrino et al. [68] are the first to use relay feedback as well as Hammerstein modeling for the identification of a buck converter. They applied the nonlinear auto-tuning method developed by Luyben and Eskinat [15] on the buck converter identification. Although there are a few works on the identification of buck converter using relay feedback (Stefanutti et al. [79], Zhao and Prodi [80], Ramana et al. [81]), they are limited only to small-signal modeling and linearization. Alonge et al. [69] identified the Hammerstein model for a buck converter with the linear subsystem as time-invariant ARX model, they used a pseudo-random binary sequence input for modeling purposes. Since the work by Balestrino et al. [68] on nonlinear identification of buck converter using relay feedback, to the author's knowledge there has been no work done in this field. Therefore, the proposed Hammerstein model identification developed in Chapter 3 is used here to identify a buck converter which is much simpler and straight forward compared to the previous work of Balestrino et al. [68].

The work presented in this chapter has been published in [82].

4.1 Buck Converter Operation

A buck converter is used to step down DC voltage in various power electronics circuits. The elementary circuit of an ideal buck converter is shown in Figure 4.1 where all the elements are considered to be ideal i.e., no voltage drop across the diode or the inductor. V_i is the input voltage which is usually fixed, $v_o(t)$ is the output voltage and $d(t)$ is the control input. A buck converter operates on fast switching i.e., it connects and disconnects the source and load at fast speed. In this manner, it achieves a chopped load voltage at the output from a constant DC input. The typical output voltage and current waveforms are given in Figure 4.2. The time periods of switching on and off are T_{on} and T_{off} in Figure 4.2. The total switching time period is $T_s = T_{on} + T_{off}$ and the

switching frequency is $f_s = \frac{1}{T_s}$. When the switch is on during the period T_{on}, the load voltage is equal to the source voltage V_i. When the switch is off during the period T_{off}, load current flows through the diode hence the load terminal is short-circuited and the load voltage is therefore zero. This is how a chopped DC voltage is produced at the load terminal. As shown in Fig 4.2, the load current is continuous however, in some cases falls to zero during part of the time period. When the current is continuous it is called continuous conduction mode (CCM) when it is discontinuous it is called the discontinuous conduction mode (DCM). In this work, only the CCM mode has been considered.

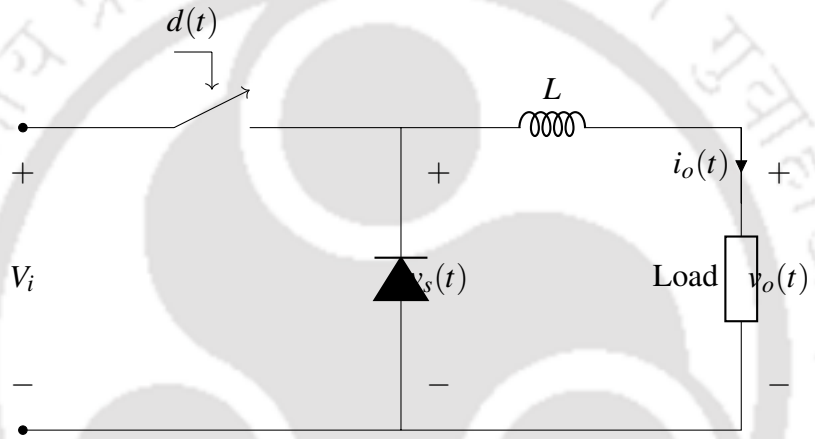

Figure 4.1: Elementary ideal buck converter

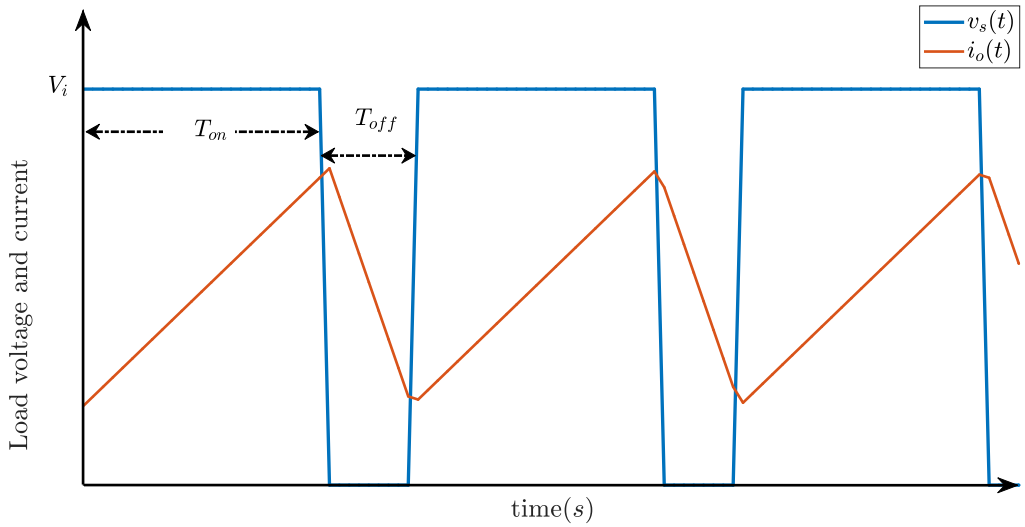

Figure 4.2: Load voltage and current waveform of an elementary ideal buck converter in CCM mode.

From Figure 4.2, the average voltage of $v_s(t)$ can be written as

$$\bar{v}_s = \frac{T_{on}}{T_s} V_i = dV_i \tag{4.1}$$

where, $d = \frac{T_{on}}{T_s}$ is called the duty cycle which is used to control the load voltage. A low pass filter is added at the output in the circuit of Figure 4.1 to pass the dc component of $v_s(t)$ and to reject its component at its switching frequency and its harmonics [83]. The output voltage is then nearly equal to the dc component of $v_s(t)$

$$v_o(t) \approx \bar{v}_s = dV_i \tag{4.2}$$

There are various control strategies to vary d however in this research the PWM scheme has been utilized. From Equation (4.2), the output voltage is directly proportional to the control input d however, this is not the case in a non-ideal buck converter. In reality, the various circuit components of the buck converter are not ideal. A non-ideal buck converter circuit is shown in Figure 4.3 which considers voltage drop across various circuit components.

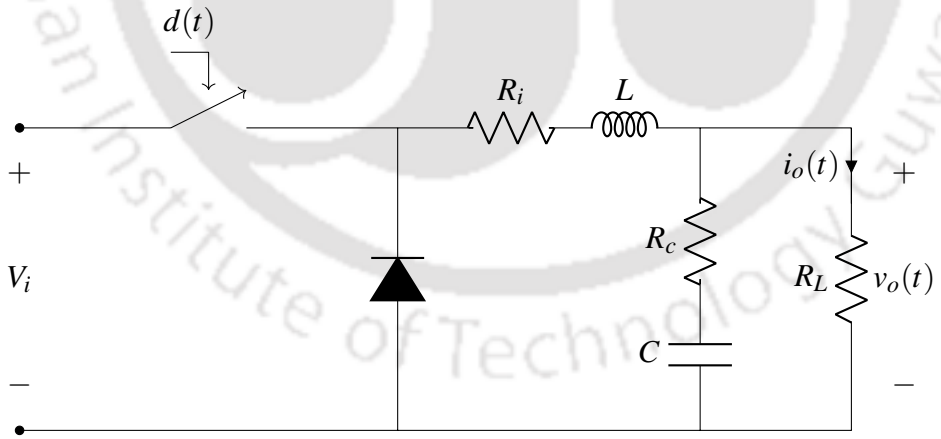

Figure 4.3: Elementary non-ideal buck converter

For control purposes, the control-to-output transfer function is required to be calculated. State space averaging technique is the most popularly used technique to find this transfer function. Considering the variation in duty cycle while the input voltage remaining constant, the control-

to-output transfer function using the state space averaging can be derived as

$$G_{vd}(s) = \frac{V_o(s)}{D(s)} = \frac{\lambda R_L(R_c C s + 1)V_i}{R_L C L s^2 + ((\lambda R_c + R_i)R_L C + \lambda L)s + \lambda(R_i + R_L)} \tag{4.3}$$

where $\lambda = \frac{R_L}{R_L + R_C}$. This transfer function describes how the average output voltage v_o varies with the variation in control input d. In an output voltage regulator system, $G_{vd}(s)$ has a key role on regulator performance evaluation. For the detailed derivation of the above equation, Chapter 8 of the book by Erickson and Maksimovic [83] is recommended.

4.2 Identification Setup and Model

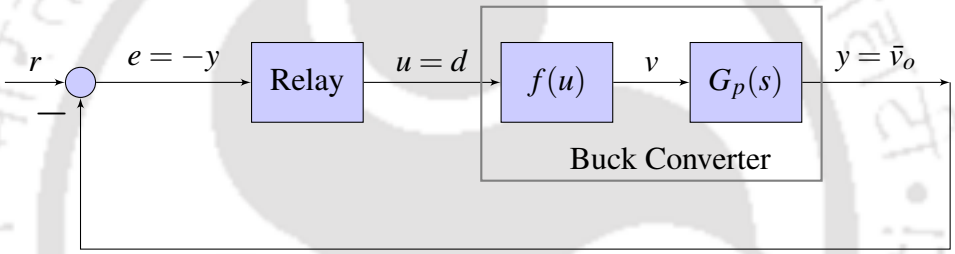

Figure 4.4: Setup used for the identification of the buck converter

The general setup used for the buck converter identification is shown in Figure 4.4 which is the same as any general relay feedback setup. The buck converter is considered to be a Hammerstein model. A Hammerstein model consists of a static nonlinearity followed by a linear subsystem. The input signal $u(t)$ in Figure 4.4 is physically the control input to the converter i.e., the duty cycle ratio. The output signal $y(t)$ is physically the output voltage $v_o(t)$ across the load. The intermediate signal $v(t)$ doesn't represent any physical signal in the buck converter circuit but it can be thought of as an intermediate voltage as suggested by Balestrino et al. [68] therefore, $v(t)$ is immeasurable. The reference signal r is not taken zero here because $u = 0, y = 0$ can not be taken a reference for oscillation as the duty ratio, $u = d$ never assumes negative values. Consequently, the relay characteristics need to be modified to get relay heights in the limit of the duty ratio variations i.e., $0 \leq u \leq 1$. The characteristics of the new relay are shown in Figure 4.5 where d_r is the reference control input and the relay height $\pm h$ is chosen in a way that $0 \leq 2h \leq 1$

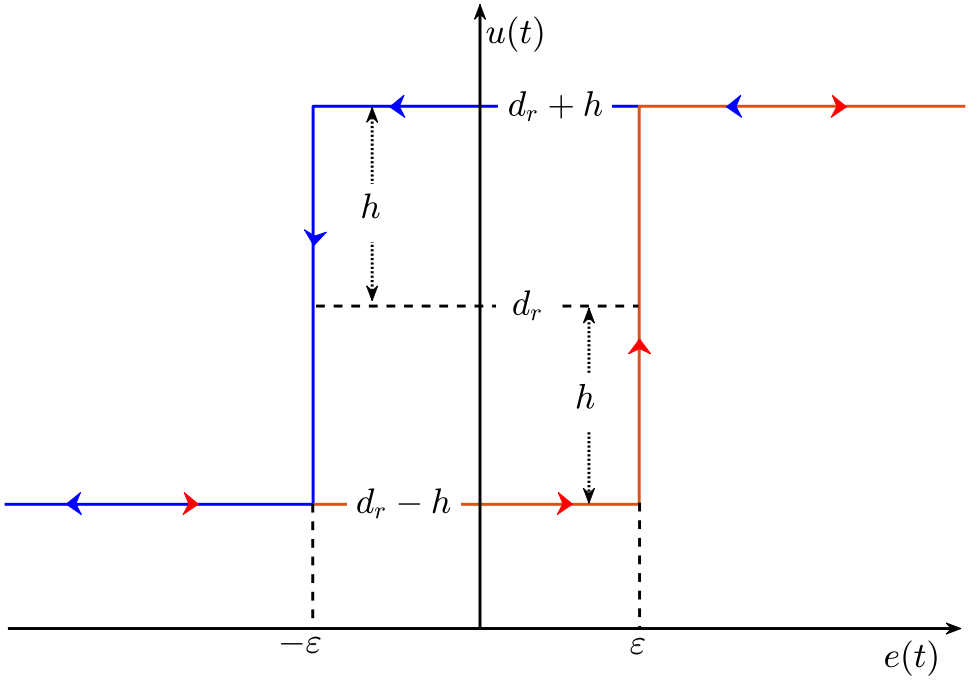

Figure 4.5: Modified relay characteristics to be used for the buck converter identification.

always.

From the average model in (4.2), it is well known that a buck converter has two left half poles and a right half zero. However, the proposed Hammerstein model identification in the previous Chapter 3 doesn't consider transfer functions with zeros. Therefore, the linear subsystem is considered as a SOPDT model having complex conjugate roots as it is well known that a buck converter's step response usually shows under-damped characteristics. As the main objective of this research is to study the static nonlinear characteristic rather than the transient behavior, this assumption of transfer function suffices the goal without any significant diversion from the actual system. Hence, the transfer function of the linear subsystem is taken as

$$G_p(s) = \frac{e^{-\theta s}}{(s+a+\mathrm{i}b)(s+a-\mathrm{i}b)} \tag{4.4}$$

where $a \pm \mathrm{i}b$ are the complex poles and θ is the time delay. The static gain is taken one as its effect can be considered along with the static nonlinearity which is considered as a polynomial of

the form described in Chapter 3 as

$$f(u(t)) = \sum_{j=0}^{p} \beta_j u^j(t) \tag{4.5}$$

where β_j's are constants and p is the order of the polynomial. The overall system dynamics of the Hammerstein system in Figure 4.4 can be written as

$$y(t) = \mathbf{C}\mathbf{X}(t) \tag{4.6}$$

$$\dot{\mathbf{X}}(t) = \mathbf{A}\mathbf{X}(t) + \mathbf{B}v(t-\theta) \tag{4.7}$$

$$v(t) = f(u(t)) \tag{4.8}$$

where,

$$\mathbf{A} = \begin{bmatrix} -a - \mathrm{i}b & 0 \\ 0 & -a + \mathrm{i}b \end{bmatrix}; \qquad \mathbf{B} = \begin{bmatrix} 1 \\ 1 \end{bmatrix}$$

$$\mathbf{C} = \frac{a^2+b^2}{-2\mathrm{i}b} \begin{bmatrix} 1 & -1 \end{bmatrix}; \qquad \mathbf{X}(t) = \begin{bmatrix} x_1(t) \\ x_2(t) \end{bmatrix}$$

4.3 Proposed Identification Procedure

The identification is done using the proposed method in Section 3.2 of Chapter 3. The input voltage V_i is fixed as we are studying the control to output response. Then, the reference input and output points are chosen. If the reference control input is taken as $u = d_r$ then the corresponding output voltage should be taken as r. An ideal buck converter should give $v_o = d_r V_i$ however, as the buck converter is considered to be non-ideal this will no longer hold. Thus, a step response with $u = d_r$ as input is needed to find $v_o = r$. However, no separate arrangement for a step response test is required, simple manipulation of the relay characteristics can be done to find r. First, the reference is set at the ideal output $v_o = d_r V_i$ then the relay is set at heights 0 and d_r with width $\varepsilon \geq 0$ which gives an output like that of a step input i.e., a non-oscillatory steady-state output. If

the system was ideal, the steady-state value of $y-r$ in Figure 4.4 should have been zero however, it will be less than zero because of the losses. The loss is measured and subtracted from the ideal output $v_o = d_r V_i$, which gives the actual output $v_o = r$. Usually, in methods of identification using relay feedback, an oscillatory output is the one that is being used for identification purposes whereas, here the information from a non-oscillatory output is being exploited.

The unknown parameters of the Hammerstein model are the poles $a \pm ib$, the time delay θ, and the coefficients of the polynomial in (4.4). The detailed procedure to calculate these parameters are described in Section 3.2 which will be reviewed here. As all the calculations for the Hammerstein model identification are done considering origin as the reference point, therefore, to bring the input oscillation around the origin, d_r is subtracted from $u(t)$. Similarly, the output is measured simply by inverting the input signal to the relay which brings the output oscillation around the origin as well. The proposed method consists of two stages: in the first stage the linear subsystem of the Hammerstein model is identified then using the obtained data, the nonlinearity is estimated in the second stage.

Linear subsystem identification includes finding $G_p(s)$. Using various points on the typical output plot of a Hammerstein model in Figure 3.2, the state space equations i.e. (4.5), (4.6), (4.7) are solved. The various time instances on the typical output plot has been described in Section 3.2. The following sets of nonlinear equations are derived to find the values of the two unknowns a and b

$$\begin{aligned}\varepsilon(a^2+b^2)\sin(bt_{\varepsilon p}) + a(\dot{y}(t_{\varepsilon p}) - \dot{y}(0))\sin(bt_{\varepsilon p}) + b(\dot{y}(t_{\varepsilon p}) + \dot{y}(0))\cos(bt_{\varepsilon p}) \\ = b\left(\dot{y}(t_{\varepsilon p})e^{at_{\varepsilon p}} + \dot{y}(0)e^{-at_{\varepsilon p}}\right)\end{aligned} \tag{4.9}$$

$$y(t_1)(a^2+b^2)\sin(bt_1) - \dot{y}(0)\Big(a\sin(bt_1) - b\cos(bt_1)\Big) = b\dot{y}(0)e^{-at_1} \tag{4.10}$$

$$y(t_1)(a^2+b^2)\sin\Big(b(t_2-t_1)\Big)+\dot{y}(t_2)\left(a\sin\Big(b(t_2-t_1)\Big)+b\cos\Big(b(t_2-t_1)\Big)\right) = b\dot{y}(t_2)e^{a(t_2-t_1)} \tag{4.11}$$

Along with equation (4.8), equations (4.9)/(4.10) are chosen based on the position of the peak of the output relative to the relay switching. In the plot of Figure 3.2, when $t_1 \leq t_0$, equations (4.8) and (4.9) are solved for finding a,b. Similarly, when $t_1 \geq t_0$, equations (4.8) and (4.10) are solved for finding a,b. To measure time delay θ, the procedure mentioned by Majhi [43] is used.

In a buck converter, the output voltage, v_o increases with the increase in the control input i.e., the duty ratio d. We are considering a nonlinear buck converter therefore, the increase in v_o with respect to d may not be linear however, it is monotonic. Thus, the nonlinearity can be estimated as a polynomial of the form in (4.4). The nonlinearity estimation includes finding the intermediate signal $v(t)$ and hence the polynomial in (4.4). The intermediate signal $v(t)$ is a square wave with asymmetric amplitudes v_1 and v_2 for positive and negative half cycles, respectively. Therefore, one relay test with a particular relay height gives two points on the polynomial curve $f(u)$ i.e., (h, v_1) and $(-h, -v_2)$. Thus, it is required to repeat the test half the number of times as the required number of points to be estimated on the polynomial. The equations for finding v_1 and v_2 is calculated in Section 3.2.2 as

$$v_1 = \frac{\dot{y}(t_{\varepsilon p})be^{at_{\varepsilon p}} + \dot{y}(0)\Big(a\sin(bt_{\varepsilon p}) - b\cos(bt_{\varepsilon p})\Big)}{\sin(bt_{\varepsilon p})} \tag{4.12}$$

$$v_2 = \frac{-\dot{y}(t_{\varepsilon m})be^{a(t_{\varepsilon m}-t_2)} + \dot{y}(t_2)\left(a\sin\Big(b(t_2-t_{\varepsilon m})\Big) + b\cos\Big(b(t_2-t_{\varepsilon m})\Big)\right)}{\sin\Big(b(t_2-t_{\varepsilon m})\Big)} \tag{4.13}$$

4.4 Simulation Results

The simulation of the buck converter identification is carried out in MATLAB's Simulink software. The set-up in the Simulink software is shown in Figure 4.6. The buck converter studied by

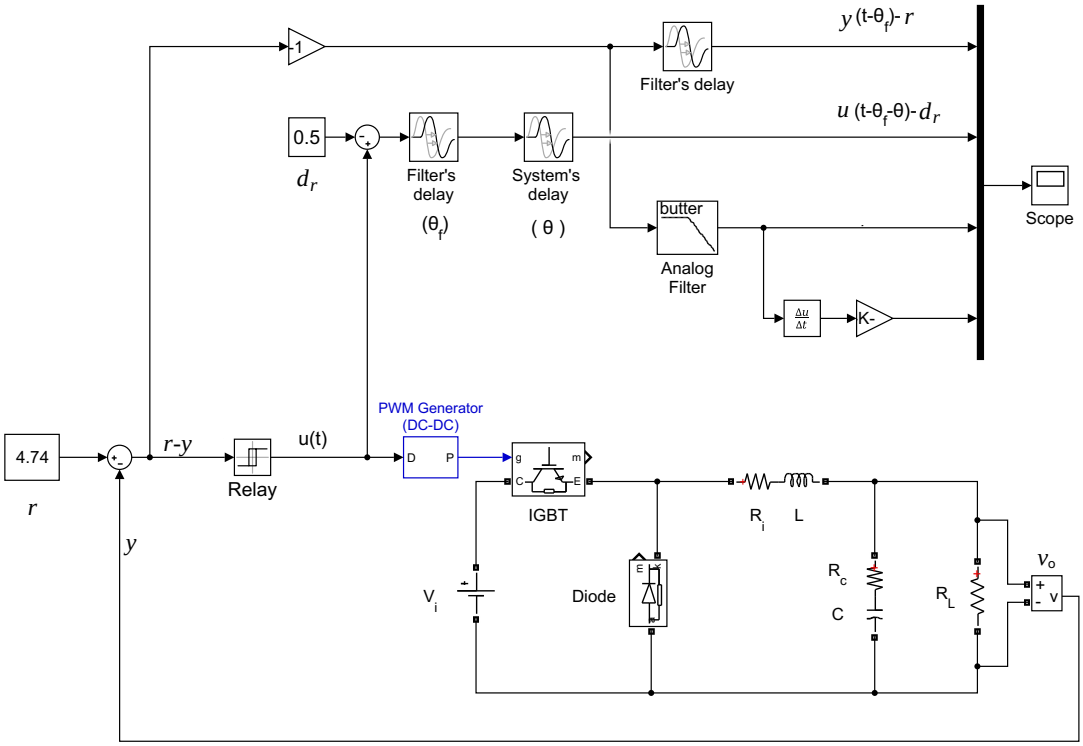

Figure 4.6: Simulink set-up used for buck converter identification

Ramana et al. [84] is considered whose specification is given in the Table 4.1.

In a buck converter, it is commonly known that the output voltage is linearly dependent on the duty ratio. However, upon simulating the specific above mentioned non-ideal buck converter, it is found that near the origin, the characteristics are not linear but for the rest of the operating region, it is linear as shown in Figure 4.7. For specific applications where the converter never operates near-zero duty ratio, it is not very efficient to identify a buck converter as a non-linear Hammerstein model. However, identifying it as a linear system is also not very useful. Every linear model like the average model will pass through the origin as $v_o = a_1 d$, where a_1 is any positive real constant. However, by extending the linear region of the buck converter towards the x-axis, it can be observed that it has a negative intercept which means it is a line of the type $v_o = a_1 d - a_0$ which defines an affine function, where a_1 and a_0 are positive real constants. Although any linear model would give a fair approximation of the buck converter's characteristics, however, at lower/higher (depending on the slope) values of the duty ratio the steady-state error will be high. The solution is to identify the system as a nonlinear or affine linear model which reduces the steady-state error. By the proposed method of identifying a Hammerstein model, an

Circuit parameter	Value
Input voltage(V_i)	10 V
Inductance(L)	560 μH
Inductor ESR (R_i)	0.12 Ω
Capacitance (C)	98 μF
Capacitor ESR (R_c)	0.365 Ω
Load Resistance (R_L)	10 Ω
Switching frequency (f_s)	20 kHz

Table 4.1: Buck converter specifications.

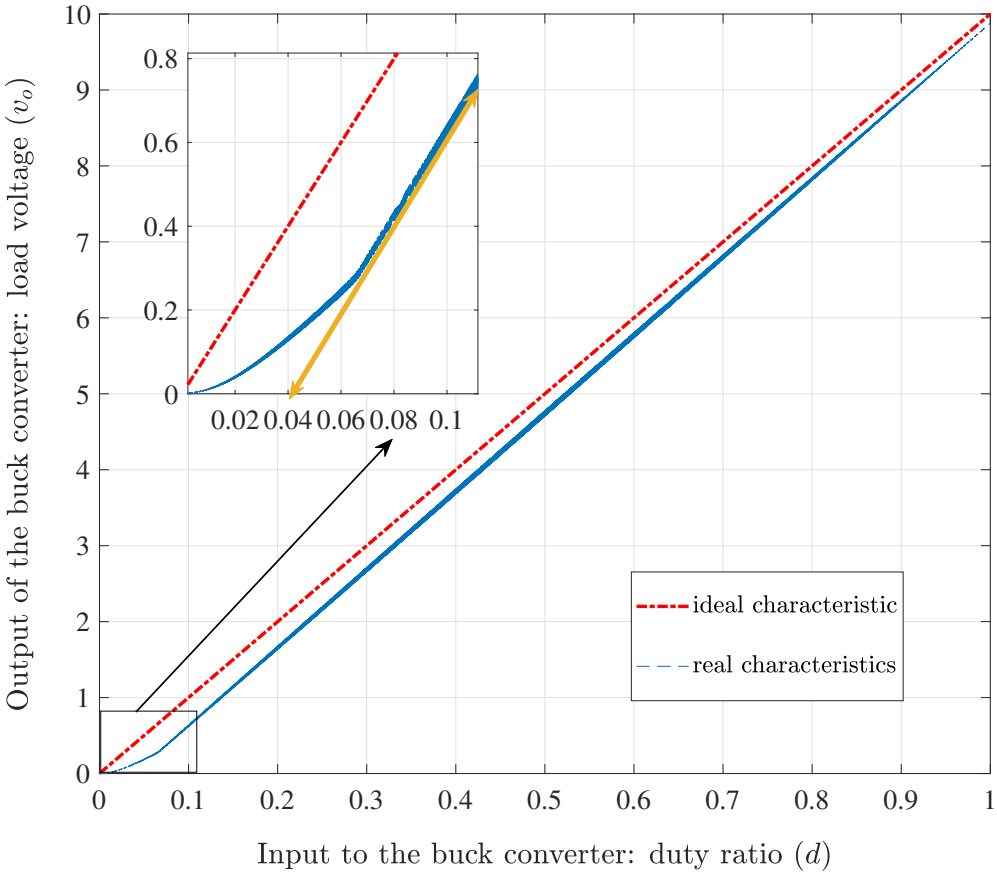

Figure 4.7: Nonlinear characteristics of the buck converter taken

affine linear model is possible with only two relay tests. However, a Hammerstein model with polynomial nonlinearity has also been identified.

As the output is not smooth due to the switching, an appropriate filter is used to get smoothness to compute the derivatives. The filter delay is measured as $\theta_f = 2 \times 10^{-5}$ sec. The reference duty cycle d_r is taken as 0.5, to bring the input oscillation around origin, $d_r = 0.5$ is subtracted from $u(t)$ as shown in the Figure 4.6. Similarly, the output is measured simply by inverting the input signal to the relay which is $y(t-\theta_f) - r$ which brings the output oscillation around the origin as well. The output voltage at $d_r = 0.5$ should be the reference voltage, r. An ideal buck converter should give $v_o = d \times V_i = 0.5 \times 10 = 5V$ however as the circuit is non-ideal, the reference voltage is measured by a relay test where the reference is set at the ideal output, i.e., $r = 5V$. The relay is set at heights 0 and 0.5 with a width $\varepsilon \geq 0$ which gives an output like that of a step input i.e., a non-oscillatory steady-state output. If the system was ideal, the steady-state value of $y(t-\theta_f) - r$ should have been zero however, it will be less than zero because of the losses. The loss is measured and subtracted from the ideal output (5V) which gives the actual output as $4.74V$. The output plot for this relay test is plotted in Figure 4.8.

Then the relay is set for parameter identification with the heights at 0.6 and 0.4 i.e., $h = 0.1$ in Figure 4.5 with the width ± 1. The delay is measured as $\theta = 2 \times 10^{-4}$. Using the observation results of the limit cycle, the parameters in (4.3) are measured as, $a = 4200$ and $b = 4372$. Hence, the linear subsystem is calculated as

$$G_p(s) = \frac{Y(s)}{V(s)} = \frac{V_o(s)}{D(s)} = \frac{e^{-2\times 10^{-4}s}}{s^2 + 8360s + 0.366 \times 10^8}$$

The intermediate signal $v(t)$ is 0 at the origin for all the calculations carried out for Hammerstein model identification. However, as the origin is not the reference point here, therefore, $v(t)$ at the reference point d_r is calculated from the above calculated transfer function as

$$v(0.5) = \frac{y|_{u=0.5}}{G_p(s)|_{s=0}} = r \times 0.366 \times 10^8 = 1.735 \times 10^8$$

Using (4.11) v_1 is calculated as 0.385×10^8 which is also v_2 as the system is linear around

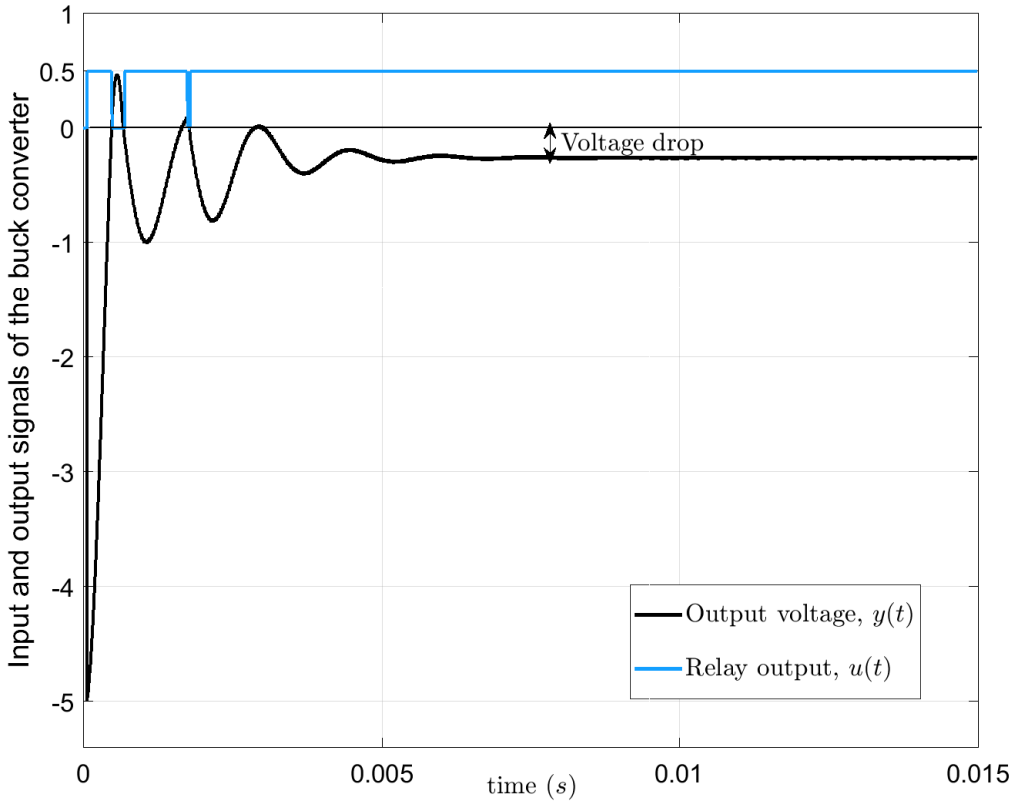

Figure 4.8: Relay feedback output for calculating the reference input, r

the operating point $d = 0.5, V_o = 4.74$. v_1 and $-v_2$ are added to the reference $v(0.5)$ to get the required points. Therefore, with $u = [0.4, 0.5, 0.6]$ and $v = 10^8 \times [1.35, 1.735, 2.12]$, the affine function is calculated as $v = 10^8(3.85u - 0.19)$.

Few more tests are done by increasing the relay height and changing its width accordingly. The result of these test is used to fit a polynomial instead of the affine function which is found to be $v = 10^8(-9.1346u^5 + 26.1582u^4 - 27.6945u^3 + 13.2244u^2 + 1.1085u)$. The transfer function of the buck converter is calculated using the formula in (4.2). The ramp and step response (for $d = 0.3$) characteristics of the identified models are shown in Figure 4.9 and Figure 4.10 which shows less steady-state error compared to the average model. Overall, estimating the non-linearity as an affine function fits more accurately compared to estimating it as a polynomial. However, near the origin i.e., when $0 \leqslant d \leqslant 0.1$, the polynomial fit is more accurate than the affine function; one can opt for either of the two based on their required operating region.

To compute the performance index, ISE, an uniform random signal varying from 0 to 0.95 (as

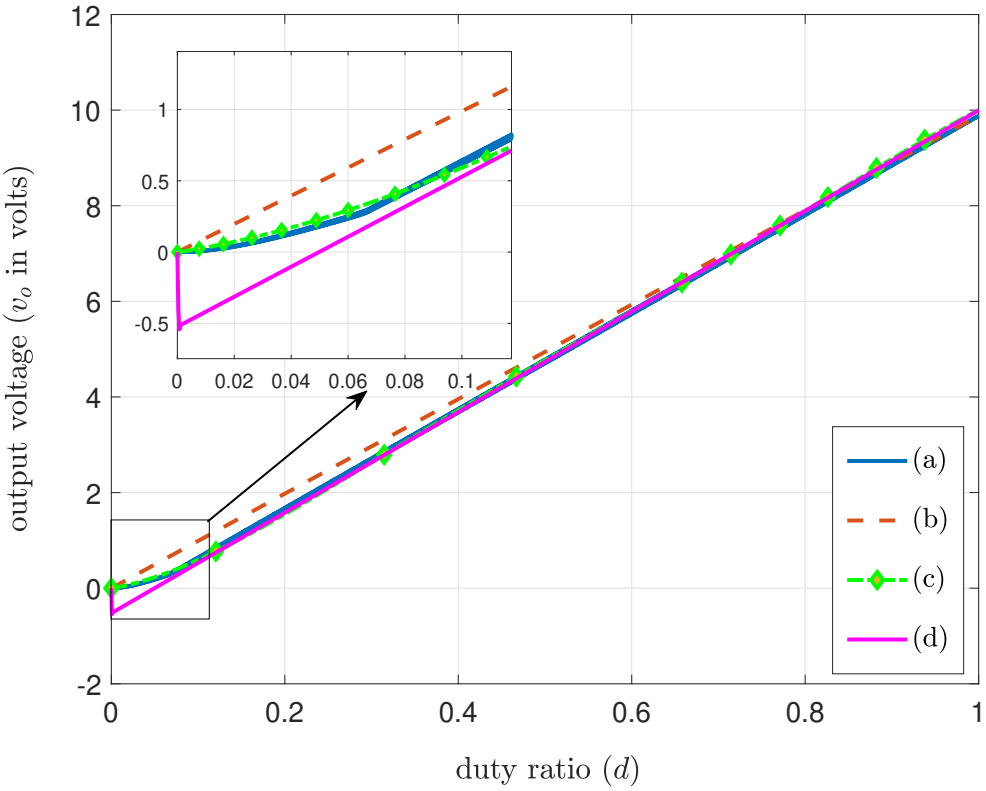

Figure 4.9: Ramp response characteristics of the buck converter: (a) original system's response (b) as average model (c) as Hammerstein model with polynomial non-linearity (d) as affine linear system.

the duty ratio $0 \geq d \geq 1$) is applied for 5 sec with sample rate of $0.01s$. The result is tabulated in Table 4.2. It can be observed that while the Hammerstein model gives the best result, both the identified models in this work gives better result compared to the average model.

4.5 Summary

A buck converter is identified as a nonlinear Hammerstein model using the method proposed in Chapter 3. The converter is modeled as an affine linear system first where the nonlinearity is estimated as an affine function. Then the converter is also modeled as a Hammerstein model with polynomial nonlinearity. Identifying the system as affine linear required only two relay tests while identifying it as a Hammerstein model required several relay tests. However, a polynomial nonlinearity gave a more accurate estimation of the system compared to the affine linear function. Both the model yield improved estimation results compared to the classical average model.

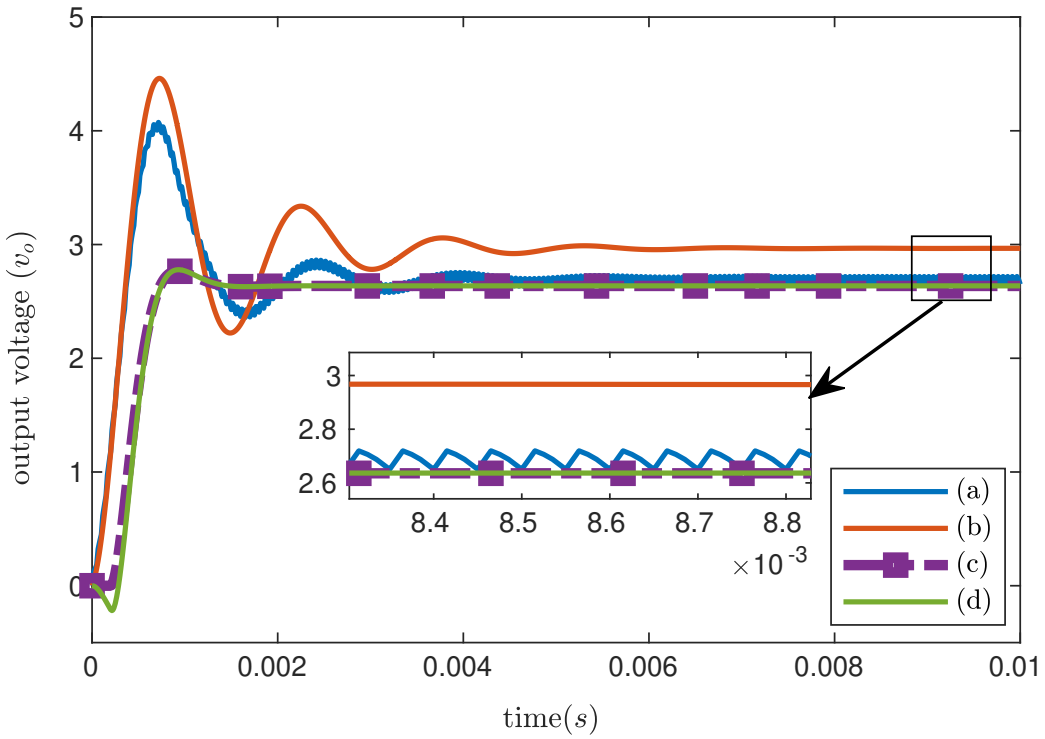

Figure 4.10: Step response characteristics of the buck converter: (a) original system's response (b) as an average model (c) as a Hammerstein model with polynomial nonlinearity (d) as affine linear system.

Identification method	Identified model	ISE
Average model using Erickson and Maksimovic [83]	$G_{vd}(s) = \dfrac{1.76\times10^8(3.577\times10^{-5}s+1)}{s^2+1828s+0.178\times10^8}$	1.5798
As affine linear by proposed method	$v = 10^8(3.85u-0.19)$ $G_p(s) = \dfrac{e^{-2\times10^{-4}s}}{s^2+8360s+0.366\times10^8}$	1.3838
As Hammerstein nonlinear by proposed method	$v = 10^8(-9.1346u^5+26.1582u^4$ $-27.6945u^3+13.2244u^2+1.1085u)$ $G_p(s) = \dfrac{e^{-2\times10^{-4}s}}{s^2+8360s+0.366\times10^8}$	1.2666

Table 4.2: Comparison of ISE of the three models.

Chapter 5

Conclusions

In this chapter, the contribution of the thesis has been summarized and a list of probable future works are given.

5.1 Thesis Contribution

A non-iterative, simple, state space based method is presented in this thesis for the identification of the Wiener and the Hammerstein models. A single common technique has been followed for both the models where a relay feedback setup has been utilized to get sustained oscillation at the output. In both the models, the typical oscillatory outputs are analysed to identify the linear subsystem first and then the static nonlinearity. Hammerstein modeling however required more than one tests for which the relay height can be pre-assigned as Chebyshev nodes in order to eradicate Runge's phenomenon of over-fitting. The proposed Hammerstein model identification method has been successfully applied to a buck converter simulation, both as a linear model as well as a nonlinear model.

This research does not aim at developing a competent method to identify Hammerstein or Wiener model over the various other approaches already existing in the literature such as LSE and Gaussian input based [53, 54, 55, 56, 85, 86, 87], correlation analysis and kernel regression estimates [57, 58, 59, 88, 61]. Although, a comparison of all available approaches would make an interesting research itself. Hence, the important point that is being stressed here is that the

scope of the research work is limited only at extending the use of relay feedback efficiently to broader domain, from linear to non-linear. Thus, the broad contributions of this thesis work focusing on the limitations of relay feedback from the literature in identifying BONL models can be summarized as

- *Applicable to unstable systems:* It is found that the equations for finding the time constants are independent of their sign. Therefore, any linear/Wiener/Hammerstein system that gives limit cycle oscillations under relay feedback can be identified irrespective of being stable or unstable.
- *Requires relatively less prior knowledge:* Given the structure of the system to be Wiener or Hammerstein, identification can be carried out without knowing the sign of the time constants or the nature of the static gain (i.e., weather linear or nonlinear).
- *Considers relatively wide cases of linear subsystems:* In most of the literature, the Wiener and the Hammerstein modeling using relay feedback are done considering only real and distinct time constants of the linear subsystem. This thesis work considers all probable cases of a second-order transfer function i.e., real roots, complex conjugate roots, repeated roots, integrating second-order, first-order, integrator and unstable cases as well.
- *Suitable for online identification:* The method is relatively simple and straight forward compared to those in the literature. Only one test with a fixed relay height is required for the Wiener model. Although, Hammerstein model requires more than one test, the relay heights can be predetermined as Chebyshev nodes which also ensures the curve fitting on the nonlinearity to be free from Runge's phenomenon of over-fitting.

5.2 Scope for Future Work

This dissertation is not a narrow down research on a specific model, it studied two major BONL models and their probable applications. Therefore, this work leaves a plenty of opportunities for future research, a few of them are mentioned below.

- The work includes solving highly nonlinear equations to find the time constants, a treaty on the solution space and developing improved numerical methods to solve these equations could be a possible future research.

- While simulations are a necessary proof for the accuracy of a method, they are nevertheless sufficient. Therefore, a theoretical analysis on the existence of solution, convergence and sensitivity would be a promising future work.

- It would be interesting to design an experiment using relay feedback such that the Hammerstein model can be identified in a single test run like the Wiener model.

- The method is restricted only to passive nonlinearity, therefore a future research can be taken on considering other class of nonlinearities such as active and dynamic nonlinearities. Also, other forms of representation beside the polynomial form can also be considered for the nonlinearity which can include nonmonotonic behaviors more efficiently. For example, Luyben and Eskinat [15] used exponential function to identify the sharp behavior of distillation column. Similarly, other forms such as rational functions, transcendental functions, orthogonal polynomials, regression analysis, Fourier series, wavelets, neural networks etc can also be investigated.

- Åström and Hägglund [14] provide a describing function approach to define the condition of oscillation for relay feedback in linear models. The presence of the unknown static nonlinearity makes it impossible to apply the same analysis for BONL models. It would be a challenging future work to analyse the condition of oscillation in such cases.

Appendix A

Chebyshev nodes

Chebyshev polynomials are integral to most areas of numerical analysis. The versatility of Chebyshev polynomials is attributed to its direct relationship with trigonometric functions "sine" and "cosine" which in turn are versatile in many kinds of naturally occurring phenomena. There are several kinds of Chebyshev polynomials, however, "Chebyshev polynomial" is used to refer explicitly to the first kind of Chebyshev polynomial which is defined as follows [89].

Definition 1. *(Chebyshev polynomial of the first kind)* The Chebyshev polynomial $T_j(q)$ of the first kind is a polynomial in q of degree j, defined by the relation

$$T_j(q) = cos(j\zeta) \quad when \quad q = cos\zeta \tag{A.1}$$

It is well known that $cos(j\zeta)$ can be expressed as a polynomial of degree j in $cos\zeta$ such as

$$\begin{aligned} cos(0\zeta) &= 1 \\ cos(1\zeta) &= cos\zeta \\ cos(2\zeta) &= 2cos^2\zeta - 1 \\ cos(3\zeta) &= 4cos^3\zeta - 3cos\zeta \\ cos(4\zeta) &= 8cos^4\zeta - 8cos^2\zeta + 1 \vdots \end{aligned} \tag{A.2}$$

Hence, using (A.1) the first few $T_j(q)$ are deduced as

$$\begin{aligned} T_0(q) &= 1 \\ T_1(q) &= q \\ T_2(q) &= 2q^2 - 1 \\ T_3(q) &= 4q^3 - 3q \\ T_4(q) &= 8q^4 - 8q^2 + 1 \\ &\vdots \end{aligned} \tag{A.3}$$

Chebyshev nodes are the roots of the Chebyshev polynomials of the first kind defined above. Chebyshev nodes are used in polynomial interpolation because they minimises the Runge's phenomenon over equally spaced node points [89]. From (A.1) it can be easily seen that the zeros of the Chebyshev polynomials of the first kind are the zeros of $cos(j\zeta)$ i.e.,

$$j\zeta = (l - \frac{1}{2})\pi, \qquad (l = 1, 2, \cdots, j). \tag{A.4}$$

where l is the number of Chebyshev node points. Hence, the zeros of $T_j(q)$ are

$$q_l = cos(\zeta_l) = cos\frac{(l - \frac{1}{2})\pi}{j}, \qquad (l = 1, 2, \cdots, j). \tag{A.5}$$

Note that the range of q is the range of $cos\zeta$ i.e., $[-1, 1]$ therefore, the above zeros of $T_j(q)$ are for interpolations only in the interval $[-1, 1]$. For zeros over any arbitrary interval $[h_1, h_2]$, an affine transform is used which gives

$$q_l = \frac{(h_1 + h_2)}{2} + \frac{(h_1 - h_2)}{2} cos\frac{(l - \frac{1}{2})\pi}{j}, \qquad (l = 1, 2, \cdots, j). \tag{A.6}$$

In this thesis work, the relay heights $\pm h$ are chosen as Chebyshev nodes in case of Hammer-

stein model identification. Therefore, the above equations of q_l give the required relay heights.

Consider Example 5 of 3.5 where the number of point to be estimated on the nonlinear curve $f(u)$ is 6 (excluding 0) in an interval of $[-2,2]$. As the proposed method uses asymmetric relay test therefore, equally positive and negative limits of the interval of estimation has been taken. It is known that one relay test gives two sets of points on the polynomial as described in Section 3.2.2. Fortunately, note again that $q = 0$ is a zero of $T_j(q)$ for all odd j, but not for even j, and these nodes/zeros are symmetrically placed in pairs on either side of $q = 0$.

Now, to get 6 sets of points, 3 relay tests are required. Note that the nonlinearity in this work is assumed to be passing through the origin therefore, zero is already a known node for interpolation. Now, if the Chebyshev nodes are calculated for $l = 6$ then one gets 7 numbers of nodes including the already known point zero which in this case is not a Chebyshev node. However, if the Chebyshev nodes are calculated for $l = 7$ then zero will come automatically as one of the Chebyshev nodes. Therefore, to get a better uniform convergence, $l = 7$ is used to calculate the required Chebyshev nodes which give

$$\begin{aligned}
q_1 &= 2cos\frac{\pi}{14} = 1.94985 \\
q_2 &= 2cos\frac{3\pi}{14} = 1.56366 \\
q_3 &= 2cos\frac{5\pi}{14} = 0.86777 \\
q_4 &= 2cos\frac{\pi}{2} = 0 \\
q_5 &= 2cos\frac{9\pi}{14} = -0.86777 \\
q_6 &= 2cos\frac{11\pi}{14} = -1.56366 \\
q_7 &= 2cos\frac{13\pi}{14} = -1.94985
\end{aligned} \tag{A.7}$$

Since a relay test with a particular height gives two points and zero is always a known interpolating node, therefore, it is beneficial to take only odd numbers for l in which zero is always a Chebyshev node.

Appendix A. Chebyshev nodes

Bibliography

[1] M. W. Lee, H.-P. Huang, and J. C. Jeng, "Identification and controller design for nonlinear processes using relay feedback," *Journal of Chemical Engineering of Japan*, vol. 37, no. 10, pp. 1194–1206, 2004.

[2] H.-P. Huang, M.-W. Lee, and Y.-T. Tang, "Identification of Wiener model using relay feedback test," *Journal of Chemical Engineering of Japan*, vol. 31, no. 4, pp. 604–612, 1998.

[3] M. Schetzen, "Nonlinear system modeling based on the Wiener theory," *Proceedings of the IEEE*, vol. 69, no. 12, pp. 1557–1573, 1981.

[4] S. H. Strogatz, *Nonlinear dynamics and chaos: with applications to physics, biology, chemistry, and engineering.* 1st ed Perseus Books, 1994.

[5] J. J. E. Slotine, W. Li *et al.*, *Applied nonlinear control*. Prentice-hall Englewood Cliffs, NJ, 1991, vol. 199.

[6] F. Giri and E. W. Bai, *Block-oriented nonlinear system identification*. Springer, 2010, vol. 1.

[7] H. P. Huang, M. W. Lee, and C. Y. Tsai, "Structure identification for block-oriented nonlinear models using relay feedback tests." *Journal of Chemical Engineering of Japan*, vol. 34, no. 6, pp. 748–756, 2001.

[8] Q. Min, Z. Xiuping *et al.*, "The modeling and equalization technique of nonlinear wireless channel," *The Open Cybernetics & Systemics Journal*, vol. 8, no. 1, pp. 297–301, 2014.

[9] C. M. Holcomb, R. A. de Callafon, and R. R. Bitmead, "Closed-loop identification of Hammerstein systems with application to gas turbines," *IFAC Proceedings Volumes*, vol. 47, no. 3, pp. 493–498, 2014.

[10] F. Jurado, "A method for the identification of solid oxide fuel cells using a Hammerstein model," *Journal of Power Sources*, vol. 154, no. 1, pp. 145–152, 2006.

[11] D. Chou, "Efficacy of Hammerstein models in capturing the dynamics of isometric muscle stimulated at various frequencies," Ph.D. dissertation, Massachusetts Institute of Technology, 2006.

[12] D. F. Wang, Y. Y. Ren, C. L. Liu, and P. Han, "Identification of thermal process using Hammerstein model based on particle swarm optimization algorithm," in *Unifying Electrical Engineering and Electronics Engineering*. Springer, 2014, pp. 1961–1968.

[13] L. Ljung, "Approaches to identification of nonlinear systems," in *Control Conference (CCC), 2010 29th Chinese*. IEEE, 2010, pp. 1–5.

[14] K. J. Åström and T. Hägglund, "Automatic tuning of simple regulators with specifications on phase and amplitude margins," *Automatica*, vol. 20, no. 5, pp. 645–651, 1984.

[15] W. L. Luyben and E. Eskinat, "Nonlinear auto-tune identification," *International Journal of Control*, vol. 59, no. 3, pp. 595–626, 1994.

[16] C. R. Arnold, "Identification of systems in terms of the Wiener model," Massachusetts Institute of Technology, Lexington Lincoln Lab, Tech. Rep., 1967.

[17] S. Billings and S. Fakhouri, "Identification of nonlinear systems using the Wiener model," *Electronics letters*, vol. 13, no. 17, pp. 502–504, 1977.

[18] W. Greblicki, "Nonparametric identification of Wiener systems," *IEEE Transactions on Information Theory*, vol. 38, no. 5, pp. 1487–1493, 1992.

[19] W. Greblicki, "Nonparametric identification of Wiener systems by orthogonal series," *IEEE Transactions on Automatic Control*, vol. 39, no. 10, pp. 2077–2086, 1994.

[20] S. Tötterman and H. T. Toivonen, "Support vector method for identification of Wiener models," *Journal of Process Control*, vol. 19, no. 7, pp. 1174–1181, 2009.

[21] Y. Fang and T. W. Chow, "Orthogonal wavelet neural networks applying to identification of Wiener model," *IEEE Transactions on Circuits and Systems I: Fundamental Theory and Applications*, vol. 47, no. 4, pp. 591–593, 2000.

[22] E.-W. Bai, "Frequency domain identification of Wiener models," *Automatica*, vol. 39, no. 9, pp. 1521–1530, 2003.

[23] F. Giri, Y. Rochdi, A. Radouane, A. Brouri, and F. Chaoui, "Frequency identification of nonparametric Wiener systems containing backlash nonlinearities," *Automatica*, vol. 49, no. 1, pp. 124–137, 2013.

[24] A. Hagenblad and L. Ljung, "Maximum likelihood estimation of Wiener models," in *Decision and Control, 2000. Proceedings of the 39th IEEE Conference on*, vol. 3. IEEE, 2000, pp. 2417–2418.

[25] A. Hagenblad, L. Ljung, and A. Wills, "Maximum likelihood identification of Wiener models," *Automatica*, vol. 44, no. 11, pp. 2697–2705, 2008.

[26] Y. Tang, L. Qiao, and X. Guan, "Identification of Wiener model using step signals and particle swarm optimization," *Expert Systems with Applications*, vol. 37, no. 4, pp. 3398–3404, 2010.

[27] D. Wang and F. Ding, "Least squares based and gradient based iterative identification for Wiener nonlinear systems," *Signal Processing*, vol. 91, no. 5, pp. 1182–1189, 2011.

[28] M. Liu, Y. Xiao, and R. Ding, "Iterative identification algorithm for Wiener nonlinear systems using the newton method," *Applied Mathematical Modelling*, vol. 37, no. 9, pp. 6584–6591, 2013.

[29] L. Zhou, X. Li, and F. Pan, "Gradient-based iterative identification for MISO Wiener nonlinear systems: application to a glutamate fermentation process," *Applied Mathematics Letters*, vol. 26, no. 8, pp. 886–892, 2013.

[30] F. Ding, X. Liu, and M. Liu, "The recursive least squares identification algorithm for a class of Wiener nonlinear systems," *Journal of the Franklin Institute*, vol. 353, no. 7, pp. 1518–1526, 2016.

[31] J. Guo, L. Y. Wang, G. Yin, Y. Zhao, and J.-F. Zhang, "Identification of Wiener systems with quantized inputs and binary-valued output observations," *Automatica*, vol. 78, pp. 280–286, 2017.

[32] M. Mohamed and I. N. Kar, "Stochastic contraction based online estimation of second order Wiener system," *ISA transactions*, vol. 69, pp. 131–139, 2017.

[33] V. Marmarelis, M. Citron, and C. Vivo, "Minimum-order Wiener modelling of spike-output systems," *Biological Cybernetics*, vol. 54, no. 2, pp. 115–123, 1986.

[34] M. J. Korenberg and I. W. Hunter, "The identification of nonlinear biological systems: Wiener kernel approaches," *Annals of Biomedical Engineering*, vol. 18, no. 6, pp. 629–654, 1990.

[35] A. Kalafatis, N. Arifin, L. Wang, and W. Cluett, "A new approach to the identification of pH processes based on the Wiener model," *Chemical Engineering Science*, vol. 50, no. 23, pp. 3693–3701, 1995.

[36] H. C. Park and J. Lee, "Step and pulse response methods for identification of Wiener processes," *AIChE Journal*, vol. 52, no. 2, pp. 668–677, 2006.

[37] J. C. Jeng, M. W. Lee, and H. P. Huang, "Identification of block-oriented nonlinear processes using designed relay feedback tests," *Industrial & Engineering Chemistry Research*, vol. 44, no. 7, pp. 2145–2155, 2005.

[38] U. Mehta and S. Majhi, "Identification of a class of Wiener and Hammerstein-type nonlinear processes with monotonic static gains," *ISA Transactions*, vol. 49, no. 4, pp. 501–509, 2010.

[39] S. Hanjalić and Ž. Jurić, "Closed-loop frequency-based identification method for Wiener type plants with a transport delay using a relay feedback," in *2012 IEEE International Conference on Control Applications*. IEEE, 2012, pp. 991–995.

[40] T. Meher and S. Majhi, "Relay-based identification of wiener model," *IET Circuits, Devices & Systems*, vol. 14, no. 3, pp. 398–406, 2020.

[41] J. W. Macki, P. Nistri, and P. Zecca, "Mathematical models for hysteresis," *SIAM review*, vol. 35, no. 1, pp. 94–123, 1993.

[42] H. K. Khalil, *Noninear systems*. Prentice-Hall, New Jersey, 1996.

[43] S. Majhi, "Relay based identification of processes with time delay," *Journal of Process Control*, vol. 17, no. 2, pp. 93–101, 2007.

[44] R. Bajarangbali, S. Majhi, and S. Pandey, "Identification of fopdt and sopdt process dynamics using closed loop test," *ISA transactions*, vol. 53, no. 4, pp. 1223–1231, 2014.

[45] M. Curve Fitting Toolbox 3.5.5, *version 9.2.0.556344 (R2017a)*. Natick, Massachusetts: The MathWorks Inc., 2017.

[46] C.-C. Yu, *Autotuning of PID controllers: A relay feedback approach*. Springer Science & Business Media, 2006.

[47] T. Meher and S. Majhi, "Relay based identification of Hammerstein model," *International Journal of Dynamics and Control*, vol. 6, no. 4, pp. 1599–1607, 2018.

[48] A. G. Bose, "A theory of nonlinear systems," 1956.

[49] N. Wiener, "Response of a non-linear device to noise," DTIC Document, Tech. Rep., 1942.

[50] S. Majhi and D. Atherton, "Autotuning and controller design for processes with small time delays," *IEE Proceedings-Control Theory and Applications*, vol. 146, no. 5, pp. 415–425, 1999.

[51] V. Ramakrishnan and M. Chidambaram, "Estimation of a SOPTD transfer function model using a single asymmetrical relay feedback test," *Computers & Chemical Engineering*, vol. 27, no. 12, pp. 1779–1784, 2003.

[52] M. Poluektov and A. Polar, "Modelling non-linear control systems using the discrete urysohn operator," *Journal of the Franklin Institute*, vol. 357, no. 6, pp. 3865–3892, 2020.

[53] K. S. Narendra and P. G. Gallman, "An iterative method for the identification of nonlinear systems using a Hammerstein model," *IEEE Transactions on Automatic Control*, vol. 11, no. 3, pp. 546–550, 1966.

[54] F. Chang and R. Luus, "A noniterative method for identification using Hammerstein model," *IEEE Transactions on Automatic Control*, vol. 16, no. 5, pp. 464–468, 1971.

[55] N. Haist, F. Chang, and R. Luus, "Nonlinear identification in the presence of correlated noise using a Hammerstein model," *IEEE Transactions on Automatic Control*, vol. 18, no. 5, pp. 552–555, 1973.

[56] T. Hsia, "A multi-stage least squares method for identifying Hammerstein model nonlinear systems," in *Decision and Control including the 15th Symposium on Adaptive Processes, 1976 IEEE Conference on*, vol. 15. IEEE, 1976, pp. 934–938.

[57] S. Billings and S. Fakhouri, "Non-linear system identification using the Hammerstein model," *International Journal of Systems Science*, vol. 10, no. 5, pp. 567–578, 1979.

[58] P. Stoica and T. Söderstrom, "Instrumental-variable methods for identification of Hammerstein systems," *International Journal of Control*, vol. 35, no. 3, pp. 459–476, 1982.

[59] W. Greblicki and M. Pawlak, "Identification of discrete Hammerstein systems using kernel

regression estimates," *IEEE Transactions on Automatic Control*, vol. 31, no. 1, pp. 74–77, 1986.

[60] W. Greblicki and M. Pawlak, "Nonparametric identification of Hammerstein systems," *IEEE Transactions on Information Theory*, vol. 35, no. 2, pp. 409–418, 1989.

[61] A. Krzyzak, "Identification of discrete Hammerstein systems by the Fourier series regression estimate," *International Journal of Systems Science*, vol. 20, no. 9, pp. 1729–1744, 1989.

[62] H. C. Park, D. G. Koo, J. H. Youn, J. Lee, and S. W. Sung, "Relay feedback approaches for the identification of Hammerstein-type nonlinear processes," *Industrial & Engineering Chemistry Research*, vol. 43, no. 3, pp. 735–740, 2004.

[63] Z. Juric, S. Hanjalic, and H. Sehovic, "Closed-loop frequency-based identification method for Hammerstein type plants with a transport delay using a relay feedback," in *2013 XXIV International Conference on Information, Communication and Automation Technologies (ICAT)*. IEEE, 2013, pp. 1–8.

[64] T. Meher and S. Majhi, "An improved relay feedback identification technique for Hammerstein model," *International Journal of Dynamics and Control*, vol. 8, no. 3, pp. 952–962, 2020.

[65] S. Pandey, S. Majhi, and P. Ghorai, "Limit cycle based identification of time delay siso processes," *IFAC Journal of Systems and Control*, vol. 6, pp. 43–52, 2018.

[66] I. Daubechies *et al.*, *Ten lectures on wavelets*. SIAM, 1992, vol. 61.

[67] M. Wavelet Toolbox 4.18, *version 9.2.0.556344 (R2017a)*. Natick, Massachusetts: The MathWorks Inc., 2017.

[68] A. Balestrino, A. Landi, M. Ould-Zmirli, and L. Sani, "Automatic nonlinear auto-tuning method for Hammerstein modeling of electrical drives," *IEEE Transactions on Industrial Electronics*, vol. 48, no. 3, pp. 645–655, 2001.

[69] F. Alonge, F. D'Ippolito, F. M. Raimondi, and S. Tumminaro, "Nonlinear modeling of dc/dc converters using the Hammerstein's approach," *IEEE Transactions on Power Electronics*, vol. 22, no. 4, pp. 1210–1221, 2007.

[70] G. Wester and R. D. Middlebrook, "Low-frequency characterization of switched dc-dc converters," *IEEE Transactions on Aerospace and Electronic Systems*, vol. AES-9, no. 3, pp. 376–385, 1973.

[71] R. Middlebrook and S. Cuk, "A general unified approach to modelling switching-converter power stages," in *Power Electronics Specialists Conference, 1976 IEEE.* IEEE, 1976, pp. 18–34.

[72] S.-P. Hsu, A. Brown, L. Rensink, and R. Middlebrook, "Modelling and analysis of switching dc-to-dc converters in constant-frequency current-programmed mode," in *Power Electronics Specialists Conference, 1979 IEEE.* IEEE, 1979, pp. 284–301.

[73] A. Pietkiewicz and D. Tollik, "Unified topological modeling method of switching dc-dc converters in duty-ratio programmed mode," *IEEE Transactions on Power Electronics*, vol. PE-2, no. 3, pp. 218–226, 1987.

[74] D. Czarkowski and M. K. Kazimierczuk, "Energy-conservation approach to modeling pwm dc-dc converters," *IEEE Transactions on Aerospace and Electronic Systems*, vol. 29, no. 3, pp. 1059–1063, 1993.

[75] A. Davoudi, J. Jatskevich, and T. De Rybel, "Numerical state-space average-value modeling of pwm dc-dc converters operating in dcm and ccm," *IEEE Transactions on Power Electronics*, vol. 21, no. 4, pp. 1003–1012, 2006.

[76] R. Tymerski, V. Vorpérian, F. C. Lee, and W. T. Baumann, "Nonlinear modeling of the pwm switch," *IEEE Transactions on Power Electronics*, vol. 4, no. 2, pp. 225–233, 1989.

[77] D. C. Hamill, J. H. Deane, and D. J. Jefferies, "Modeling of chaotic dc-dc converters by

iterated nonlinear mappings," *IEEE Transactions on Power Electronics*, vol. 7, no. 1, pp. 25–36, 1992.

[78] C. K. Tse and K. M. Adams, "Quasi-linear modeling and control of dc-dc converters," *IEEE Transactions on Power Electronics*, vol. 7, no. 2, pp. 315–323, 1992.

[79] W. Stefanutti, P. Mattavelli, S. Saggini, and M. Ghioni, "Autotuning of digitally controlled dc–dc converters based on relay feedback," *IEEE Transactions on Power Electronics*, vol. 22, no. 1, pp. 199–207, 2007.

[80] Z. Zhao and A. Prodi, "Limit-cycle oscillations based auto-tuning system for digitally controlled dc–dc power supplies," *IEEE Transactions on Power Electronics*, vol. 22, no. 6, pp. 2211–2222, 2007.

[81] K. V. Ramana, S. Majhi, and A. K. Gogoi, "Identification of dc–dc buck converter dynamics using relay feedback method with experimental validation," *IET Circuits, Devices & Systems*, 2018.

[82] T. Meher, S. Majhi, and K. V. Ramana, "Hammerstein modeling of buck converter using relay feedback," in *TENCON 2019-2019 IEEE Region 10 Conference (TENCON)*. IEEE, 2019, pp. 637–642.

[83] R. W. Erickson and D. Maksimovic, *Fundamentals of power electronics*. Springer Science & Business Media, 2007.

[84] K. V. Ramana, S. Majhi, and A. K. Gogoi, "Modeling and estimation of dc–dc buck converter dynamics using relay feedback output with performance evaluation," *IEEE Transactions on Circuits and Systems II: Express Briefs*, vol. 66, no. 3, pp. 427–431, 2018.

[85] B. Zhang and Z. Mao, "Bias compensation principle based recursive least squares identification method for Hammerstein nonlinear systems," *Journal of the Franklin Institute*, vol. 354, no. 3, pp. 1340–1355, 2017.

[86] L. Ma and X. Liu, "A novel apso-aided weighted lssvm method for nonlinear Hammerstein system identification," *Journal of the Franklin Institute*, vol. 354, no. 4, pp. 1892–1906, 2017.

[87] F. Ding, H. Chen, L. Xu, J. Dai, Q. Li, and T. Hayat, "A hierarchical least squares identification algorithm for Hammerstein nonlinear systems using the key term separation," *Journal of the Franklin Institute*, vol. 355, no. 8, pp. 3737–3752, 2018.

[88] W. Greblicki and M. Pawlak, "Recursive nonparametric identification of Hammerstein systems," *Journal of the Franklin Institute*, vol. 326, no. 4, pp. 461–481, 1989.

[89] J. C. Mason and D. C. Handscomb, *Chebyshev polynomials*. CRC Press, 2002.

List of Publications

Journals

1. Trusna Meher and Somanath Majhi, ”Relay based identification of Wiener model”, *IET Circuits, Devices & Systems*, vol. 14, issue 3, pp. 398-406, 2020.

2. Trusna Meher and Somanath Majhi, ”An improved relay feedback identification technique for Hammerstein model”, *International Journal of Dynamics and Control*, vol. 8, issue 3, pp.952-962, 2020.

3. Trusna Meher and Somanath Majhi, ”Relay based identification of Hammerstein model”, *International Journal of Dynamics and Control*, vol. 6, issue 4, pp. 1599–1607, 2018.

Conferences

1. T. Meher, S. Majhi and K. V. Ramana, ”Hammerstein Modeling of Buck Converter using Relay Feedback”, *2019 IEEE Region 10 Conference (TENCON)*, Kochi, India, 2019, pp. 637-642.